Novel CH-π Interactions of Polyethylene Glycols and Crown Ethers with Biological Aromatic Compounds

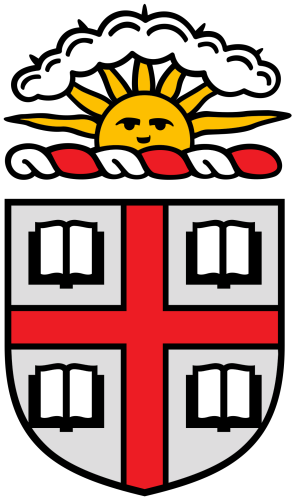

Author: Ainsley Baker

Research Advisor: Amit Basu, Ph.D

Brown University

Department of Chemistry

April 2023

Submitted in partial fulfillment of the honors requirements for the degree of Bachelor of Science in Chemical Biology

TABLE OF CONTENTS

ABSTRACT

We report the preliminary evidence of a novel CH-π interaction between polyethylene glycol and aromatic compounds as well as crown ethers and aromatic compounds. Polyethylene glycol (PEG), an extensively common ether polymer found in a variety of products, has recently taken up the public spotlight as the allergenic component of the Pfizer and Moderna SARS-CoV-2 vaccines. PEG hypersensitivities remain underdiagnosed, and the immunogenicity of PEG has not yet been completely demystified. From previous investigations, an increased incidence of non-hydrogen bonding aromatic residue contacts in the anti-PEG antibody antigen-binding site provokes a question of a potentially new aromatic-PEG interaction. Similarly to the discovery and characterization of the CH-π interactions that are critical to carbohydrate binding by proteins, ^{1}H NMR is utilized to observe the upfield change in chemical shift of the participating PEG-CH hydrogens in the presence of amino acid-derived aromatic compounds. The data shows that polyethylene glycol and crown ether both show significant upfield shifting of interior hydrogens in the presence of these aromatic compounds. Though further studies are required to flesh out the entire character of these interactions, these preliminary results suggest a previously unconsidered intermolecular force with potential importance regarding PEG immunogenicity.

ACKNOWLEDGEMENTS

Firstly, I would like to thank Dr. Amit Basu for the years of guidance, mentorship, and friendship that he has graciously provided to me. He has been a champion of solving all of the polyethylene glycol problems I create since day one, and the freedom of independent scientific inquiry that he provided to me has made my experience in the chemistry department far more fulfilling than I ever anticipated. Dr. Basu has always cultivated a collaborative environment in which this work could grow, and I am immensely grateful to have had such a talented, bright and kind advisor to pioneer my undergraduate degree.

I would also like to thank Brown University for awarding a Karen T. Romer Undergraduate Teaching and Research Award (UTRA) to us for the summer of 2021, seeding the two years of work that were to follow. Without this opportunity, my undergraduate education would not have been even half as valuable as it is now, and it cannot be credited enough for the work that this thesis contains.

I also must thank Sebastian Rueda, Janet Muzulu, and Raj Hoshing, for their guiding hand as graduate students in the Basu lab during my work. They gave me my license to drive *Cronus* and answered a million and one of my questions while completing research of their own, for which I will always be grateful.

I would additionally like to thank my family and friends for supporting me throughout my time at Brown despite the troubled nature of these last 4 years, especially to my mother: I love you, always.

Lastly, I would like to thank Dr. Frank Gasparro for forcing me write college-length lab reports in AP Chemistry, citing the fact that I would “obviously be a chemistry major one day,” despite my ample protest. You were right.

INTRODUCTION

Polyethylene Glycol

Polyethylene glycol (PEG) is a pervasive polyether compound found in an extensive range of applications. PEG polymer chains can vary in weight, from 400 to 8000 grams per mole or higher, and have smaller-weight relatives with similar properties, such as tetraethylene glycol. It is in your home as a preservative and emulsifier in shampoos and cosmetics, in your laxatives as an active ingredient, and of more recent interest, in the lipid nanoparticle drug delivery systems utilized in the SARS-CoV-2 vaccines (Sellaturay et al., 2021). The lipid nanoparticle system used for these vaccines and many other pharmaceuticals requires the process of coating liposomes and micelles with PEG, which is referred to as "PEGylation." This is done in order to increase solubility of the drug-encapsulating liposomes while in circulation, increasing drug delivery (Harris and Chess, 2003).

Though it is of high utility in multiple settings, PEG usage does have an important drawback that has recently become of a higher concern: an underappreciated immunogenicity. PEG allergies are increasing in incidence (Kozma et al., 2020), but remain underdiagnosed (Sellaturay et al., 2021). PEG has been identified as the allergenic ingredient of the COVID-19 vaccines in cases of anaphylaxis (Sellaturay et al., 2021) and other hypersensitive responses, thought to be IgE-mediated (Wylon et al., 2016). Beyond hypersensitivity, the aforementioned PEGylated pharmaceuticals additionally activate an antibody-mediated response, referred to as the accelerated blood clearance (ABC) phenomenon, in which anti-PEG IgM binds the PEG coating and activates complement, resulting in decreased efficacy and circulation time (Mohamed et al., 2019). Insight into the mechanisms of PEG immunogenicity would offer promising help to those affected, and aromatic compounds seem like an interesting starting point.

Previous Evidence of Aromatic Compound Interactions

Aromatic compounds appear to be related to PEG binding in immunological responses and other interactions, an association previously observed but not well characterized. The binding site of an anti-PEG antibody has been detailed structurally with x-ray crystallography and contains a number of non-hydrogen bonding aromatic residues in proximity to bound PEG (Lee et al., 2020). As shown in Figure 1, antibody crystallized in complex with PEG demonstrates numerous contacts with aromatic residues in a way important to PEG capture in the binding site. The conformation of the PEG molecules is of note as well, as it assumes a crown ether-like conformation when bound by the antibody, resulting in an anti R-O-C-C-H conformation for the C-H making contact with the aromatic residues. The conformational constraints of the binding site point in an interesting direction towards aromatic-PEG interactions.

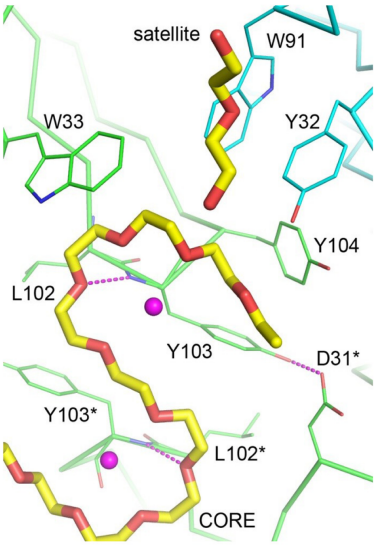

Figure 1: X-ray crystal structure of PEG in the anti-PEG antibody binding site (Lee et al., 2020).

Tetraethylene glycol, a smaller weight PEG, has further been shown to interact preferentially with aromatic protein functional groups over other functional groups (Knowles et al., 2015). Knowles et al. measured solute accumulation of PEGs and glycerol on various functional group model compounds and then compiled this information into predictive models of how PEGs and glycerol would behave with a model dipeptide expressing the functional groups investigated (Figure 2). In this model, it can be seen that the PEG interior groups would interact favorably with the aromatic and amine functional groups of the dipeptide.

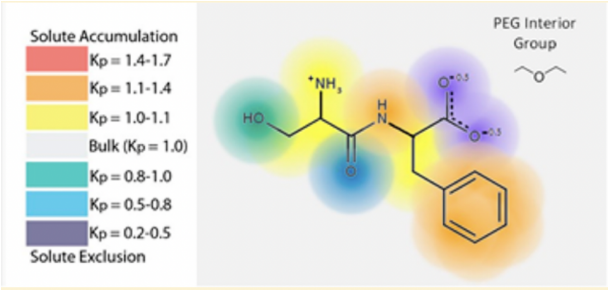

Figure 2: Predicted solute accumulation of the interior PEG groups at functional groups of the Ser-Phe model dipeptide (Knowles et al., 2015).

PEG-aromatic interactions are not just of potential immunological application – PEG is recommended for phenol spill cleanup and skin contact, though the mechanism is not well understood (Phenol SOP, 2022). All of these hints at an aromatic compound and PEG interaction point toward the unique delocalized π system of electrons common to aromatic compounds as a perpetrator.

CH-π Interactions

Interactions of a similar nature have been previously reported. CH-π interactions are a group of intermolecular interactions of particular importance to carbohydrate binding, in which

electron-poor CH bonds coordinate with electron-rich π systems on aromatic compounds. This leads to "stacking" of carbohydrates and aromatics, and the interaction is very important for stabilizing carbohydrates bound by proteins (Asensio et al., 2012). Similarly to the anti-PEG antibody binding site, carbohydrate binding sites in proteins also show increased numbers of aromatic residues (Hudson et al., 2015). X-ray crystallography of carbohydrates bound by proteins show the effect of aromatic residues in the binding sites, including the stacking effect, as can be seen in Figure 3.

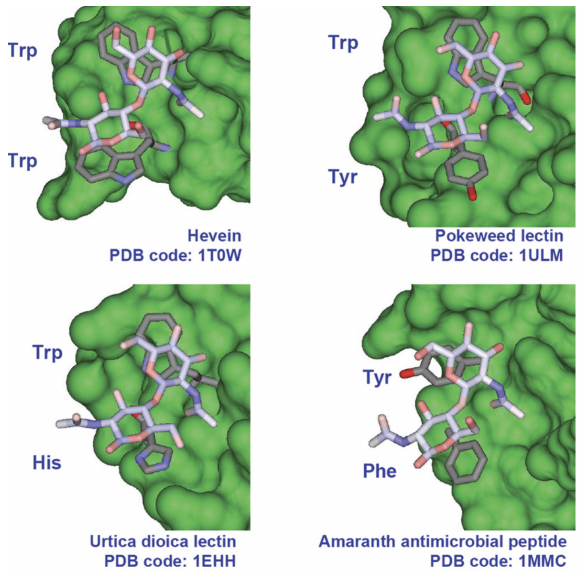

Figure 3: Carbohydrates bound by proteins (Asensio et al., 2012).

These carbohydrate CH-π interactions have been detected experimentally using NMR. In the ^{1}H NMR environment, the circular nature of an aromatic π system induces a smaller magnetic environment orthogonal to the plane of the aromatic ring. If the CH-π interactions are occurring, the field created by the aromatic system should induce shielding of protons in proximity to the field, resulting in changes in the chemical shifts of CH protons participating in said CH-π interaction. In 2005, Fernández-Alonso et al. were able to demonstrate carbohydrate

CH-π interactions by use of this property with simple ^{1}H NMR experiments. Solutions of the carbohydrate in D_2O with and without an aromatic compound were used to record ^{1}H NMR spectra, showing a significant change upfield in the chemical shifts of the carbohydrate CH protons as seen in Figure 4. The changes in chemical shift can be expressed at the scale of parts per billion (ppb). This ^{1}H NMR technique was used again by Hudson et al. in 2015, allowing for them to use the resulting shift changes to generate a heat map of carbohydrate-π interactions on the carbohydrate protons (Figure 5).

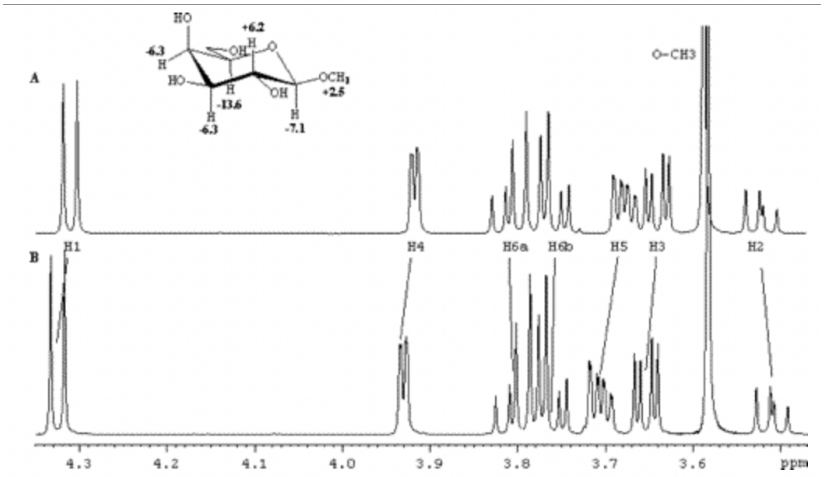

Figure 4: Chemical shift perturbations of methyl β-galactoside in D_2O with (A) and without (B) 200 mM phenol (Fernández-Alonso et al., 2005)

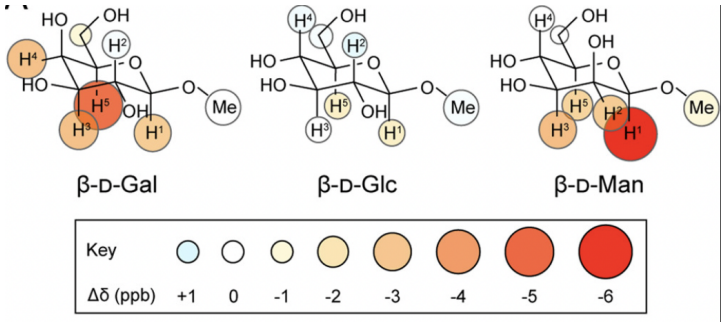

Figure 5: Heat map of chemical shift perturbations of methyl glycosides by indole (Hudson et al. 2015)

This ^{1}H NMR simple solution technique has been the basis for NMR experiments to assess carbohydrate-aromatic interactions, and it can act as a guiding light for PEG-aromatic interaction assessment. In similar NMR findings from 2008, the ^{1}H NMR data was interpreted alongside DFT modeling of the compound interactions to not only develop a 3D model for the interaction but also an approximate ratio of complex formation in solution (Vandenbussche et al., 2008). These 2008 studies suggested that the electron density of the aromatic ring is crucial to the hydrophobic interaction occurring. Additionally, the stereochemistry of carbohydrate protons is of importance, as C-H bonds orthogonal to the plane of the aromatic ring were those participating the most in the interaction. This experimental model might transfer excellently to the investigation of PEG-aromatic reactions, providing a robust avenue for investigation.

In order to demonstrate the hypothetical PEG-π interaction, ^{1}H NMR would be a brilliant first step. Upon confirmation of PEG-π interactions, factors impacting binding, such as PEG stereochemistry and electron density of the aromatics, can then be manipulated in order to paint a clearer picture of the binding mechanism. By showing the upfield shifting of PEG protons when in solution with aromatic compounds, the binding of these two molecules can be confirmed. Diffusion ordered spectroscopy (DOSY) can be used as well to quantify the strength of the binding interaction. DOSY allows for the fraction of bound aromatic compound to be compared when in the absence and presence of PEG, a technique used previously to probe the binding of indole and carbohydrates (Muzulu and Basu, 2021).

Molecular Orbital Stabilization

Determination of PEG-π interactions by the same means of CH-π interactions additionally allows for expansion of CH-π explanations of binding to be extended to PEG-π,

painting a far clearer picture of PEG interaction predictability moving forward. One common theme of mechanism for RH-π interactions is molecular orbital stabilization. In SH-π interactions that have been reported, stabilization of the electron deficient S-H σ* molecular orbital by the π system is thought to be the underlying mechanism of the the interaction (Forbes et al., 2017). Beyond this, the "gauche effect" of electronegative X atoms in an X-C-C-X bond preferring the gauche conformation is typically described by hyperconjugation, as can be seen in Figure 6 (Alabugin et al., 2011). Hyperconjugation is characterized by the delocalization of (typically σ-character) electrons into empty orbitals, in this case empty and adjacent σ* orbitals. This stabilization model is most important to highly electronegative atoms, but may prove potentially extendable to the interactions of ether oxygens in PEG, as it is an effect that dominates the conformational preferences of the PEG monomer, ethylene glycol (Alabugin et al., 2011).

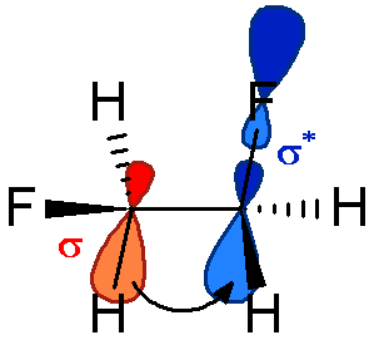

Figure 6: Hyperconjugation causing the gauche effect in 1,2-difluoroethane

By quantifying binding of PEG and aromatic compounds with H^1NMR, a novel interaction can be characterized and extended to both PEG allergy interventions and other molecular interactions with similar mechanisms. PEG alternatives that lack features important to the PEG-π interaction can be introduced as less allergenic alternatives, such as polyamine alternatives developed previously that show decreased immunogenicity when used for

PEGylation (Engler et al., 2015). Ether-π interactions in other compounds, like smaller weight ethylene glycols, can be expanded upon to generate a better understanding of how the body interacts with these molecules. Characterization of the PEG-π interaction would open an avenue into a wide new frontier of intermolecular interactions.

RESULTS AND DISCUSSION

Characterization of PEG-π Interactions

Ethylene glycol (**1**) was selected as the monomer control version of PEG, as it does not contain the repeated interior ether groups characteristic of other PEGs. Diethylene glycol (**2**), triethylene glycol (**3**), and tetraethylene glycol (**4**) were used as very small weight versions of PEG, in order to ascertain whether the number of interior ethers is important to the interactions. The crown ethers, 15-crown-5 (**6**) and 18-crown-6 (**7**), were used as conformationally constrained versions of PEG that have no PEG terminal hydroxyl groups. 1,5-pentanediol (**8**) is used as a non-ether analog to diethylene glycol as a control for terminal hydroxyl groups. All of these compounds mentioned up to this point are referred to as PEG-related compounds, glycol-related compounds, or "glycols" in this research. Phenol (**10**) and indole (**9**) were selected as model compounds for tyrosine and tryptophan residues in binding sites. L-tyrosine methyl ester hydrochloride (**12**) and L-tryptophan methyl ester hydrochloride (**13**) were additionally selected to emulate tyrosine and tryptophan residues, and L-alanine methyl ester hydrochloride (**11**) was used as a non-aromatic standard of comparison. 4-nitrophenol (**14**) and 3-cyanophenol (**15**) were used as electron-deficient variants of phenol.

From the experimental ^{1}H NMR spectra collected, changes in chemical shifts were obtained using the following formula:

$$\Delta\delta_{x\ mM\ of\ aromatic\ compound} = \delta_{x\ mM\ of\ aromatic\ compound} - \delta_{0\ mM\ of\ aromatic\ compound}$$

The changes in chemical shift for each glycol were calculated in Tables 1-7. Hydrogen assignments in Tables 1-7 refer to the hydrogen environment labels in Figure 11.

^{1}H NMR spectra reveal that PEG 8000 and related compounds experience significant upfield shifting of interior hydrogens in the presence of phenol, as seen in Table 1. Ethylene glycol, which lacks “interior” hydrogens adjacent to ether oxygens, did not present any upfield shifting, and instead saw downfield shifting. Downfield shifting is typically attributed to hydrogen bonding for X-H····H hydrogen bonds, where X is an electron withdrawing group. In the context of this research, downfield shifting is moreso considered the opposite of upfield shifting, with numerous potential contributions to the shift. As data is discussed, rather than upfield and downfield shifting being antithetical, downfield shifting is instead representative of a loss of upfield shift. Generally, as the concentration of the aromatic compound increases, downfield shifting increases for non-participating hydrogens. This is highlighted by the significant downfield shift of the HOD peaks in each titration. The “reference frame” for chemical shift seems to be always shifting downfield, as in both participating non-participating hydrogens are shifting downfield with increased aromatic concentration, and so upfield shifting becomes less pronounced in some titrations, like the 4-nitrophenol and 3-cyanophenol titrations (Tables 6 and 7). Additional justification for this idea can be seen in the L-alanine methyl ester hydrochloride titrations in Table 3, in which a compound that would prefer mostly hydrogen bonding induces downfield shifting in non-hydrogen bonding protons.

Table 1. Changes in ^{1}H NMR chemical shifts (in ppb) of PEG 8000 and related compounds in increasing concentrations of **10**.

PEG-related compound	*Hydrogen*	10 mM	100 mM	150 mM	200 mM
Ethylene glycol (**1**)	HOD	0.9	12.3	—	22.4
	H_a	0.1	4.3	—	9.1
Diethylene glycol (**2**)	HOD	0.9	10.6	—	23.15
	H_a	0.35	1.7	—	3.95
	H_b	-0.45	-2.25	—	-3.5
Triethylene glycol (**3**)	HOD	1.15	10.05	15.7	—
	H_a	0.05	0.65	1.65	—
	H_b	-0.5	-4	-3.5	—
	H_c	-0.65	-6.2	-8.55	—
Tetraethylene glycol (**4**)	HOD	1.9	10.3	—	22.85
	H_a	0.1	0.7	—	1.8
	H_b	-1	-3.9	—	-7.75
	$H_{interior}$	-1.65	-7.85	—	-14.7
PEG 8000 (**5**)	HOD	2.75	9.55	16.75	—
	$H_{interior}$	-1.3	-10	-15.1	—
1,5-pentanediol (**8**)	HOD	1.1	11.2	23.4	—
	H_a	0	-0.3	0.5	—
	H_b	-0.1	-0.8	-0.7	—
	H_c	-0.2	-1.7	-2.6	—
15-crown-5 (**6**)	HOD	0.7	9.0	—	17.6
	H_a	-1.3	-10.2	—	-20.3
18-crown-6 (**7**)	HOD	2.5	12.1	—	25.8
	H_a	-1.4	-11.2	—	-21.5

Free amino acid side chain analogues

The ^{1}H NMR spectra demonstrate numerous things. As polyethylene glycol weight increases and chain length increases, the magnitude of the upfield shift increases, which can be seen in Table 1. Phenol shows shift changes in the -20 ppb range, which is a high amount compared to interactions seen previously in carbohydrates (Hudson et al. 2015). Notably, the crown ethers break the trend of increasing PEG weight, as their upfield shifts are even higher than PEG 8000, despite being of a much smaller chain length. Crown ethers only have "interior" hydrogens, hydrogens only adjacent to ether groups, and so are an interesting point of comparison for the polyethylene glycols, especially since PEG is seen taking a crown ether-like conformation when bound by antibody (Lee et al., 2020). 1,5-pentanediol was included in the phenol titrations as a non-ether control, but interestingly followed the same trend of upfield shifting as its glycol analogue, diethylene glycol (Table 1).

Table 2. Changes in ^{1}H NMR chemical shifts (in ppb) of PEG 8000 and related compounds in increasing concentrations of **9**.

PEG-related compound	*Hydrogen*	4 mM	7.5 mM	10 mM
Ethylene glycol (**1**)	HOD	1.6	3.4	3.1
	H_a	-1.2	-0.2	-0.1
Tetraethylene glycol (**4**)	HOD	1.8	4.5	3.0
	H_a	0.1	-0.3	-0.7
	H_b	-0.8	-1.2	-1.2
	$H_{interior}$	-1.0	-1.9	-2.6
PEG 8000 (**5**)	HOD	2.7	2.3	1.8
	$H_{interior}$	-1.1	-3.0	-4.5

Indole titrations presented similar results, however due to the lower concentration of indole, shift changes are smaller in magnitude (Table 2). The lower concentrations are due to indole's limited solubility in D_2O, so to remedy this, the amino acid methyl esters were introduced as substitutes later on. Ethylene glycol does not show significant upfield shifting of hydrogens in indole, further suggesting the importance of the interior ether groups to the interactions. The extended size and electron density of the indole π system compared to the phenol π system would suggest that it should interact more favorably than phenol with PEG, which may be suggested by the trend of this data.

Table 3. Changes in ^{1}H NMR chemical shifts (in ppb) of PEG 8000 and related compounds in increasing concentrations of **11**.

PEG-related compound	*Hydrogen*	4 mM	40 mM	80 mM
Ethylene glycol (**1**)	HOD	0.9	2.3	2.7
	H_a	0.3	0.1	0.5
Tetraethylene glycol (**4**)	HOD	1.1	2.7	3.9
	H_a	0.1	0.1	-0.1
	H_b	0.1	0.4	1.4
	$H_{interior}$	0.4	0.9	0.9
PEG 8000 (**5**)	HOD	1.2	2.6	3.7
	$H_{interior}$	-0.3	-0.3	0.1
18-crown-6 (**7**)	HOD	1.6	1.8	2.3
	H_a	0.2	3.1	6.0

Methyl ester hydrochloride amino acid analogues

Methyl ester hydrochlorides were introduced as a way to work around the water insolubility of indole, allowing for higher concentration ratios of glycols and aromatic compounds to be achieved. L-alanine methyl ester hydrochloride is used as a non-aromatic

standard to ensure that interactions with the additional functionalities of the amino acids do not interfere with the aromatic interactions. This is confirmed to be true by the lack of significant upfield shifting of glycol protons when in solution with L-alanine methyl ester hydrochloride.

Table 4. Changes in ^{1}H NMR chemical shifts (in ppb) of PEG 8000 and related compounds in increasing concentrations of **13**.

PEG-related compound	*Hydrogen*	4 mM	7.5 mM	10 mM	40 mM	80 mM
Ethylene glycol (**1**)	HOD	1.7	4	4.6	—	—
	H_a	1.2	3.3	2.8	—	—
Tetraethylene glycol (**4**)	HOD	3.1	3.2	4.3	13.7	25
	H_a	0.6	1.2	2.7	7.6	14
	H_b	0.9	1.5	1.9	4.3	6.5
	$H_{interior}$	0.4	0.5	0.8	0.9	-0.6
PEG 8000 (**5**)	HOD	3.3	2.3	2.8	12.7	23.5
	$H_{interior}$	0.8	0.3	-0.6	-1.4	-3.2
18-crown-6 (**7**)	HOD	0.8	4.1	4.4	13.1	23.8
	H_a	-1.3	-0.4	-1.2	-5.1	-12.8

As suspected, the aromatic amino acid L-tryptophan methyl ester hydrochloride indeed showed upfield shifting of the interior hydrogens more clearly than the low concentrations of indole. If the π system is truly responsible for binding, then indole and L-tryptophan methyl ester would result in the highest upfield shifts due to their enhanced aromaticity. This is seen to be true for 18-crown-6 (Figure 9), but for PEG 8000 and tetraethylene glycol, phenol upfield shift exceeds that of L-tryptophan methyl ester (Figure 7, Figure 8). L-alanine methyl ester was used

as a control non-aromatic methyl ester amino acid, and the results suggest no upfield shifting patterns resembling that of the aromatic compounds (Table 3).

Table 5. Changes in ^{1}H NMR chemical shifts (in ppb) of PEG 8000 and related compounds in increasing concentrations of **12**.

PEG-related compound	*Hydrogen*	4 mM	40 mM	80 mM
Ethylene glycol (**1**)	HOD	1.0	7.3	11.1
	H_a	0.3	5.4	8.9
Tetraethylene glycol (**4**)	HOD	0.4	4.9	9.8
	H_a	0.7	4.8	7.6
	H_b	0.5	3.3	6.0
	$H_{interior}$	0.7	3.0	4.5
PEG 8000 (**5**)	HOD	0.9	4.2	4.0
	$H_{interior}$	0.9	2.4	4.1
18-crown-6 (**7**)	HOD	1.8	5.2	9.6
	H_a	-0.3	1.9	2.6

L-tyrosine methyl ester intriguingly follows a similar pattern in which shift change decreases from exterior to interior hydrogens, but these values of shift change still all remain downfield (Table 5). This is in line with what is discussed at the beginning of this section, in which the reference frame shifts downfield while specific participating hydrogens shift upfield, still resulting in a net shift downfield. This convolution makes the L-tyrosine methyl ester data more difficult to expand to general trends.

Table 6. Changes in ^{1}H NMR chemical shifts of PEG 8000 and related compounds in increasing concentrations of **14**.

Glycol-related compound	*Hydrogen*	4 mM	40 mM	80 mM
Ethylene glycol (**1**)	HOD	1.2	11.5	24.1
	H_a	1.0	8.0	18.7
Tetraethylene glycol (**4**)	HOD	1.2	11.9	22.7
	H_a	0.9	7.0	13.7
	H_b	0.6	5.2	10.0
	$H_{interior}$	0.4	3.8	7.6
PEG 8000 (**5**)	HOD	0.2	9.7	9.4
	$H_{interior}$	-1.2	0.4	0.9
18-crown-6 (**7**)	HOD	0.4	10.4	20.4
	H_a	0.6	1.7	3.5

Table 7. Changes in ^{1}H NMR chemical shifts of PEG 8000 and related compounds in increasing concentrations of **15**.

Glycol-related compound	*Hydrogen*	4 mM	40 mM	80 mM
Ethylene glycol (**1**)	HOD	0.8	9.5	19.6
	H_a	0.1	6.5	13.7
Tetraethylene glycol (**4**)	HOD	1.0	8.8	19.1
	H_a	0.6	3.7	10.0
	H_b	0.3	2.6	6.2
	$H_{interior}$	0.3	1.4	3.6
PEG 8000 (**5**)	HOD	0.9	9.0	16.5
	$H_{interior}$	0.2	-0.3	-0.8
18-crown-6 (**7**)	HOD	1.9	8.3	17.3
	H_a	0.6	-0.2	0.2

Electron-deficient phenols

4-nitrophenol and 3-cyanophenol titrations were carried out in order to determine how much electron density in the π system affects the binding interaction. It is predicted that the cyano group would be less electron-withdrawing than the nitro group, and this is reflected in the data. 4-nitrophenol and 3-cyanophenol both show a diminished upfield shift of interior hydrogens, but still follow the pattern of shift changes between exterior and interior hydrogens seen in previous titrations (Table 7). 4-nitrophenol, with a stronger electron-withdrawing group, shows less upfield shifting than 3-cyanophenol, both of which are weaker than the upfield shifting in phenol (Figure 7, Figure 8, Figure 9)). These patterns suggest that electron density is the primary effector of upfield shifting in the polyethylene glycol interior hydrogens.

Comparison of chemical shift changes across all aromatic compounds

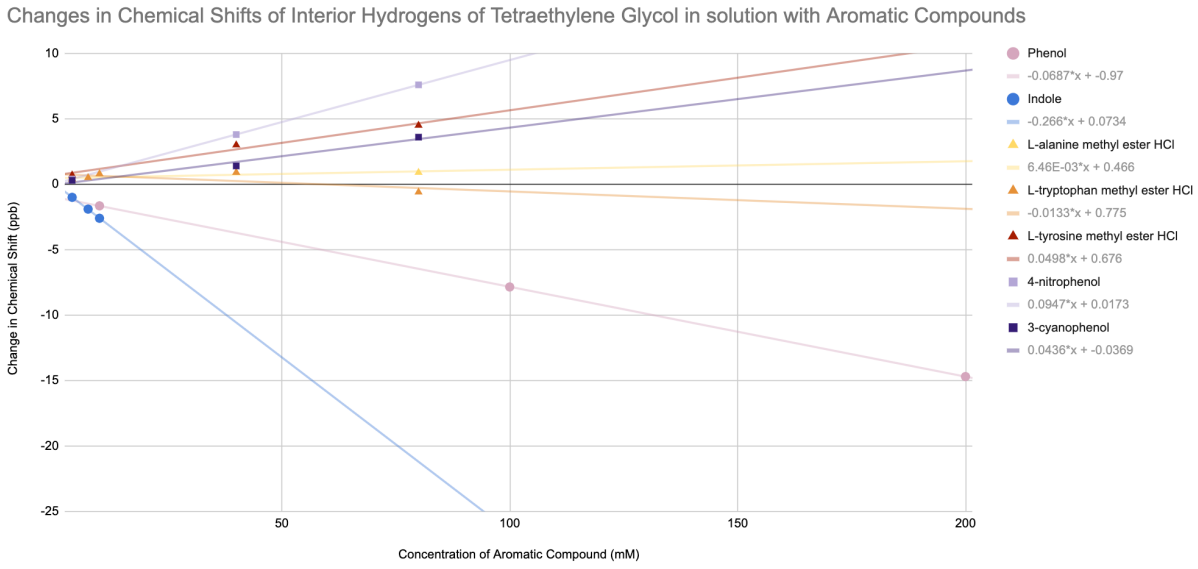

Figure 7: Changes in Chemical Shift of Tetraethylene Glycol (**4**) Interior Hydrogens in Various Aromatic Compound Concentrations. Refers to data in Tables 1-8.

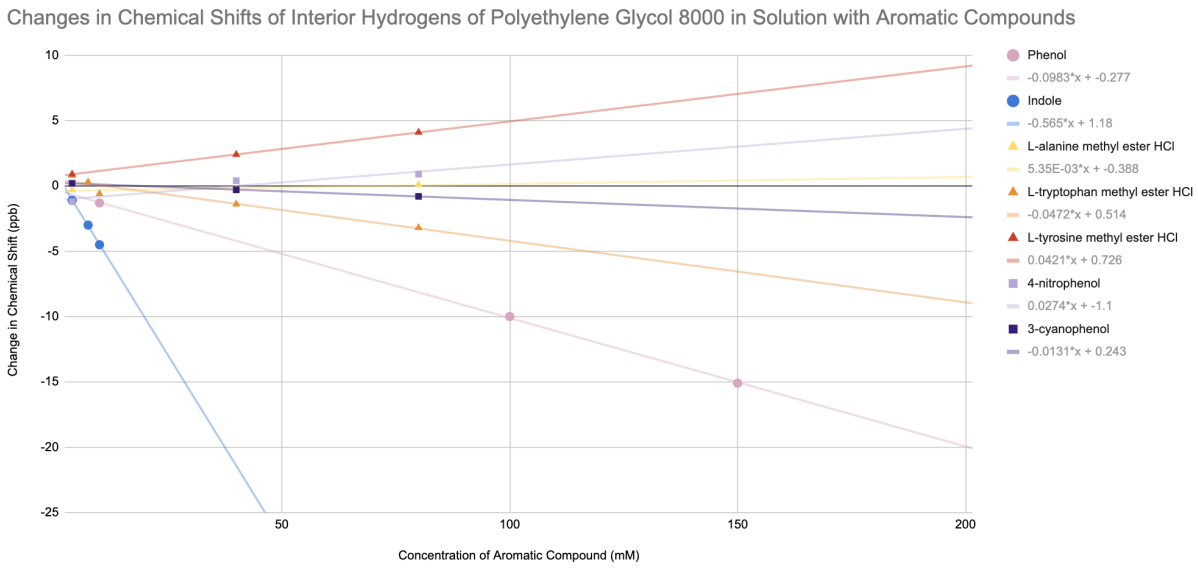

Figure 8: Changes in Chemical Shift of Polyethylene Glycol 8000 (**5**) Interior Hydrogens in Various Aromatic Compound Concentrations. Refers to data in Tables 1-8.

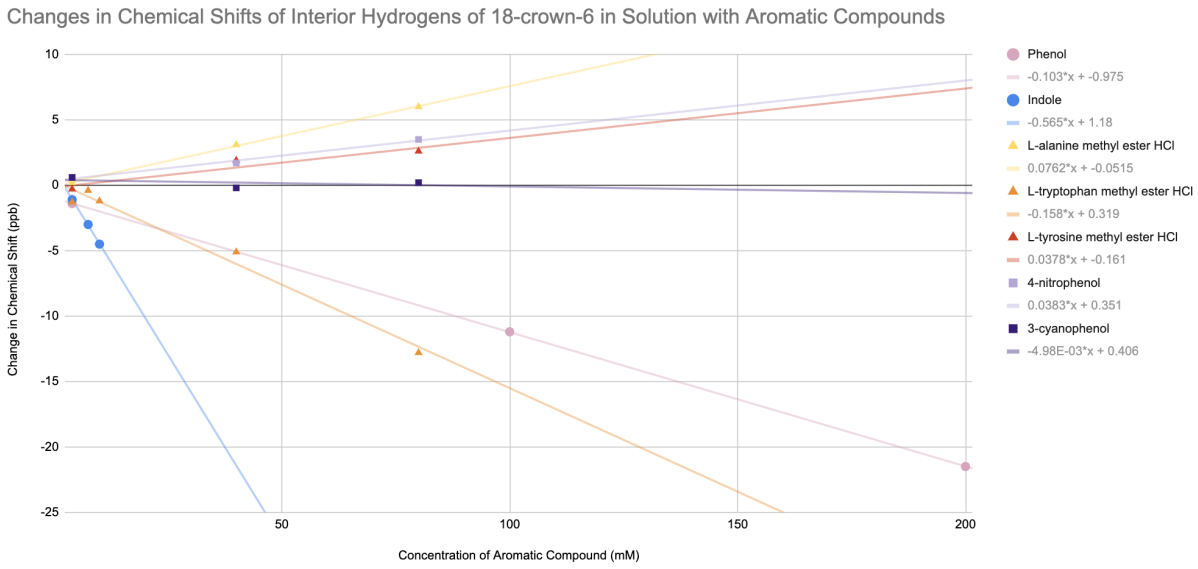

Figure 9: Changes in Chemical Shift of 18-crown-6 (**7**) Interior Hydrogens in Various Aromatic Compound Concentrations. Refers to data in Tables 1-8.

Trendlines in Figures 7, 8, and 9 show a highly linear relationship between aromatic compound concentrations and chemical shift changes. The nature of this mathematically is not

yet known and demands further investigation. Trendlines with negative slope can be grouped as definitive CH-π interactions, whereas positive trendlines require consideration of confounding hydrogen-bonding factors.

Table 8. 2D DOSY NMR Diffusion Constants for indole and acetone in D_2O, with (4 mM) and without (0 mM) PEG 8000. Indole diffusion constant ratios are colored in comparison to the acetone diffusion constant ratio.

Compound	*Hydrogen*	*Peak, ppm*	$D_{0\ mM\ PEG\ 8000}$	$D_{4\ mM\ PEG\ 8000}$	$D_{0\ mM\ PEG\ 8000}/D_{4\ mM\ PEG\ 8000}$
Indole	a	7.654	7.78E-10	6.47E-10	1.2
	b	7.489	7.24E-10	6.47E-10	1.12
	c	7.338	6.83E-10	6.58E-10	1.04
	d	7.182	7.23E-10	6.63E-10	1.09
	e	7.089	7.15E-10	6.69E-10	1.07
	f	6.53	7.55E-10	6.65E-10	1.14
PEG 8000	interior	3.637	N/A	4.90E-11	N/A
Acetone	a	2.159	9.64E-10	9.37E-10	**1.03**
HOD	HOD	4.709	1.68E-09	1.64E-09	1.02

Characterization of PEG-π Binding Strength

Due to the chain length and hydrophilicity of PEG 8000, addition of PEG 8000 to D_2O solutions results in a change in viscosity. This change in viscosity causes a change in the diffusion constant of HOD, which is typically used as the internal standard for comparison. To remedy this, acetone was introduced as a new internal standard after showing no changes in PEG 8000 or indole chemical shifts with ^1H NMR when mixed. The diffusion constant of acetone should only change with viscosity, as it should not bind indole or PEG sufficiently. Using the Stokes-Einstein equation for diffusion constant approximation:

$$D = \frac{k_b T}{6\pi\mu r}$$

where k_b is the Boltzmann constant, T is the temperature of the solution, μ is the solvent viscosity, and r is the solute hydrodynamic radius, an equation relating the diffusion constant (*D*) of acetone in solution with and without PEG to the viscosity of water (μ) with and without PEG can then be derived:

$$\frac{D_{acetone\ (no\ PEG)}}{D_{acetone\ (PEG)}} = \frac{\mu_{D2O\ (PEG)}}{\mu_{D2O\ (no\ PEG)}}$$

Due to the change in viscosity, a decrease in D_{indole} when in solution with PEG 8000 cannot be assumed to be due to binding. Instead, to demonstrate binding, the ratios of diffusion constants are used. If solely D_{indole} is changing solely because of the viscosity change, then the ratio of acetone diffusion constants and the ratio of indole diffusion constants will be the same. However, if binding is indeed happening, the following relationship would be observed:

$$\frac{D_{acetone\ (no\ PEG)}}{D_{acetone\ (PEG)}} < \frac{D_{indole\ (no\ PEG)}}{D_{indole\ (PEG)}}$$

Indeed, this difference in diffusion constants was seen for all of the indole hydrogens (Table 8), indicating that PEG 8000 and indole do bind to a significant degree.

CONCLUSIONS

From the data, it can be seen that PEG exhibits detectable CH-π binding interactions with a variety of aromatic compounds. The upfield shifting seen in the ^{1}H NMR data resembles that of confirmed carbohydrate-aromatic binding in previous publications, resembling their recorded magnitudes as well - typical shift perturbations for a 1:1 ratio of aromatic compound and carbohydrate were observed to be on a scale of around 5-6 ppb, as can be seen in Figure 5, whereas shifts around 5 ppb were observed here with a 10:1 ratio of aromatic compound and glycol. Even at 10:1, some chemical shift changes were in the 10-12 ppb range (Table 1). The chain length of the PEG seems to have had an effect as well, though it is not yet seen whether or not this is due to an increased number of available contact points skewing the average proton shift or due to length of the chain somehow enhancing the mechanism, though the former is more likely.

Crown ethers exhibited even stronger binding interactions with the same set of aromatic compounds. As we have seen, this is notable since PEG assumes a crown ether-like conformation when bound by anti-PEG antibodies (Lee et al., 2020). This would suggest that the crown ether stereochemistry is highly optimal for CH-π aromatic binding, considering the crown ether RO-C-C-OR bond is confined to the gauche conformation.

The electron density of the aromatic ring was additionally shown to affect the degree of interaction between PEG and the aromatic compounds. Use of electron-deficient phenols correlated with a loss of interaction proportional to the strength of the electron-withdrawing groups used (Table 6 and 7). This observation aligns with properties of the CH-π interactions determined in the carbohydrate studies (Vandenbussche et al., 2008), suggesting that the same mechanisms might be responsible.

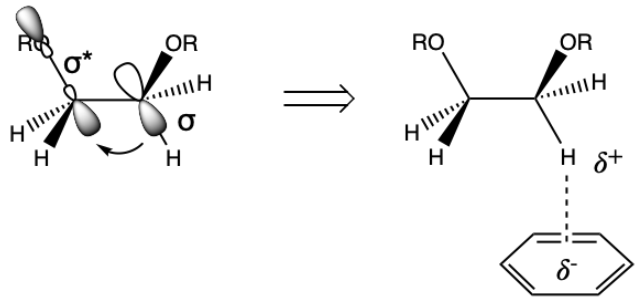

Figure 10. A proposed hyperconjugation explanation of the PEG-π interaction. This has not been completely verified by data in this report, but stands to inspire further computational modeling experiments.

Extending this model to PEG is not outside the scope of reason, as the gauche oxygen effect is already understood for ethylene glycol and is rationalized by hyperconjugation as we mentioned previously (Alabugin et al., 2011). Combined with the data suggesting the importance of the gauche RO-C-C-OR conformation to the PEG-π interaction, and that the electron density of the aromatic ring similarly impacts the interaction, it is possible hyperconjugation plays a new important role in CH-π interactions.

In order to flesh out this model, computational modeling would contribute massively. The most advisable next step for this research would be to supplement experimental data with atomic simulation calculations. Construction of a diffusion-inclusive DFT computational model from a combination of previous literature with experimental data would allow for a freer venue of experimentation. Furthermore, an adjacent performance of conformational studies with these combinations of PEG-relatives and aromatic compounds would drastically improve upon rationalizing a model for these interactions.

Based on the gauche oxygen effect and previous XH-π studies, a preliminary hypothesis for the contribution of hyperconjugation to the PEG-π reaction can be generated, as seen in

Figure 10. Further DOSY experiments would be of additional help to create a robust proof of the interaction.

These findings demonstrate the clear existence of a novel polyethylene glycol CH-π interaction, something that seems to have been hiding in the corners of the literature but was not yet experimentally demonstrated. Though the grander intentions of this work were to specify the mechanisms of PEG immunogenicity, these findings in their preliminary nature open up a massive door to potential avenues of exploration. Beyond the notion resulting from these findings that there may be *far more* CH-π interactions out there, hiding from our view and understanding, preliminary identification of the PEG CH-π interaction creates a new set of potential investigations, similar to the sugar CH-π interactions that were discussed at the beginning of this work. The polyethylene glycol CH-π interaction is highly specific to its class of PEG-related compounds, allowing for it to potentially inform future selection and development of non-immunogenic PEG alternatives. Expansions on this work could puncture a massive hole in our current understanding of CH-π interactions, doing the justice deserved for a still-developing field of intermolecular interactions with widespread chemical, physical, and biological potential.

MATERIALS AND METHODS

All compounds were purchased from chemical suppliers and used as received. All NMR experiments were performed with samples in Wilmad WG-1241 600 MHz NMR tubes. Peak assignments were decided based on knowledge of structures as well as spectral data from the SDBS database (SDBS). Spectra were calibrated manually by assigning the DSS peak to 0 ppm.

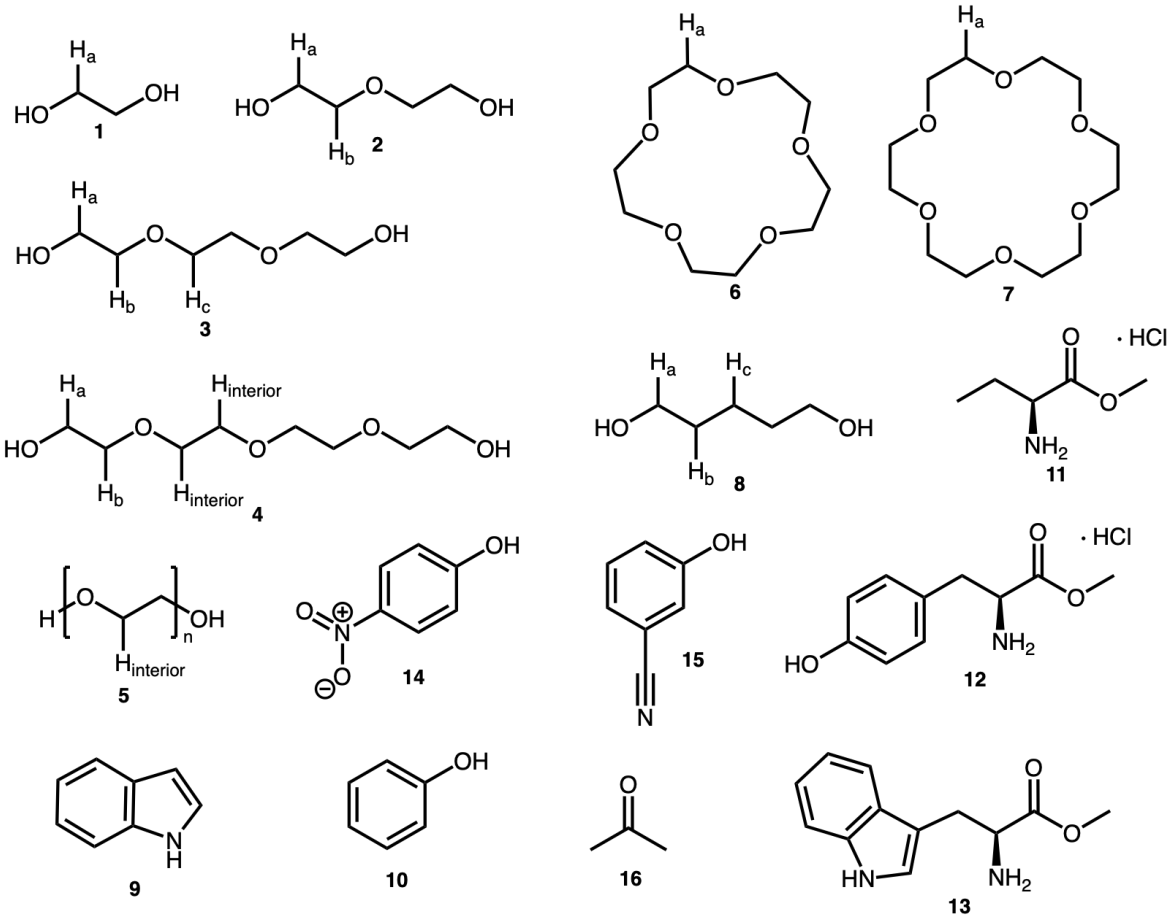

Figure 11: Compounds used in experiments. Hydrogens labeled H_x refer to unique ^{1}H NMR proton environments. Symmetrical hydrogens with identical environments are not labeled. Hydrogens labeled $H_{interior}$ refer to hydrogens with technically distinct environments that are not distinguishable in 600 MHz H^{1}NMR. Names of compounds used: ethylene glycol (**1**), diethylene glycol (**2**), triethylene glycol (**3**), tetraethylene glycol (**4**), polyethylene glycol (**5**), 15-crown-5 (**6**), 18-crown-6 (**7**), 1,5-pentanediol (**8**), indole (**9**), phenol (**10**), L-alanine methyl ester hydrochloride (**11**), L-tyrosine methyl ester hydrochloride (**12**), L-tryptophan methyl ester hydrochloride (**13**), 4-nitrophenol (**14**), 3-cyanophenol (**15**), acetone (**16**). For all uses of **5** in this report, the specific type of PEG is PEG 8000. H_a of PEG 8000 is not labeled here, as it is almost always indistinguishable in the ^{1}H NMR spectra.

Phenol ^{1}H NMR Titrations

Phenol D_2O stock solution was prepared by dissolving a weighed amount of phenol (**10**) in D_2O. A second phenol stock solution of the same concentration was additionally prepared a week later, due to suspicion that the first stock solution had partially oxidized to p-benzoquinone, turning the stock solution from colorless to light pink. This was not verified by NMR, but NMR samples made before stock turned pink do not show contaminant peaks. Phenol titrations were completed with compounds **1**, **2**, **3**, **4**, **5**, **6**, **7**, and **8**. All glycols were dissolved in D_2O to create stock solutions of known concentration for use in sample preparation. 2,2-Dimethyl-2-silapentane-5-sulfonate (DSS) was included as an internal standard for NMR samples, prepared as a separate D_2O stock solution for addition to samples.

Titrations were completed by preparing four NMR samples for each glycol with a set glycol concentration (10 mM) and increasing phenol concentrations (0 mM, 10 mM, 100 mM, 200 mM). Samples were prepared by delivering the necessary amounts of glycol stock solution, phenol stock solution, DSS stock solution, and additional D_2O to an Eppendorf tube via micropipette. Eppendorf tube samples were then transferred to 600 MHz NMR tubes via Pasteur pipette. Samples were prepared in Eppendorf tubes instead of NMR tubes due to the viscosity of many stock solutions, which prohibited proper mixing in the NMR tube. The NMR tubes were then individually mixed for several seconds on a Fisher Vortex Genie 2 to ensure a homogeneous sample was obtained.

An ^{1}H NMR spectrum was then obtained for each sample using the 600 MHz NMR spectrometer. The resulting spectra were calibrated using the DSS internal standard peak and autophased. The peaks of each spectrum were recorded, and the integrations were calculated to assist in assigning peaks to protons. The chemical shifts of all glycol protons were recorded for

each concentration of phenol, and the changes in chemical shift at increasing phenol concentrations were then calculated using the equation described in the Results and Discussion section. The resulting changes in chemical shifts are tabulated in the Results and Discussion section.

For diethylene glycol (**2**), triethylene glycol (**3**), tetraethylene glycol (**4**), and polyethylene glycol 8000 (**5**), two titrations were performed. Sample preparation details are in *LabArchives: Experimental Notebook/Sample Preparation/Sample Contents and Shifts.* Resulting NMR spectra are included in the appendix. An example figure of titration spectral data is included in Figure 12.

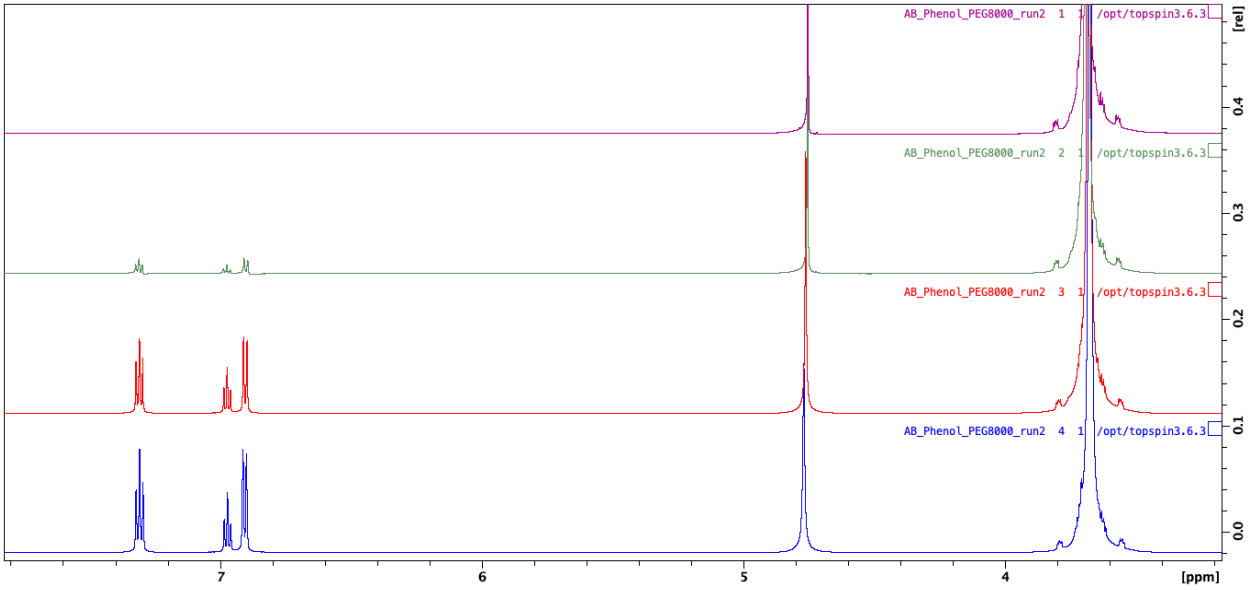

Figure 12: ^{1}H NMR spectra of PEG 8000 (**5**) at increasing concentrations of phenol (**10**). From top to bottom: (a) 10 mM PEG 8000, 20 uM DSS, in D_2O; (b) 10 mM PEG 8000, 10 mM phenol, 20 uM DSS, in D_2O; (c) 10 mM PEG 8000, 20 mM phenol, 20 uM DSS, in D_2O; (d) 10 mM PEG 8000, 200 mM phenol, 20 uM DSS, in D_2O. [*Peak assignments (from left to right): triplet, H_{phenol}; triplet, H_{phenol}; doublet, H_{phenol}; singlet, HOD; singlet, $H_{interior}$ (PEG 8000); triplet (hard to make out), H_b (PEG 8000)] LabArchives: Experimental Notebook/Phenol Titrations Raw Data*

Indole ^{1}H NMR Titrations

Indole (**9**) was purified the day of use by sublimation. Sublimed indole was recollected, weighed, and used to prepare an indole D_2O stock solution for use only that day, as indole oxidizes when exposed to air for too long, even in solution. Indole titrations were carried out with the glycols **1**, **4**, and **5**. All glycols were dissolved in D_2O to create stock solutions of known concentration for use in sample preparation. 2,2-Dimethyl-2-silapentane-5-sulfonate (DSS) was included as an internal standard for NMR samples, prepared as a separate D_2O stock solution for addition to samples.

Titrations were completed by preparing four NMR samples for each glycol with a set glycol concentration (10 mM) and increasing indole concentrations (0 mM, 4 mM, 7.5 mM, 10 mM). Lower concentrations than the phenol titrations were used due to the significantly less water-soluble nature of indole. Samples were prepared by delivering the necessary amounts of glycol stock solution, indole stock solution, DSS stock solution, and additional D_2O to an Eppendorf tube via micropipette. Eppendorf tube samples were then transferred to 600 MHz NMR tubes via Pasteur pipette. The NMR tubes were then individually mixed for several seconds on a Fisher Vortex Genie 2 to ensure a homogeneous sample was obtained.

An ^{1}H NMR spectrum was then obtained for each sample using the 600 MHz NMR spectrometer. The resulting spectra were calibrated using the DSS internal standard peak and autophased. The peaks of each spectrum were recorded and the integrations were calculated to assist in assigning peaks to protons. The chemical shifts of all glycol protons were recorded for each concentration of indole, and the changes in chemical shift at increasing indole concentrations were then calculated using the equation described in the Results and Discussion section. The resulting changes in chemical shifts are tabulated in the Results and Discussion

section. Sample preparation details are in *LabArchives: Experimental Notebook/Sample Preparation/Sample Contents and Shifts.* Resulting NMR spectra are included in the appendix.

L-Alanine Methyl Ester Hydrochloride ^{1}H NMR Titrations.

L-alanine methyl ester hydrochloride (**11**) D_2O stock solution was prepared using a weighed amount of L-alanine methyl ester hydrochloride. L-alanine methyl ester hydrochloride was used as a non-aromatic standard to determine if glycol binding to the amino acid methyl esters was due to a non-aromatic group.

L-alanine methyl ester hydrochloride titrations were completed with the glycols **4**, **5**, and **7**. Titration with **1** was performed at a later date. All glycols were dissolved in D_2O to create stock solutions of known concentration for use in sample preparation. 2,2-Dimethyl-2-silapentane-5-sulfonate (DSS) was included as an internal standard for NMR samples, prepared as a separate D_2O stock solution for addition to samples.

Titrations were completed by preparing four NMR samples for each glycol with a set glycol concentration (4 mM) and increasing L-alanine methyl ester hydrochloride concentrations (0 mM, 4 mM, 40 mM, 80 mM). Samples were prepared by delivering the necessary amounts of glycol stock solution, L-alanine methyl ester hydrochloride stock solution, DSS stock solution, and additional D_2O to an Eppendorf tube via micropipette. Eppendorf tube samples were then transferred to 600 MHz NMR tubes via Pasteur pipette. Samples were prepared in Eppendorf tubes instead of NMR tubes due to the viscosity of many stock solutions, which prohibited proper mixing in the NMR tube. The NMR tubes were then individually mixed for several seconds on a Fisher Vortex Genie 2 to ensure a homogeneous sample was obtained.

An ^{1}H NMR spectrum was then obtained for each sample using the 600 MHz NMR spectrometer. The resulting spectra were calibrated using the DSS internal standard peak and autophased. The peaks of each spectrum were recorded and the integrations were calculated to assist in assigning peaks to protons. The chemical shifts of all glycol protons were recorded for each concentration of L-alanine methyl ester hydrochloride, and the changes in chemical shift at increasing L-alanine methyl ester hydrochloride concentrations were then calculated using the equation described in the Results and Discussion section. The resulting changes in chemical shifts are tabulated in the Results and Discussion section. Sample preparation details are in *LabArchives: Experimental Notebook/Sample Preparation/Sample Contents and Shifts.*

L-Tryptophan Methyl Ester Hydrochloride ^{1}H NMR Titrations.

L-tryptophan methyl ester hydrochloride (**13**) D_2O stock solution was prepared using a weighed amount of L-tryptophan methyl ester hydrochloride. L-tryptophan methyl ester hydrochloride titrations were completed with glycols **1**, **4**, **5**, and **7**. All glycols were dissolved in D_2O to create stock solutions of known concentration for use in sample preparation. 2,2-Dimethyl-2-silapentane-5-sulfonate (DSS) was included as an internal standard for NMR samples, prepared as a separate D_2O stock solution for addition to samples.

Titrations were completed by preparing four NMR samples for each glycol with a set glycol concentration (4 mM) and increasing L-tryptophan methyl ester hydrochloride concentrations (0 mM, 4 mM, 40 mM, 80 mM). A set of titrations was first completed with lower L-tryptophan methyl ester hydrochloride concentrations (0 mM, 4 mM, 7.5 mM, 10 mM), but this was revised to higher concentrations in order to increase the scale of chemical shift changes. Samples were prepared by delivering the necessary amounts of glycol stock solution,

L-tryptophan methyl ester hydrochloride stock solution, DSS stock solution, and additional D_2O to an Eppendorf tube via micropipette. Eppendorf tube samples were then transferred to 600 MHz NMR tubes via Pasteur pipette. The NMR tubes were then individually mixed for several seconds on a Fisher Vortex Genie 2 to ensure a homogeneous sample was obtained.

An ^1H NMR spectrum was then obtained for each sample using the 600 MHz NMR spectrometer. The resulting spectra were calibrated using the DSS internal standard peak and autophased. The peaks of each spectrum were recorded and the integrations were calculated to assist in assigning peaks to protons. The chemical shifts of all glycol protons were recorded for each concentration of L-tryptophan methyl ester hydrochloride, and the changes in chemical shift at increasing L-tryptophan methyl ester hydrochloride concentrations were then calculated using the equation described in the Results and Discussion section. The resulting changes in chemical shifts are tabulated in the Results and Discussion section. Sample preparation details are in *LabArchives: Experimental Notebook/Sample Preparation/Sample Contents and Shifts.* Resulting NMR spectra are included in the appendix.

L-tyrosine Methyl Ester Hydrochloride ^1H NMR Titrations.

L-tyrosine methyl ester hydrochloride (**12**) D_2O stock solution was prepared using a weighed amount of L-tyrosine methyl ester hydrochloride. L-tyrosine methyl ester hydrochloride titrations were completed with glycols **1**, **4**, **5**, and **7**. All glycols were dissolved in D_2O to create stock solutions of known concentration for use in sample preparation. 2,2-Dimethyl-2-silapentane-5-sulfonate (DSS) was included as an internal standard for NMR samples, prepared as a separate D_2O stock solution for addition to samples.

Titrations were completed by preparing four NMR samples for each glycol with a set glycol concentration (4 mM) and increasing L-tyrosine methyl ester hydrochloride concentrations (0 mM, 4 mM, 40 mM, 80 mM). Samples were prepared by delivering the necessary amounts of glycol stock solution, L-tyrosine methyl ester hydrochloride stock solution, DSS stock solution, and additional D_2O to an Eppendorf tube via micropipette. Eppendorf tube samples were then transferred to 600 MHz NMR tubes via Pasteur pipette. The NMR tubes were then individually mixed for several seconds on a Fisher Vortex Genie 2 to ensure a homogeneous sample was obtained.

An ^1H NMR spectrum was then obtained for each sample using the 600 MHz NMR spectrometer. The resulting spectra were calibrated using the DSS internal standard peak and autophased. The peaks of each spectrum were recorded and the integrations were calculated to assist in assigning peaks to protons. The chemical shifts of all glycol protons were recorded for each concentration of L-tyrosine methyl ester hydrochloride, and the changes in chemical shift at increasing L-tyrosine methyl ester hydrochloride concentrations were then calculated using the equation described in the Results and Discussion section. The resulting changes in chemical shifts are tabulated in the Results and Discussion section. Sample preparation details are in *LabArchives: Experimental Notebook/Sample Preparation/Sample Contents and Shifts.* Resulting NMR spectra are included in the appendix.

4-nitrophenol ^1H NMR Titrations

4-nitrophenol (**14**) D_2O stock solution was prepared using a weighed amount of 4-nitrophenol dissolved in D_2O. 4-nitrophenol titrations were completed with glycols **1**, **4**, **5**, and **7**. All glycols were dissolved in D_2O to create stock solutions of known concentration for use in

sample preparation. 2,2-Dimethyl-2-silapentane-5-sulfonate (DSS) was included as an internal standard for NMR samples, prepared as a separate D_2O stock solution for addition to samples.

Titrations were completed by preparing four NMR samples for each glycol with a set glycol concentration (4 mM) and increasing 4-nitrophenol concentrations (0 mM, 4 mM, 40 mM, 80 mM). Samples were prepared by delivering the necessary amounts of glycol stock solution, 4-nitrophenol stock solution, DSS stock solution, and additional D_2O to an Eppendorf tube via micropipette. Eppendorf tube samples were then transferred to 600 MHz NMR tubes via Pasteur pipette. The NMR tubes were then individually mixed for several seconds on a Fisher Vortex Genie 2 to ensure a homogeneous sample was obtained.

An ^1H NMR spectrum was then obtained for each sample using the 600 MHz NMR spectrometer. The resulting spectra were calibrated using the DSS internal standard peak and autophased. The peaks of each spectrum were recorded and the integrations were calculated to assist in assigning peaks to protons. The chemical shifts of all glycol protons were recorded for each concentration of 4-nitrophenol, and the changes in chemical shift at increasing 4-nitrophenol concentrations were then calculated using the equation described in the Results and Discussion section. The resulting changes in chemical shifts are tabulated in the Results and Discussion section. Sample preparation details are in *LabArchives: Experimental Notebook/Sample Preparation/Sample Contents and Shifts.* Resulting NMR spectra are included in the appendix.

3-cyanophenol ^1H NMR Titrations

3-cyanophenol (**15**) D_2O stock solution was prepared using a weighed amount of 3-cyanophenol dissolved in D_2O. 3-cyanophenol titrations were completed with glycols **1**, **4**, **5**,

and **7**. All glycols were dissolved in D_2O to create stock solutions of known concentration for use in sample preparation. 2,2-Dimethyl-2-silapentane-5-sulfonate (DSS) was included as an internal standard for NMR samples, prepared as a separate D_2O stock solution for addition to samples.

Titrations were completed by preparing four NMR samples for each glycol with a set glycol concentration (4 mM) and increasing 3-cyanophenol concentrations (0 mM, 4 mM, 40 mM, 80 mM). Samples were prepared by delivering the necessary amounts of glycol stock solution, 3-cyanophenol stock solution, DSS stock solution, and additional D_2O to an Eppendorf tube via micropipette. Eppendorf tube samples were then transferred to 600 MHz NMR tubes via Pasteur pipette. The NMR tubes were then individually mixed for several seconds on a Fisher Vortex Genie 2 to ensure a homogeneous sample was obtained.

An ^1H NMR spectrum was then obtained for each sample using the 600 MHz NMR spectrometer. The resulting spectra were calibrated using the DSS internal standard peak and autophased. The peaks of each spectrum were recorded and the integrations were calculated to assist in assigning peaks to protons. The chemical shifts of all glycol protons were recorded for each concentration of 3-cyanophenol, and the changes in chemical shift at increasing 3-cyanophenol concentrations were then calculated using the equation described in the Results and Discussion section. The resulting changes in chemical shifts are tabulated in the Results and Discussion section. Sample preparation details are in *LabArchives: Experimental Notebook/Sample Preparation/Sample Contents and Shifts.* Resulting NMR spectra are included in the appendix.

Indole/PEG 8000 DOSY

Indole (**9**) was purified the day of use by sublimation. Sublimed indole was recollected, weighed, and used to prepare an indole D_2O stock solution for use only that day, as indole oxidizes when exposed to air for too long, even in solution. PEG 8000 (**5**) D_2O stock solution and acetone (**16**) D_2O stock solution were also prepared for sample creation. Acetone stock was prepared directly before addition to samples in order to minimize evaporation. 2,2-Dimethyl-2-silapentane-5-sulfonate (DSS) was included as an internal standard for NMR samples, prepared as a separate D_2O stock solution for addition to samples.

The DOSY experiments were completed by preparing two NMR samples, one with PEG 8000 (4 mM indole, 4 mM PEG 8000, 4 mM acetone), and one without PEG 8000 (4 mM indole, 4 mM acetone). Acetone is included in both samples in order to provide an internal standard for comparison, as PEG 8000 changes the viscosity of the solution. Samples were prepared by delivering the necessary amounts of PEG 8000 stock solution, indole stock solution, acetone stock solution, DSS stock solution, and additional D_2O to an Eppendorf tube via micropipette. Eppendorf tube samples were then transferred to 600 MHz NMR tubes via Pasteur pipette. The NMR tubes were then individually mixed for several seconds on a Fisher Vortex Genie 2 to ensure a homogeneous sample was obtained.

A 2D DOSY experiment was then performed on each of the two samples. Using the diffusion curves for each peak in a sample, the diffusion coefficients of each proton were calculated using the Bruker NMR Topspin Software. DOSY parameters are included with the spectra. The resulting diffusion coefficients are tabulated in the Results and Discussion section. Sample preparation details are in *LabArchives: Experimental Notebook/Sample Preparation/Sample Contents and Shifts.* Resulting NMR spectra are included in the appendix.

REFERENCES

Alabugin, I. V.; Gilmore, K. M.; Peterson, P. W. Hyperconjugation. *WIREs Computational Molecular Science* **2011**, *1* (1), 109-141. https://doi.org/10.1002/wcms.6

Asensio, J. L.; Ardá, A.; Cañada, F. J.; Jiménez-Barbero, J. Carbohydrate–Aromatic Interactions. *Accounts of Chemical Research* **2012**, *46* (4), 946–954. https://doi.org/10.1021/ar300024d

Cox, F.; Khalib, K.; Conlon, N. PEG That Reaction: A Case Series of Allergy to Polyethylene Glycol. *The Journal of Clinical Pharmacology* **2021**, *61*, *6*, 832-835. https://doi.org/10.1002/jcph.1824

Engler, A. C.; Ke, X.; Gao, S.; Chan, J. M. W.; Coady, D. J.; Ono, R. J.; Lubbers, R.; Nelson, A.; Yang, Y. Y.; Hedrick, J. L. Hydrophilic Polycarbonates: Promising Degradable Alternatives to Poly(ethylene glycol)-Based Stealth Materials. *Macromolecules* **2015**, *48*, *6*, 1673-1678. https://doi.org/10.1021/acs.macromol.5b00156

Fernández-Alonso, M. del C.; Cañada, F. J.; Jiménez-Barbero, J.; Cuevas, G. Molecular Recognition of Saccharides by Proteins. Insights on the Origin of the Carbohydrate-Aromatic Interactions. *Journal of the American Chemical Society* **2005**, *127, 20,* 7379-7386.

Forbes, C. R.; Sinha, S. K.; Ganguly, H. K.; Bai, S.; Yap, G. P. A.; Patel, S.; Zondlo, N. J. Insights into Thiol-Aromatic Interactions: A Stereoelectronic Basis for S-H/π Interactions. *Journal of the American Chemical Society* **2017**, *139, 5*, 1842-1855. https://doi.org/10.1021/jacs.6b08415

Harris, J. M.; Chess, R. B. Effect of PEGylation on Pharmaceuticals. *Nature* **2003**, *2*, 214-221. https://doi.org/10.1038/nrd1033

Hudson, K. L.; Bartlett, G. J.; Diehl, R. C.; Agirre, J.; Gallagher, T.; Kiessling, L. L.; Woolfson, D. N. Carbohydrate-Aromatic Interactions in Proteins. *Journal of the American Chemical Society* **2015**, *137*, 15152-15160. https://doi.org/10.1021/jacs.5b08424

Hwang, J.; Li, P.; Smith, M. D.; Warden, C. E.; Sirianni, D. A.; Vik, E. C.; Maier, J. M.; Yehl, C. J.; Sherrill, C. D.; Shimizu, K. D. Tipping the Balance between S-π and O-π Interactions. *Journal of the American Chemical Society* **2018**, *140, 41,* 13301-13307. https://doi.org/10.1021/jacs.8b07617

Knowles, D. B.; Shkel, I. A.; Phan, N. M.; Sternke, M.; Lingeman, E.; Cheng, X.; Cheng, L.; O'Connor, K.; Record, M. T. Chemical Interactions of Polyethylene Glycols (PEGs) and Glycerol with Protein Functional Groups: Applications to Effects of PEG and Glycerol on Protein Processes. *Biochemistry* **2015**, *54, 22,* 3528-3542. https://doi.org/10.1021/acs.biochem.5b00246

Kozma, G. T.; Shimizu, T.; Ishida, T.; Szebeni, J. Anti-PEG antibodies: Properties, formation, testing and role in adverse immune reactions to pegylated nano-biopharmaceuticals. *Advanced Drug Delivery Reviews* **2020**, *154-155*, 163-175. https://doi.org/10.1016/j.addr.2020.07.024

Lee, C.-C..; Su, Y.-C.; Ko, T.-P.; Lin, L.-L.; Yang, C.-Y.; Chang, S. S.-C.; Roffler, S. R.; Wang, A. H.-J. Structural basis of polyethylene glycol recognition by antibody. *Journal of Biomedical Science* **2020**, *27*, *12*. https://doi.org/10.1186/s12929-019-0589-7

Li, P.; Vik, E. C.; Maier, J. M.; Karki, I.; Strickland, S. M. S.; Umana, J. M.; Smith, M. D.; Pellechia, P. J.; Shimizu, K. D. Electrostatically Driven CO-π Aromatic Interactions.

Journal of the American Chemical Society **2019**, *141*, 12513-12517. http://doi.org/10.1021/jacs.9b06363

Li, P.; Parker, T. M.; Hwang, J.; Deng, F.; Smith, M. D.; Pellechia, P. J.; Sherrill, C. D.; Shimizu, K. D. The CH-π Interactions of Methyl Ethers as a Model for Carbohydrate-*N*-Heteroarene Interactions. *Organic Letters* **2014***, 16, 19,* 5064-5067. https://doi.org/10.1021/ol502418k

Mohamed, M.; Abu Lila, A. S.; Shimizu, T.; Alaaeldin, E.; Hussein, A.; Sarhan, H. A.; Szebeni, J.; Ishida, T. PEGylated liposomes: immunological responses. *Science and Technology of Advanced Materials* **2019**, *20, 1,* 710-724. https://doi.org/10.1080/14686996.2019.1627174

Muzulu, J.; Basu, A. Detection of Ligand Binding to Glycopolymers Using Saturation Transfer Difference NMR. *Physical Chemistry Chemical Physics* **2021**, *23,* 21934-21940.

Phenol; Standard Operating Procedure. Retrieved from Yale University Environmental Health and Safety. **2022**. https://ehs.yale.edu/sites/default/files/files/phenol-sop.pdf

Sasaki, H.; Daicho, S.; Yamada, Y.; Nibu, Y. Comparable Strength of OH-O versus OH-π Hydrogen Bonds in Hydrogen-Bonded 2,3-Benzofuran Clusters with Water and Methanol. *The Journal of Physical Chemistry A* **2013**, *117, 15,* 3183-3189. https://doi.org/10.1021/jp400676x

SDBSWeb : https://sdbs.db.aist.go.jp (National Institute of Advanced Industrial Science and Technology)

Sellaturay, P.; Nasser, S.; Islam, S.; Gurugama, P.; Ewan, P. W. Polyethylene glycol (PEG) is a cause of anaphylaxis to the Pfizer/BioNTech mRNA COVID-19 vaccine. *Clinical & Experimental Allergy* **2021**, *51*, *6*, 861-863. https://doi.org/10.1111/cea.13874

Shiraishi, K.; Yokoyama, M. Toxicity and immunogenicity concerns related to PEGylated-micelle carrier systems: a review. *Science and Technology of Advanced Materials* **2019**, *20*, *1*, 324-336. https://doi.org/10.1080/14686996.2019.1590126

Wylon, K.; Dölle, S.; Worm, M. Polyethylene glycol as a cause of anaphylaxis. *Allergy, Asthma & Clinical Immunology* **2016**, *12* (67), 1-3. https://doi.org/10.1186/s13223-016-0172-7

Wenande, E. C.; Skov, P. S.; Mosbech, H.; Poulsen, L. K.; Garvey, L. H. Inhibition of polyethylene glycol-induced histamine release by monomeric ethylene and diethylene glycol: A case of probable polyethylene glycol allergy. *Journal of Allergy and Clinical Immunology* **2013**, *131, 5,* 1425-1427. https://doi.org/10.1016/j.jaci.2012.09.037

Vandenbussche, S.; Díaz, D.; Fernández-Alonso, M. C.; Pan, W.; Vincent, S. P.; Cuevas, G.; Cañada, F. J.; Jiménez-Barbero, J.; Bartik, K. Aromatic-Carbohydrate Interactions: An NMR and Computational Study of Model Systems. *Chem. Eur. J.* **2008**, *14*, 7570-7578. https://doi.org/10.1002/chem.200800247

APPENDIX

^{1}H NMR Spectra

Appendix 1a-h: ^{1}H NMR spectra of phenol titrations with various PEG-related compounds.

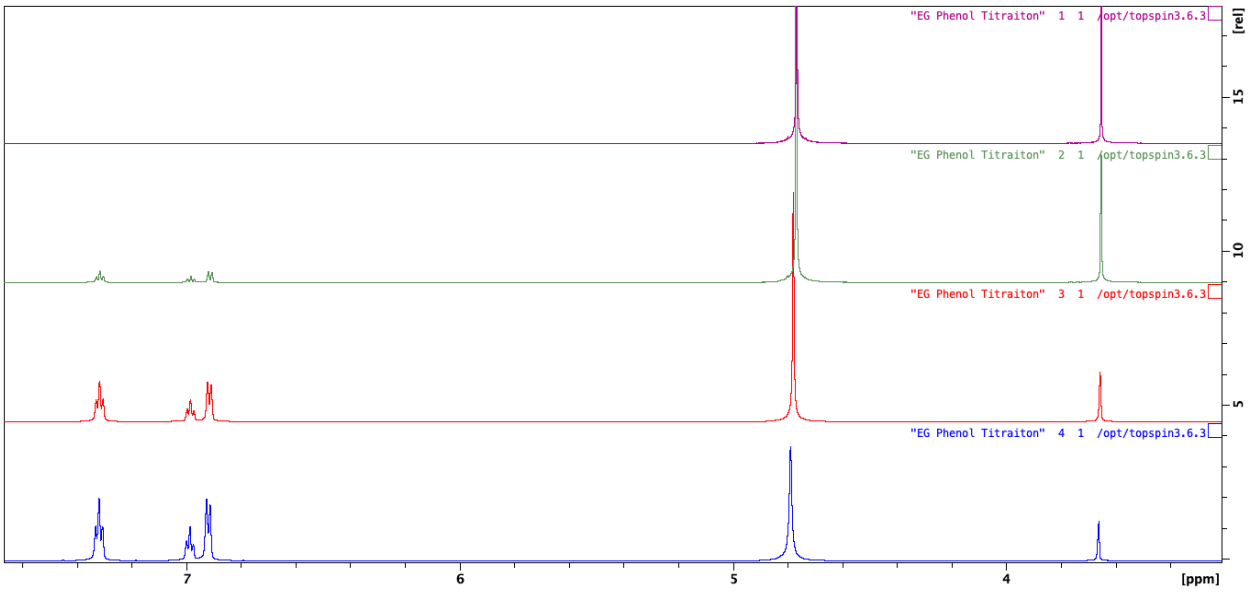

Appendix 1a: ^{1}H NMR spectra of ethylene glycol (**1**) at increasing concentrations of phenol (**10**). From top to bottom: (a) 10 mM ethylene glycol, 20 uM DSS, in D_2O; (b) 10 mM ethylene glycol, 10 mM phenol, 20 uM DSS, in D_2O; (c) 10 mM ethylene glycol, 20 mM phenol, 20 uM DSS, in D_2O; (d) 10 mM ethylene glycol, 200 mM phenol, 20 uM DSS, in D_2O. [*Peak assignments (from left to right): triplet: H_{phenol}, triplet: H_{phenol}, doublet: H_{phenol}, singlet: HOD, singlet: H_a (ethylene glycol)] LabArchives: Experimental Notebook/Phenol Titrations Raw Data.*

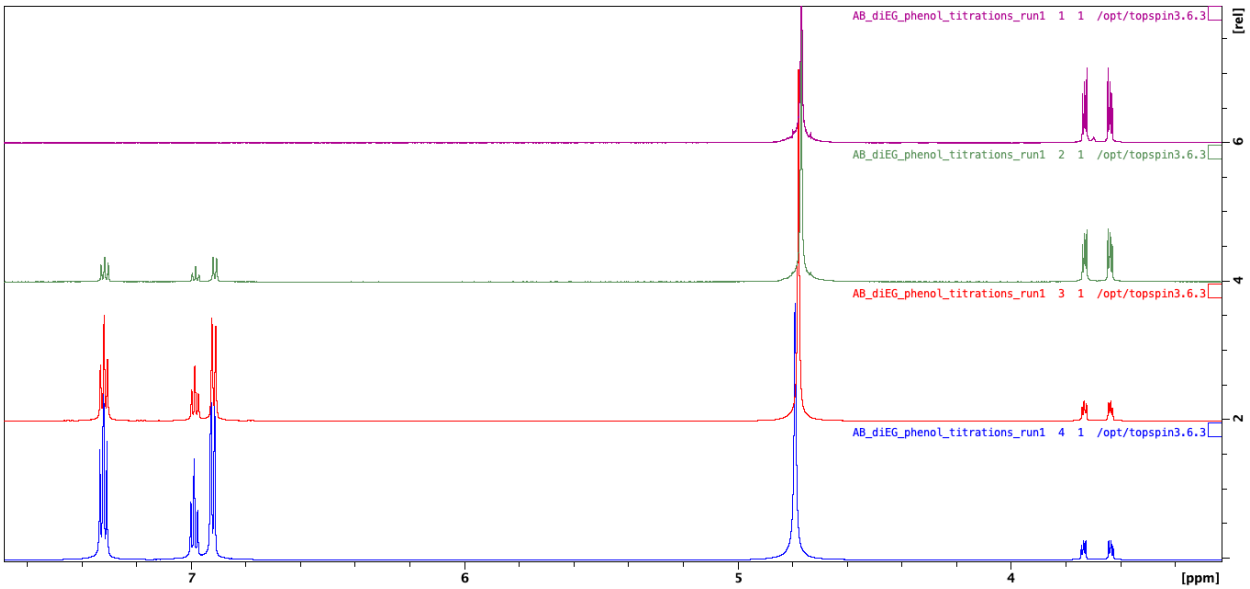

Appendix 1b: ^{1}H NMR spectra of diethylene glycol (**2**) at increasing concentrations of phenol (**10**). From top to bottom: (a) 10 mM diethylene glycol, 20 uM DSS, in D_2O; (b) 10 mM diethylene glycol, 10 mM phenol, 20 uM DSS, in D_2O; (c) 10 mM diethylene glycol, 20 mM phenol, 20 uM DSS, in D_2O; (d) 10 mM diethylene glycol, 200 mM phenol, 20 uM DSS, in D_2O. [*Peak assignments (from left to right): triplet: H_{phenol}, triplet: H_{phenol}, doublet: H_{phenol}, singlet: HOD, triplet: H_a (diethylene glycol), triplet: H_b (diethylene glycol)] LabArchives: Experimental Notebook/Phenol Titrations Raw Data*

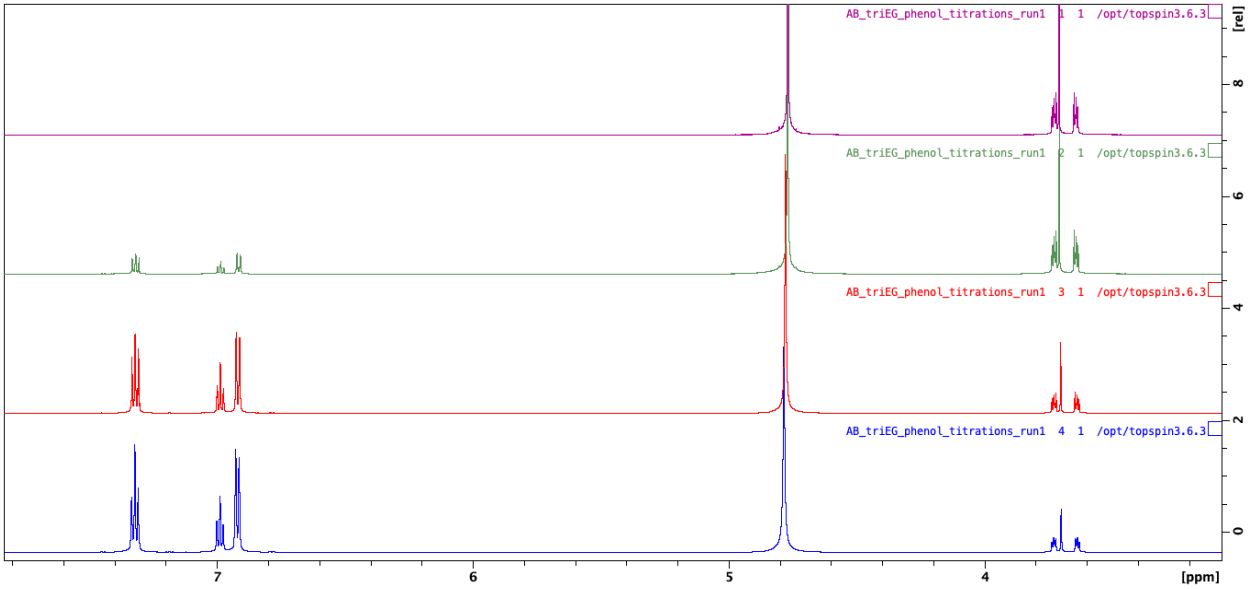

Appendix 1c: ^{1}H NMR spectra of triethylene glycol (**3**) at increasing concentrations of phenol (**10**). From top to bottom: (a) 10 mM triethylene glycol, 20 uM DSS, in D_2O; (b) 10 mM triethylene glycol, 10 mM phenol, 20 uM DSS, in D_2O; (c) 10 mM triethylene glycol, 20 mM phenol, 20 uM DSS, in D_2O; (d) 10 mM triethylene glycol, 150 mM phenol*, 20 uM DSS, in D_2O. *Note: 150 mM was used instead of 200 due to a viscosity issue. [*Peak assignments (from left to right): triplet: H_{phenol}, triplet: H_{phenol}, doublet: H_{phenol}, singlet: HOD, triplet: H_a (triethylene*

glycol), singlet: H_c (triethylene glycol), triplet: H_b (triethylene glycol)] LabArchives: Experimental Notebook/Phenol Titrations Raw Data

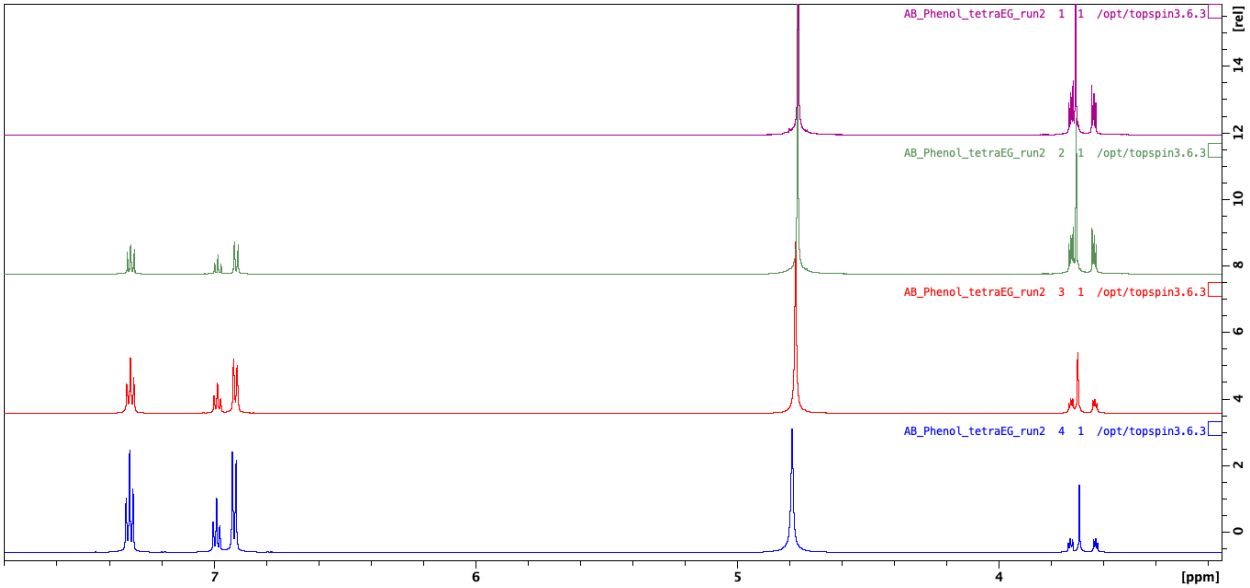

Appendix 1d: ^{1}H NMR spectra of tetraethylene glycol (**4**) at increasing concentrations of phenol (**10**). From top to bottom: (a) 10 mM tetraethylene glycol, 20 uM DSS, in D_2O; (b) 10 mM tetraethylene glycol, 10 mM phenol, 20 uM DSS, in D_2O; (c) 10 mM tetraethylene glycol, 20 mM phenol, 20 uM DSS, in D_2O; (d) 10 mM tetraethylene glycol, 200 mM phenol, 20 uM DSS, in D_2O. [*Peak assignments (from left to right): triplet: H_{phenol}, triplet: H_{phenol}, doublet: H_{phenol}, singlet: HOD, triplet: H_a (tetraethylene glycol), singlet: $H_{interior}$ (tetraethylene glycol), triplet: H_b (tetraethylene glycol)] LabArchives: Experimental Notebook/Phenol Titrations Raw Data*

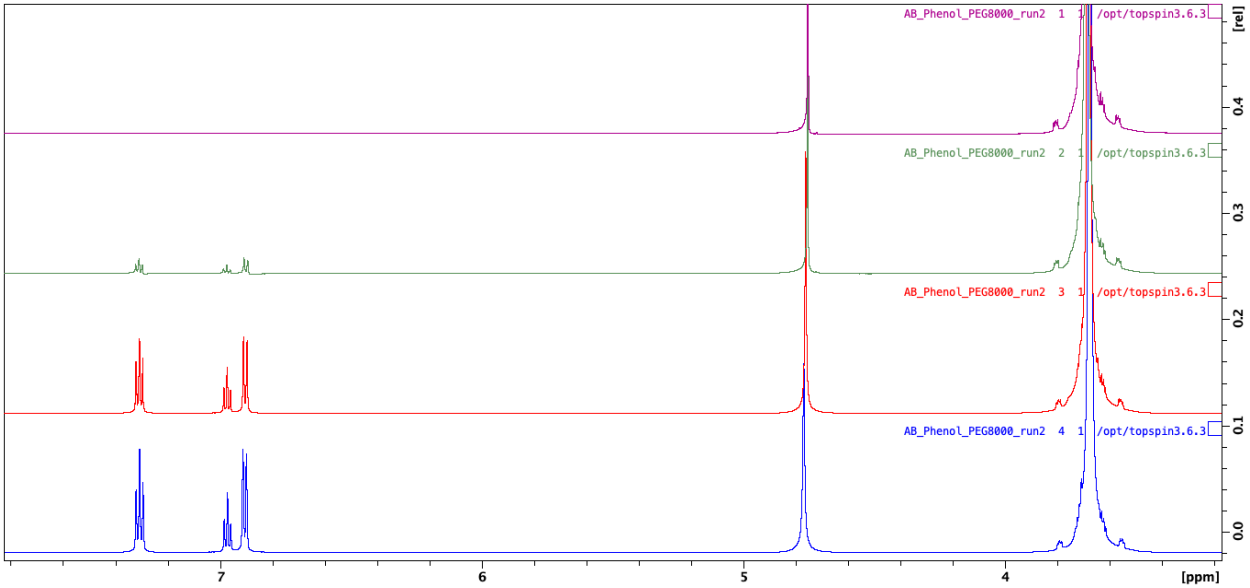

Appendix 1e: ^{1}H NMR spectra of PEG 8000 (**5**) at increasing concentrations of phenol (**10**). From top to bottom: (a) 10 mM PEG 8000, 20 uM DSS, in D_2O; (b) 10 mM PEG 8000, 10 mM phenol, 20 uM DSS, in D_2O; (c) 10 mM PEG 8000, 20 mM phenol, 20 uM DSS, in D_2O; (d) 10

mM PEG 8000, 200 mM phenol, 20 uM DSS, in D_2O. [*Peak assignments (from left to right): triplet: H_{phenol}, triplet: H_{phenol}, doublet: H_{phenol}, singlet: HOD, singlet: $H_{interior}$ (PEG 8000), triplet (hard to make out): H_b (PEG 8000)] LabArchives: Experimental Notebook/Phenol Titrations Raw Data*

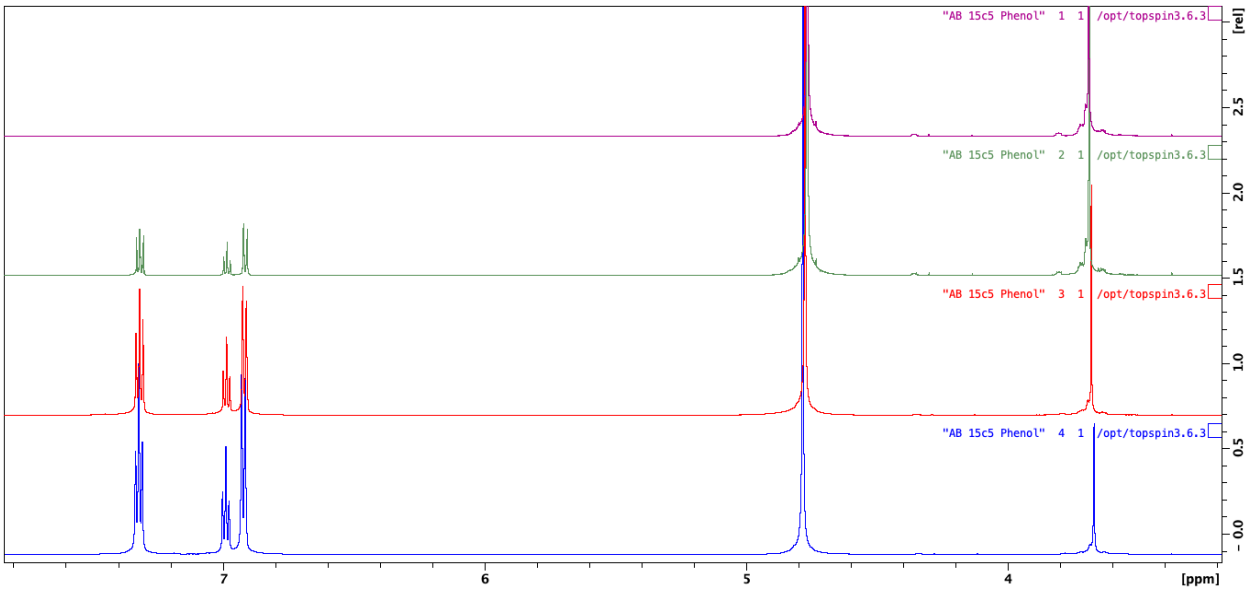

Appendix 1f: ^{1}H NMR spectra of 15-crown-5 (**6**) at increasing concentrations of phenol (**10**). From top to bottom: (a) 10 mM 15-crown-5, 20 uM DSS, in D_2O; (b) 10 mM 15-crown-5, 10 mM phenol, 20 uM DSS, in D_2O; (c) 10 mM 15-crown-5, 20 mM phenol, 20 uM DSS, in D_2O; (d) 10 mM 15-crown-5, 200 mM phenol, 20 uM DSS, in D_2O. [*Peak assignments (from left to right): triplet: H_{phenol}, triplet: H_{phenol}, doublet: H_{phenol}, singlet: HOD, singlet: H_a (15-crown-5)] LabArchives: Experimental Notebook/Phenol Titrations Raw Data*

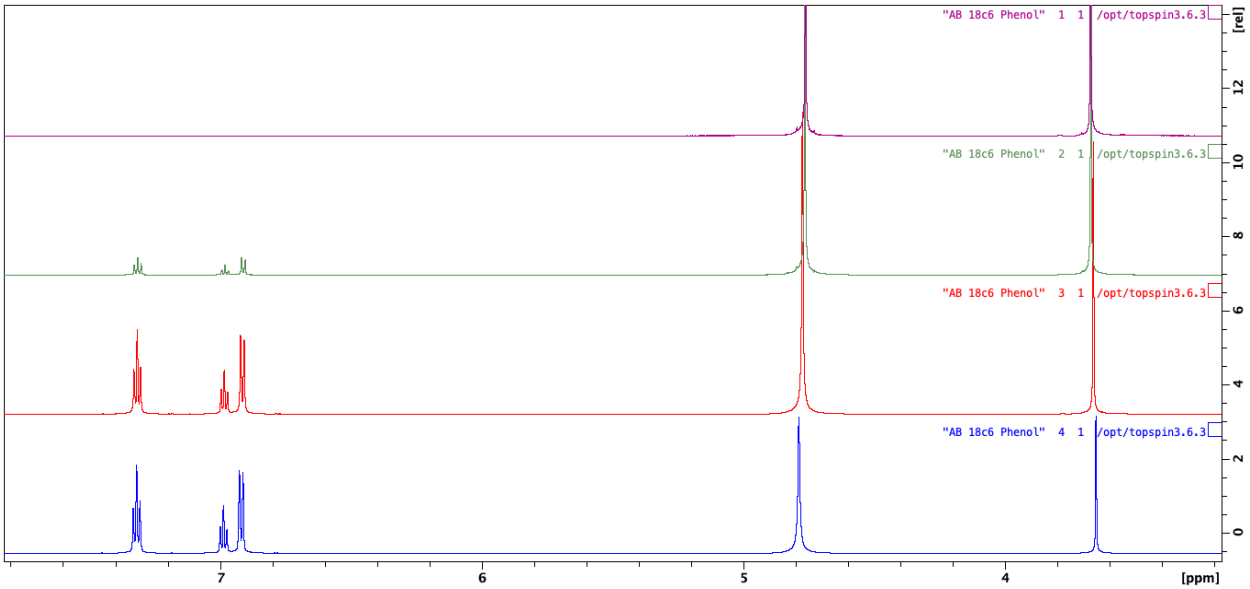

Appendix 1g: ^{1}H NMR spectra of 18-crown-6 (**7**) at increasing concentrations of phenol (**10**). From top to bottom: (a) 10 mM 18-crown-6, 20 uM DSS, in D_2O; (b) 10 mM 18-crown-6, 10

mM phenol, 20 uM DSS, in D_2O; (c) 10 mM 18-crown-6, 20 mM phenol, 20 uM DSS, in D_2O; (d) 10 mM 18-crown-6, 200 mM phenol, 20 uM DSS, in D_2O. [*Peak assignments (from left to right): triplet: H_{phenol}, triplet: H_{phenol}, doublet: H_{phenol}, singlet: HOD, singlet: H_a (18-crown-6)] LabArchives: Experimental Notebook/Phenol Titrations Raw Data*

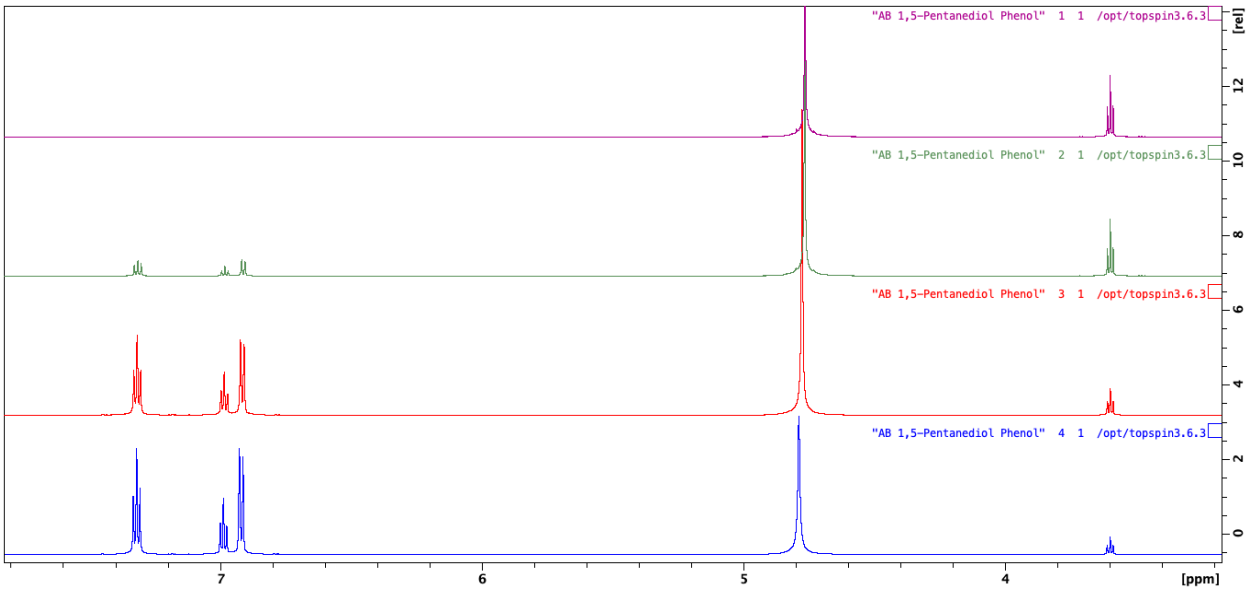

Appendix 1h: ^{1}H NMR spectra of 1,5-pentanediol (**8**) at increasing concentrations of phenol (**10**). From top to bottom: (a) 10 mM 1,5-pentanediol, 20 uM DSS, in D_2O; (b) 10 mM 1,5-pentanediol, 10 mM phenol, 20 uM DSS, in D_2O; (c) 10 mM 1,5-pentanediol, 20 mM phenol, 20 uM DSS, in D_2O; (d) 10 mM 1,5-pentanediol, 200 mM phenol, 20 uM DSS, in D_2O. [*Peak assignments (from left to right): triplet: H_{phenol}, triplet: H_{phenol}, doublet: H_{phenol}, singlet: HOD, triplet: H_a (1,5-pentanediol). H_b and H_c are not visible in this image.] LabArchives: Experimental Notebook/Phenol Titrations Raw Data*

Appendix 2a-c: ^{1}H NMR spectra of indole titrations with various PEG-related compounds.

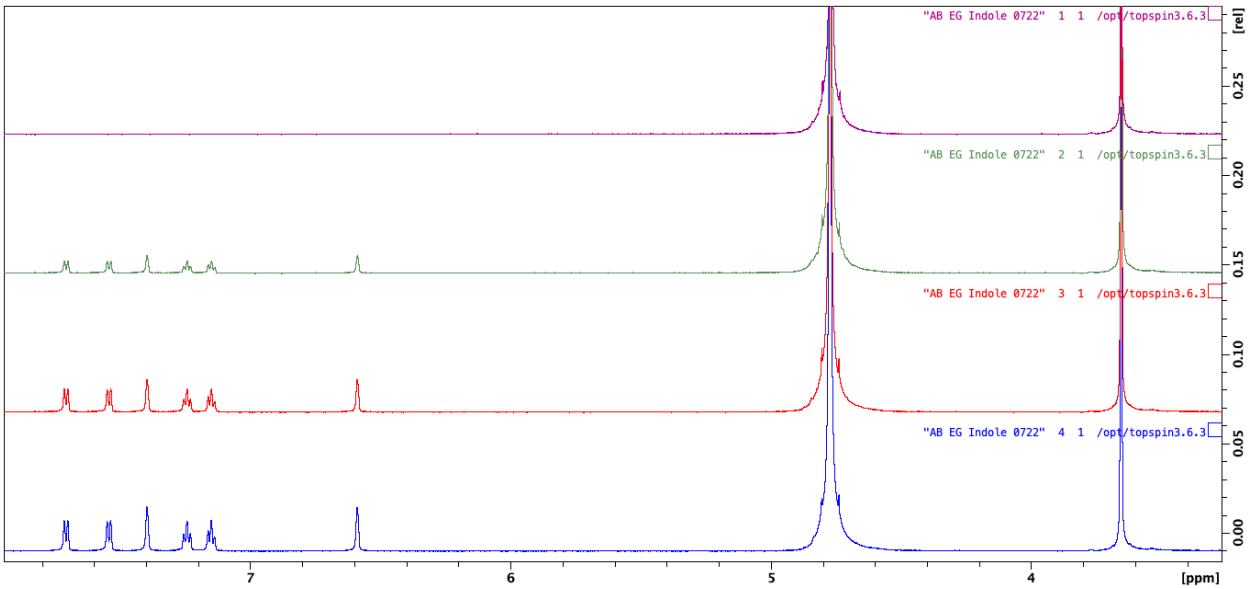

Appendix 2a: ^{1}H NMR spectra of ethylene glycol (**1**) at increasing concentrations of indole (**9**). From top to bottom: (a) 4 mM ethylene glycol, 20 uM DSS, in D_2O; (b) 4 mM ethylene glycol, 4 mM indole, 20 uM DSS, in D_2O; (c) 4 mM ethylene glycol, 7.5 mM indole, 20 uM DSS, in D_2O; (d) 4 mM ethylene glycol, 10 mM indole, 20 uM DSS, in D_2O. [*Peak assignments (from left to right): doublet: H_{indole}, doublet: H_{indole}, singlet: H_{indole}, triplet: H_{indole}, triplet: H_{indole}, singlet: H_{indole}, singlet: HOD, singlet: H_a (ethylene glycol)] LabArchives: Experimental Notebook/Indole Titrations Raw Data*

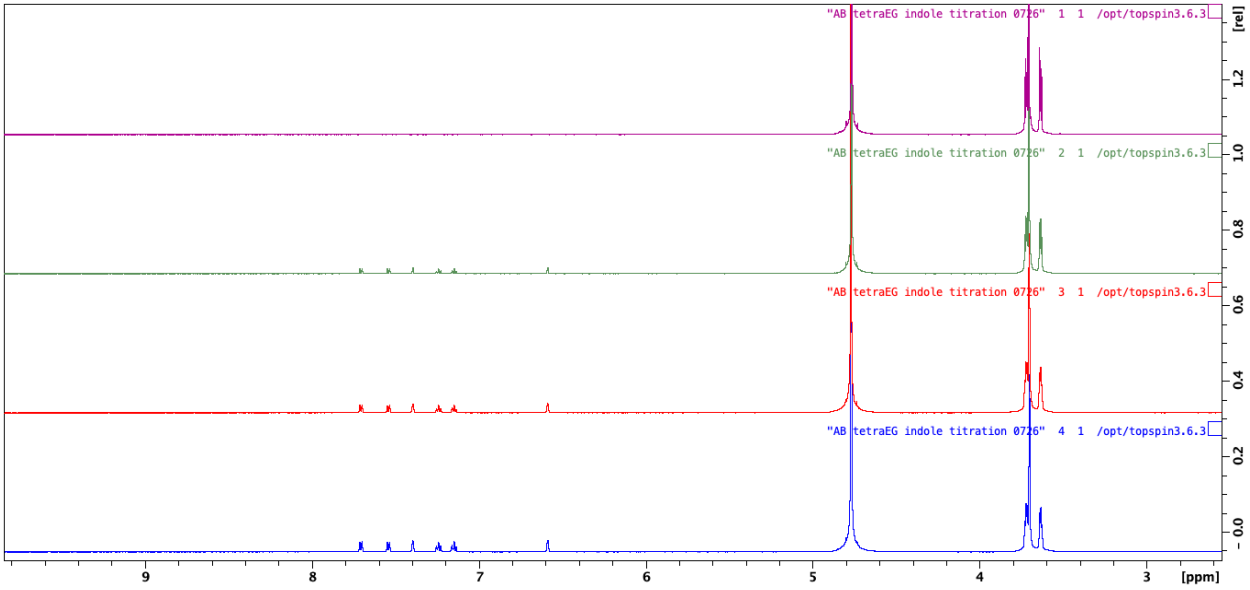

Appendix 2b: ^{1}H NMR spectra of tetraethylene glycol (**4**) at increasing concentrations of indole (**9**). From top to bottom: (a) 4 mM tetraethylene glycol, 20 uM DSS, in D_2O; (b) 4 mM tetraethylene glycol, 4 mM indole, 20 uM DSS, in D_2O; (c) 4 mM tetraethylene glycol, 7.5 mM indole, 20 uM DSS, in D_2O; (d) 4 mM tetraethylene glycol, 10 mM indole, 20 uM DSS, in D_2O. [*Peak assignments (from left to right): doublet: H_{indole}, doublet: H_{indole}, singlet: H_{indole}, triplet: H_{indole}, triplet: H_{indole}, singlet: H_{indole}, singlet: HOD, triplet: H_a (tetraethylene glycol), singlet:*

$H_{interior}$ (tetraethylene glycol), triplet: H_b (tetraethylene glycol)] LabArchives: Experimental Notebook/Indole Titrations Raw Data

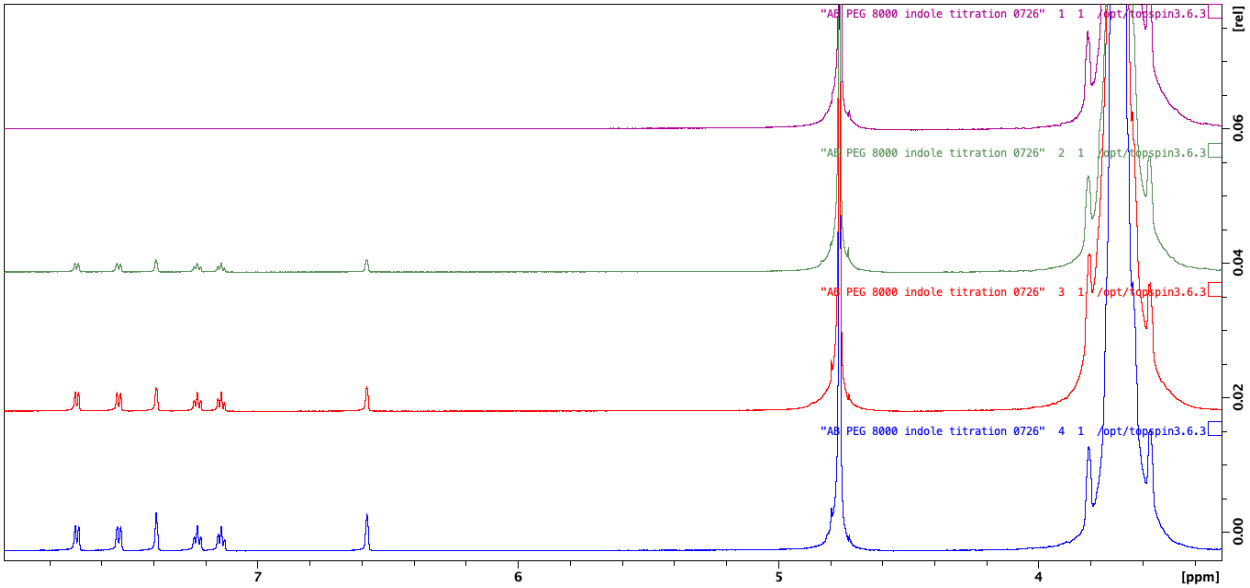

Appendix 2c: ^{1}H NMR spectra of PEG 8000 (**5**) at increasing concentrations of indole (**9**). From top to bottom: (a) 4 mM PEG 8000, 20 uM DSS, in D_2O; (b) 4 mM PEG 8000, 4 mM indole, 20 uM DSS, in D_2O; (c) 4 mM PEG 8000, 7.5 mM indole, 20 uM DSS, in D_2O; (d) 4 mM PEG 8000, 10 mM indole, 20 uM DSS, in D_2O. [*Peak assignments (from left to right): doublet: H_{indole}, doublet: H_{indole}, singlet: H_{indole}, triplet: H_{indole}, triplet: H_{indole}, singlet: H_{indole}, singlet: HOD, singlet: $H_{interior}$ (PEG 8000)] LabArchives: Experimental Notebook/Indole Titrations Raw Data*

Appendix 3a-d: ^{1}H NMR spectra of L-alanine methyl ester hydrochloride titrations with various

PEG-related compounds.

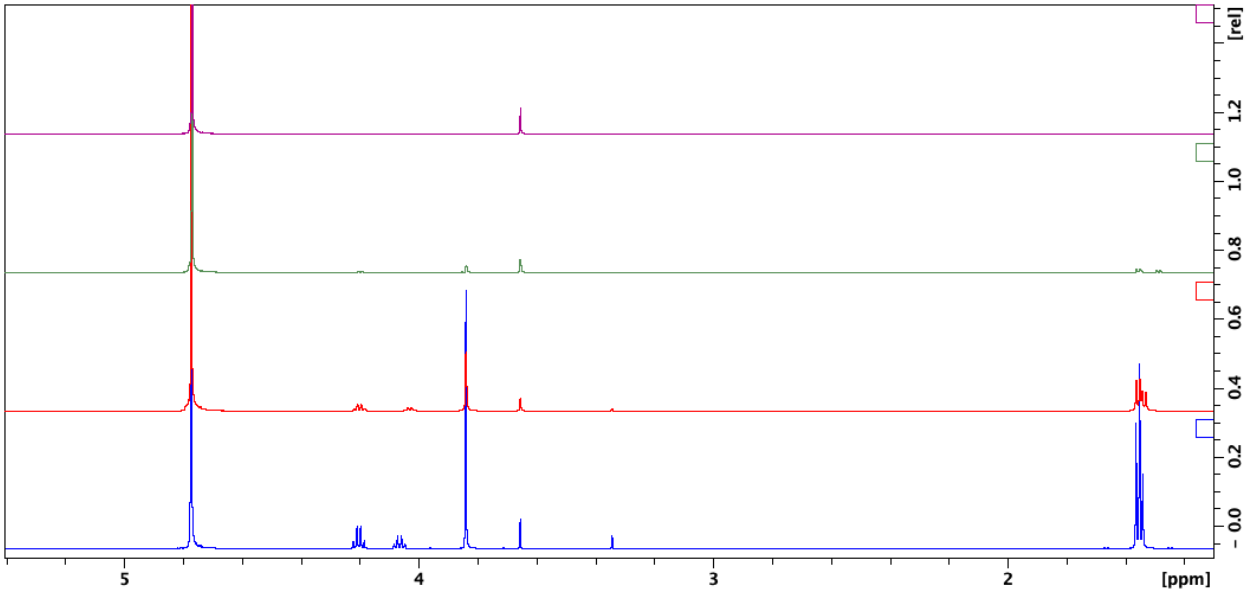

Appendix 3a: ^{1}H NMR spectra of ethylene glycol (**1**) at increasing concentrations of L-alanine methyl ester hydrochloride (**11**). From top to bottom: (a) 4 mM ethylene glycol, 20 uM DSS, in D_2O; (b) 4 mM ethylene glycol, 4 mM L-alanine methyl ester HCl, 20 uM DSS, in D_2O; (c) 4 mM ethylene glycol, 40 mM L-alanine methyl ester HCl, 20 uM DSS, in D_2O; (d) 4 mM ethylene glycol, 80 mM L-alanine methyl ester HCl, 20 uM DSS, in D_2O. *[Peak assignments (from left to right): singlet: HOD, quadruplet: $H_{\text{L-alanine met est HCl}}$, quadruplet: $H_{\text{L-alanine (contaminant)}}$, singlet: $H_{\text{L-alanine met est HCl}}$, singlet: H_a (ethylene glycol), doublet: $H_{\text{L-alanine met est HCl}}$, doublet: $H_{\text{L-alanine (contaminant)}}$] LabArchives: Experimental Notebook/L-alanine methyl ester HCl Titrations Raw Data*

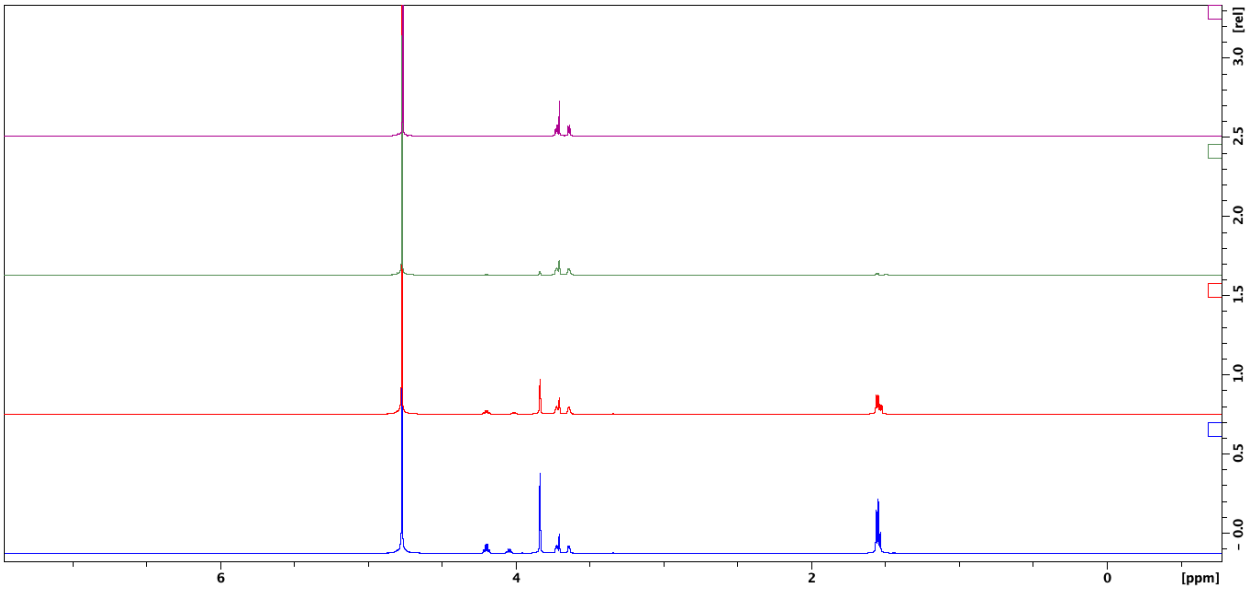

Appendix 3b: ^{1}H NMR spectra of tetraethylene glycol (**4**) at increasing concentrations of L-alanine methyl ester hydrochloride (**11**). From top to bottom: (a) 4 mM tetraethylene glycol, 20 uM DSS, in D_2O; (b) 4 mM tetraethylene glycol, 4 mM L-alanine methyl ester HCl, 20 uM DSS, in D_2O; (c) 4 mM tetraethylene glycol, 40 mM L-alanine methyl ester HCl, 20 uM DSS, in D_2O;

(d) 4 mM tetraethylene glycol, 80 mM L-alanine methyl ester HCl, 20 uM DSS, in D_2O. *[Peak assignments (from left to right): singlet: HOD, quadruplet: $H_{L\text{-alanine met est HCl}}$, quadruplet: $H_{L\text{-alanine (contaminant)}}$, singlet: $H_{L\text{-alanine met est HCl}}$, triplet: H_a (tetraethylene glycol), singlet: $H_{interior}$ (tetraethylene glycol), triplet: H_b (tetraethylene glycol), doublet: $H_{L\text{-alanine met est HCl}}$, doublet: $H_{L\text{-alanine (contaminant)}}$] LabArchives: Experimental Notebook/L-alanine methyl ester HCl Titrations Raw Data*

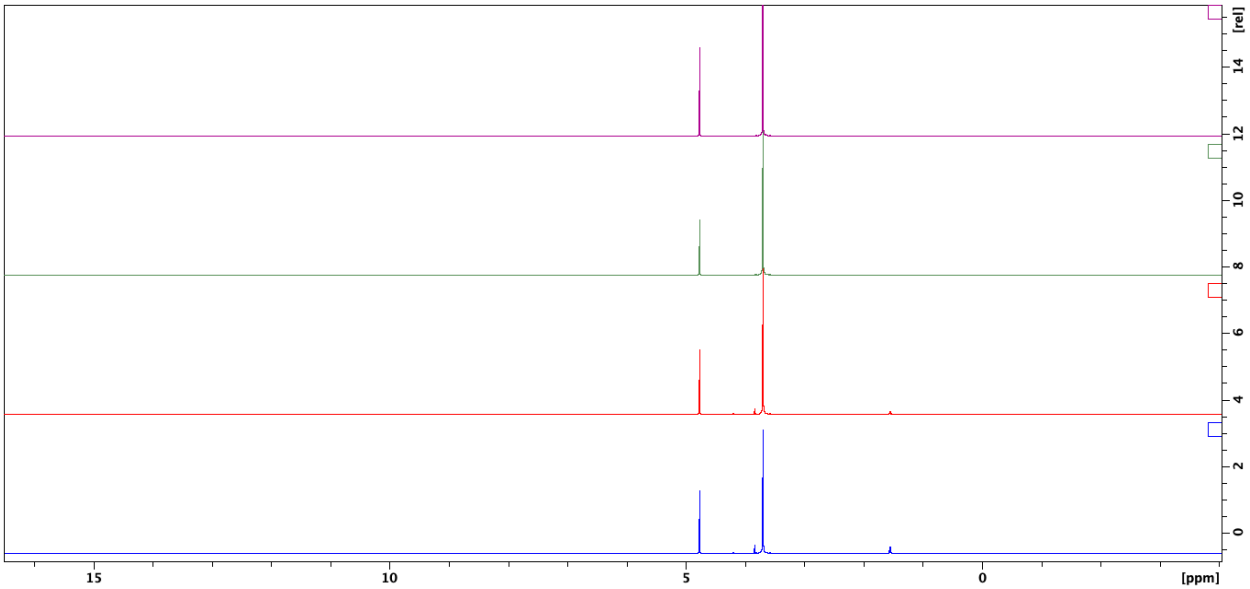

Appendix 3c: ^{1}H NMR spectra of PEG 8000 (**5**) at increasing concentrations of L-alanine methyl ester hydrochloride (**11**). From top to bottom: (a) 4 mM PEG 8000, 20 uM DSS, in D_2O; (b) 4 mM PEG 8000, 4 mM L-alanine methyl ester HCl, 20 uM DSS, in D_2O; (c) 4 mM PEG 8000, 40 mM L-alanine methyl ester HCl, 20 uM DSS, in D_2O; (d) 4 mM PEG 8000, 80 mM L-alanine methyl ester HCl, 20 uM DSS, in D_2O. *[Peak assignments (from left to right): singlet: HOD, quadruplet: $H_{L\text{-alanine met est HCl}}$, quadruplet: $H_{L\text{-alanine (contaminant)}}$, singlet: $H_{L\text{-alanine met est HCl}}$, singlet: $H_{interior}$ (PEG 8000), doublet: $H_{L\text{-alanine met est HCl}}$, doublet: $H_{L\text{-alanine (contaminant)}}$] LabArchives: Experimental Notebook/L-alanine methyl ester HCl Titrations Raw Data*

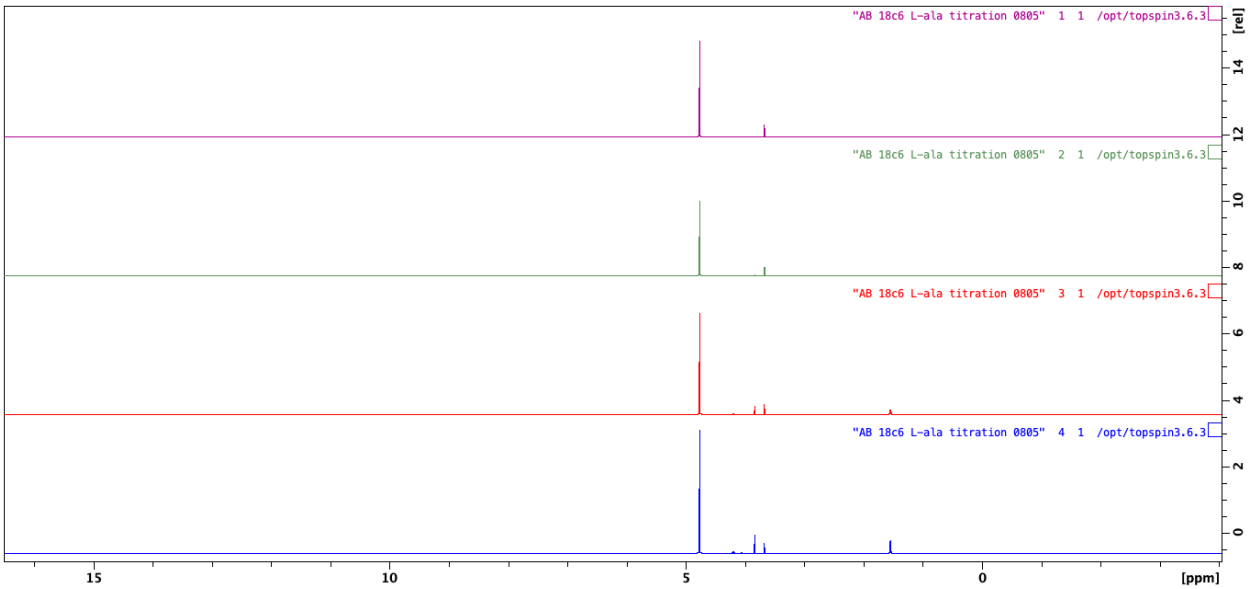

Appendix 3d: ^{1}H NMR spectra of 18-crown-6 (**7**) at increasing concentrations of L-alanine methyl ester hydrochloride (**11**). From top to bottom: (a) 4 mM 18-crown-6, 20 uM DSS, in D_2O; (b) 4 mM 18-crown-6, 4 mM L-alanine methyl ester HCl, 20 uM DSS, in D_2O; (c) 4 mM 18-crown-6, 40 mM L-alanine methyl ester HCl, 20 uM DSS, in D_2O; (d) 4 mM 18-crown-6, 80 mM L-alanine methyl ester HCl, 20 uM DSS, in D_2O. *[Peak assignments (from left to right): singlet: HOD, quadruplet: $H_{L\text{-alanine met est HCl}}$, quadruplet: $H_{L\text{-alanine (contaminant)}}$, singlet: $H_{L\text{-alanine met est HCl}}$, singlet: H_a (18-crown-6), doublet: $H_{L\text{-alanine met est HCl}}$, doublet: $H_{L\text{-alanine (contaminant)}}$] LabArchives: Experimental Notebook/L-alanine methyl ester HCl Titrations Raw Data*

Appendix 4a-d: ^{1}H NMR spectra of L-tryptophan methyl ester hydrochloride with various PEG-related compounds.

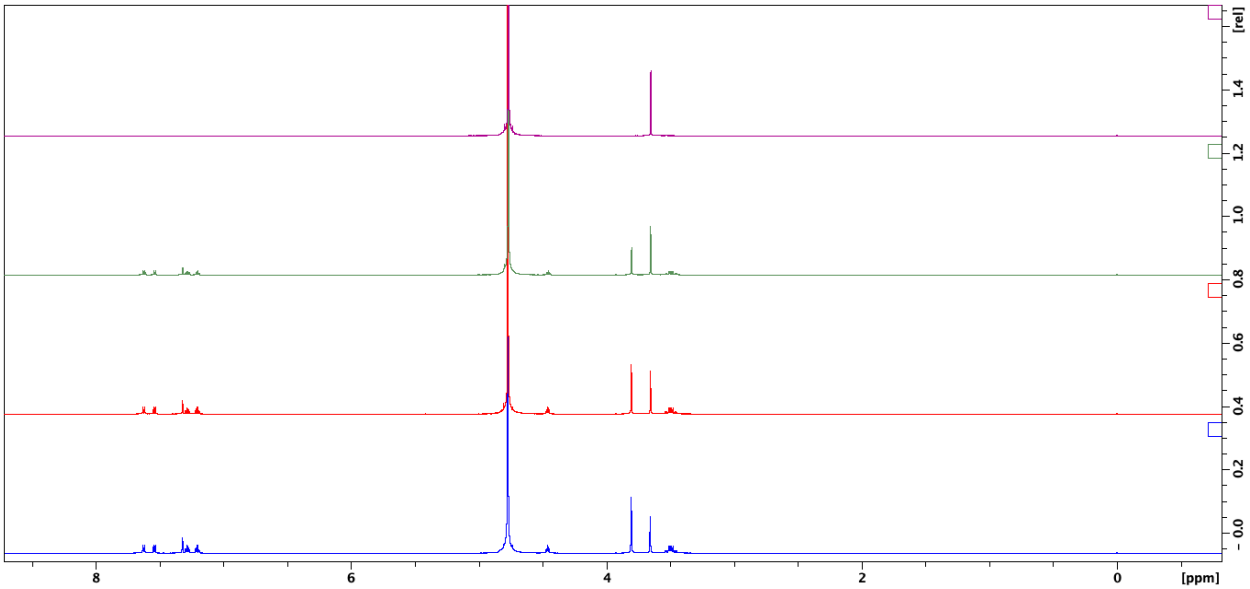

Appendix 4a: ^{1}H NMR spectra of ethylene glycol (**1**) at increasing concentrations of L-tryptophan methyl ester hydrochloride (**13**). From top to bottom: (a) 4 mM ethylene glycol, 20

uM DSS, in D_2O; (b) 4 mM ethylene glycol, 4 mM L-tryptophan methyl ester HCl, 20 uM DSS, in D_2O; (c) 4 mM ethylene glycol, 7.5 mM L-tryptophan methyl ester HCl, 20 uM DSS, in D_2O; (d) 4 mM ethylene glycol, 10 mM L-tryptophan methyl ester HCl, 20 uM DSS, in D_2O. [*Peak assignments (from left to right): doublet:* $H_{\text{L-tryptophan met est HCl}}$, *doublet:* $H_{\text{L-tryptophan met est HCl}}$, *singlet:* $H_{\text{L-tryptophan met est HCl}}$, *triplet:* $H_{\text{L-tryptophan met est HCl}}$, *triplet:* $H_{\text{L-tryptophan met est HCl}}$, *singlet: HOD, multiplet:* $H_{\text{L-tryptophan met est HCl}}$, *singlet:* $H_{\text{L-tryptophan met est HCl}}$, *singlet:* H_a *(ethylene glycol), multiplet:* $H_{\text{L-tryptophan met est HCl}}$*] LabArchives: Experimental Notebook/L-tryptophan methyl ester HCl Titrations Raw Data*

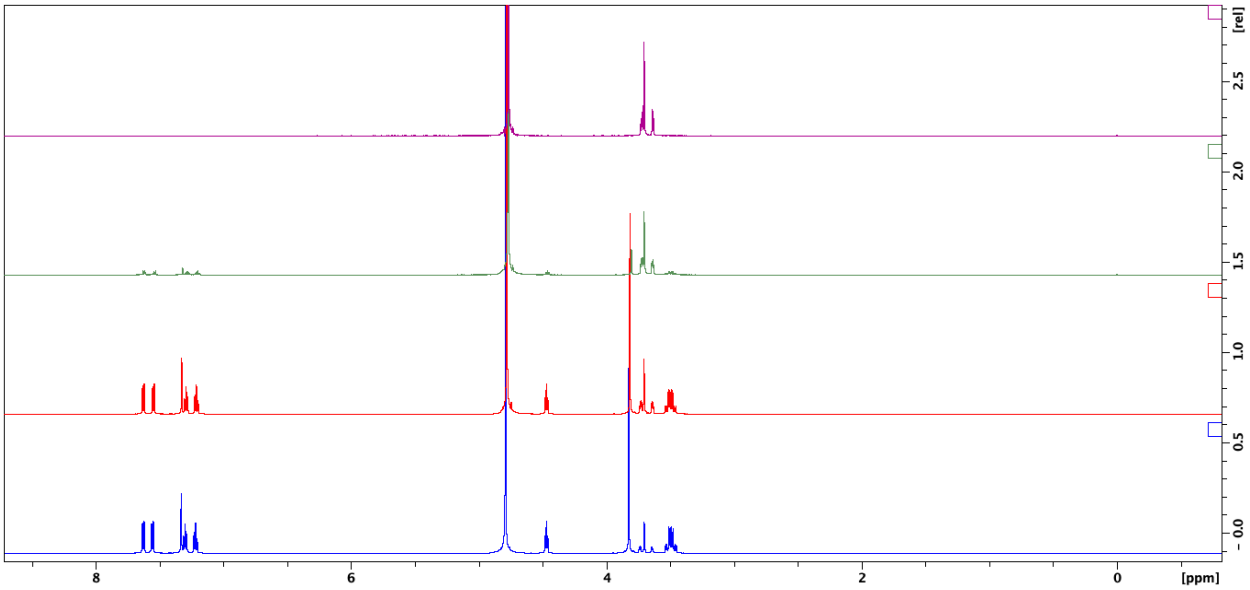

Appendix 4b: ^{1}H NMR spectra of tetraethylene glycol (**4**) at increasing concentrations of L-tryptophan methyl ester hydrochloride (**13**). From top to bottom: (a) 4 mM tetraethylene glycol, 20 uM DSS, in D_2O; (b) 4 mM tetraethylene glycol, 4 mM L-tryptophan methyl ester HCl, 20 uM DSS, in D_2O; (c) 4 mM tetraethylene glycol, 40 mM L-tryptophan methyl ester HCl, 20 uM DSS, in D_2O; (d) 4 mM tetraethylene glycol, 80 mM L-tryptophan methyl ester HCl, 20 uM DSS, in D_2O. [*Peak assignments (from left to right): doublet:* $H_{\text{L-tryptophan met est HCl}}$, *doublet:* $H_{\text{L-tryptophan met est HCl}}$, *singlet:* $H_{\text{L-tryptophan met est HCl}}$, *triplet:* $H_{\text{L-tryptophan met est HCl}}$, *triplet:* $H_{\text{L-tryptophan met est HCl}}$, *singlet: HOD, multiplet:* $H_{\text{L-tryptophan met est HCl}}$, *singlet:* $H_{\text{L-tryptophan met est HCl}}$, *triplet:* H_a *(tetraethylene glycol), singlet:* $H_{interior}$ *(tetraethylene glycol), triplet:* H_b *(tetraethylene glycol), multiplet:* $H_{\text{L-tryptophan met est HCl}}$*] LabArchives: Experimental Notebook/L-tryptophan methyl ester HCl Titrations Raw Data*

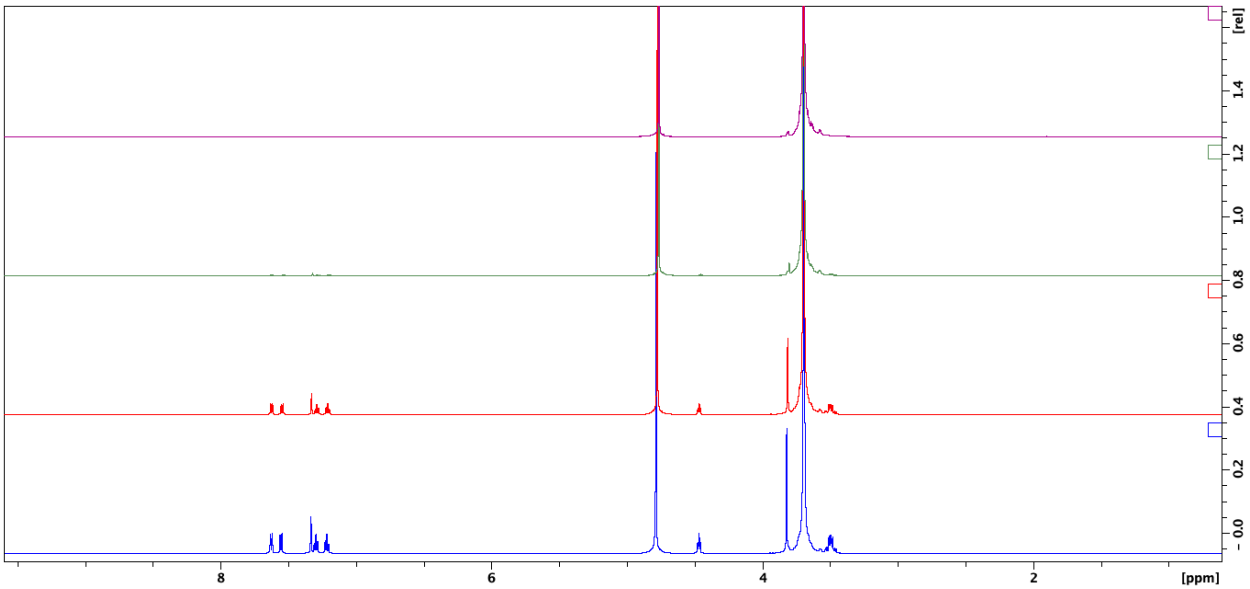

Appendix 4c: ^{1}H NMR spectra of PEG 8000 (**5**) at increasing concentrations of L-tryptophan methyl ester hydrochloride (**13**). From top to bottom: (a) 4 mM PEG 8000, 20 uM DSS, in D_2O; (b) 4 mM PEG 8000, 4 mM L-tryptophan methyl ester HCl, 20 uM DSS, in D_2O; (c) 4 mM PEG 8000, 40 mM L-tryptophan methyl ester HCl, 20 uM DSS, in D_2O; (d) 4 mM PEG 8000, 80 mM L-tryptophan methyl ester HCl, 20 uM DSS, in D_2O. [*Peak assignments (from left to right): doublet:* $H_{\text{L-tryptophan met est HCl}}$, *doublet:* $H_{\text{L-tryptophan met est HCl}}$, *singlet:* $H_{\text{L-tryptophan met est HCl}}$, *triplet:* $H_{\text{L-tryptophan met est HCl}}$, *triplet:* $H_{\text{L-tryptophan met est HCl}}$, *singlet: HOD, multiplet:* $H_{\text{L-tryptophan met est HCl}}$, *singlet:* $H_{\text{L-tryptophan met est HCl}}$, *singlet:* H_{interior} *(PEG 8000), multiplet:* $H_{\text{L-tryptophan met est HCl}}$*] LabArchives: Experimental Notebook/L-tryptophan methyl ester HCl Titrations Raw Data*

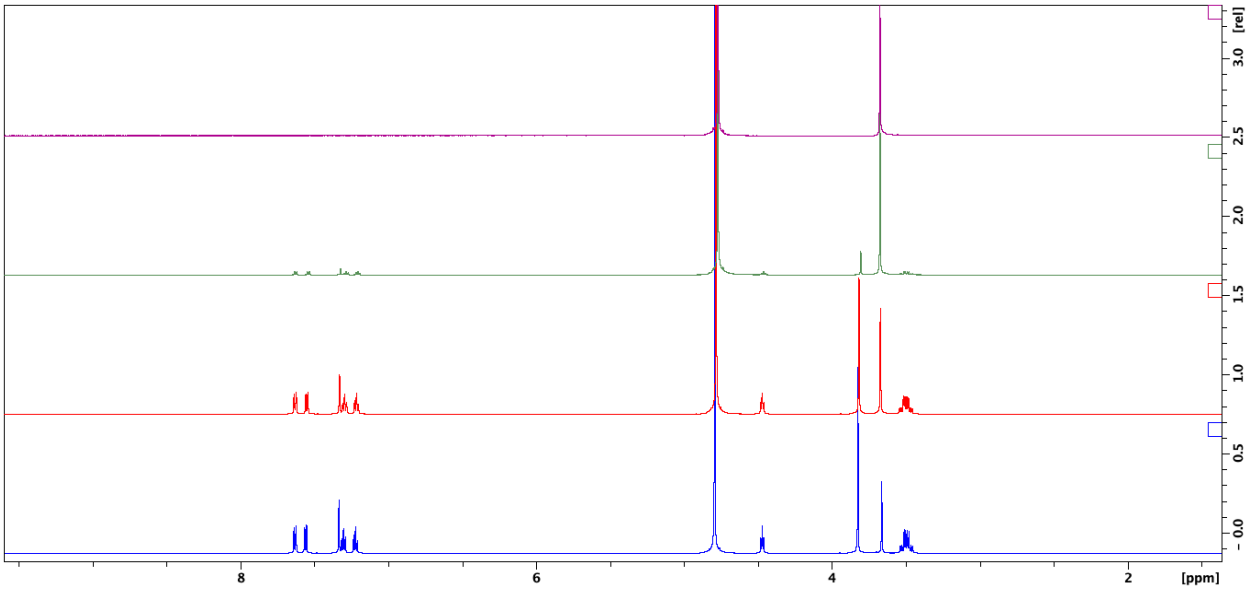

Appendix 4d: ^{1}H NMR spectra of 18-crown-6 (**7**) at increasing concentrations of L-tryptophan methyl ester hydrochloride (**13**). From top to bottom: (a) 4 mM 18-crown-6, 20 uM DSS, in D_2O; (b) 4 mM 18-crown-6, 4 mM L-tryptophan methyl ester HCl, 20 uM DSS, in D_2O; (c) 4 mM 18-crown-6, 40 mM L-tryptophan methyl ester HCl, 20 uM DSS, in D_2O; (d) 4 mM 18-crown-6,

80 mM L-tryptophan methyl ester HCl, 20 uM DSS, in D_2O. [*Peak assignments (from left to right): doublet: $H_{L\text{-tryptophan met est HCl}}$, doublet: $H_{L\text{-tryptophan met est HCl}}$, singlet: $H_{L\text{-tryptophan met est HCl}}$, triplet: $H_{L\text{-tryptophan met est HCl}}$, triplet: $H_{L\text{-tryptophan met est HCl}}$, singlet: HOD, multiplet: $H_{L\text{-tryptophan met est HCl}}$, singlet: $H_{L\text{-tryptophan met est HCl}}$, singlet: H_a (18-crown-6), multiplet: $H_{L\text{-tryptophan met est HCl}}$] LabArchives: Experimental Notebook/L-tryptophan methyl ester HCl Titrations Raw Data*

Appendix 5a-d: ^{1}H NMR spectra of L-tyrosine methyl ester hydrochloride with various PEG-related compounds.

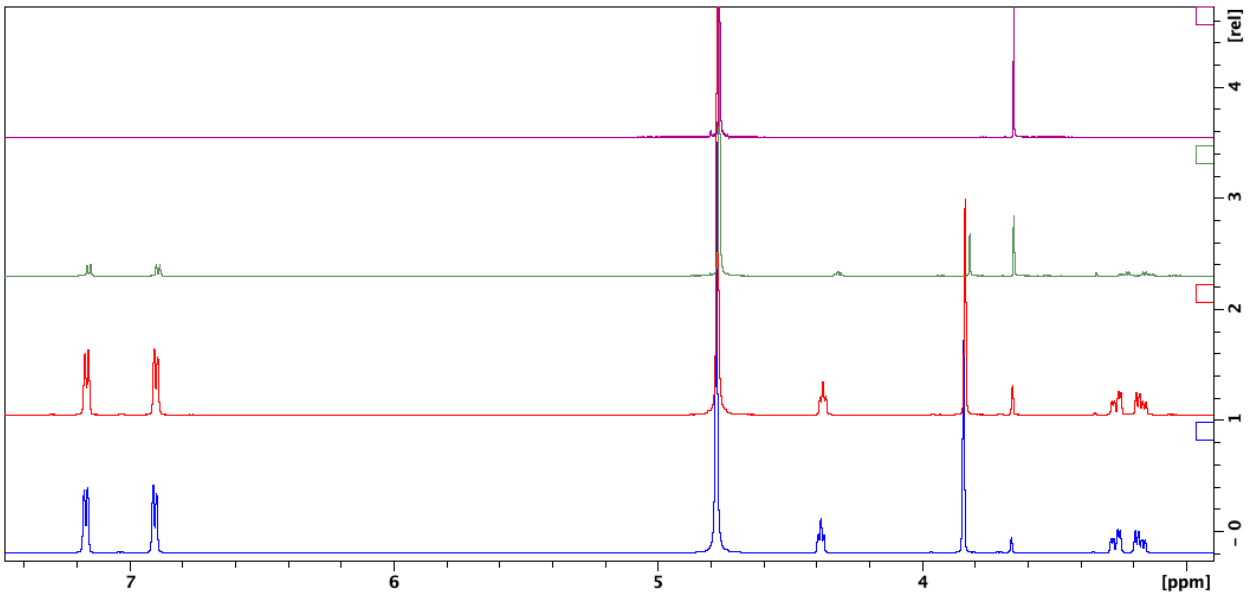

Appendix 5a: ^{1}H NMR spectra of ethylene glycol (**1**) at increasing concentrations of L-tyrosine methyl ester hydrochloride (**12**). From top to bottom: (a) 4 mM ethylene glycol, 20 uM DSS, in D_2O; (b) 4 mM ethylene glycol, 4 mM L-tyrosine methyl ester HCl, 20 uM DSS, in D_2O; (c) 4 mM ethylene glycol, 40 mM L-tyrosine methyl ester HCl, 20 uM DSS, in D_2O; (d) 4 mM ethylene glycol, 80 mM L-tyrosine methyl ester HCl, 20 uM DSS, in D_2O. [*Peak assignments (from left to right): doublet: $H_{L\text{-tyrosine met est HCl}}$, doublet: $H_{L\text{-tyrosine met est HCl}}$, singlet: HOD, triplet: $H_{L\text{-tyrosine met est HCl}}$, singlet: $H_{L\text{-tyrosine met est HCl}}$, singlet: H_a (ethylene glycol), multiplet: $H_{L\text{-tyrosine met est HCl}}$] LabArchives: Experimental Notebook/L-tyrosine methyl ester HCl Titrations Raw Data*

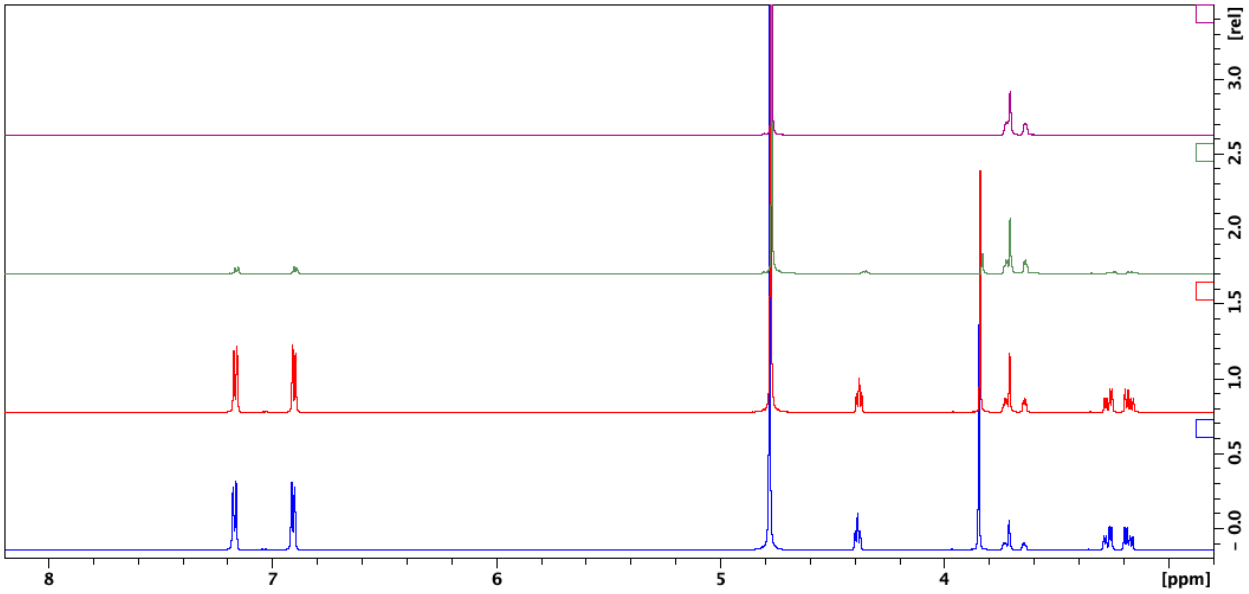

Appendix 5b: ^{1}H NMR spectra of tetraethylene glycol (**4**) at increasing concentrations of L-tyrosine methyl ester hydrochloride (**12**). From top to bottom: (a) 4 mM tetraethylene glycol, 20 uM DSS, in D_2O; (b) 4 mM tetraethylene glycol, 4 mM L-tyrosine methyl ester HCl, 20 uM DSS, in D_2O; (c) 4 mM tetraethylene glycol, 40 mM L-tyrosine methyl ester HCl, 20 uM DSS, in D_2O; (d) 4 mM tetraethylene glycol, 80 mM L-tyrosine methyl ester HCl, 20 uM DSS, in D_2O. [*Peak assignments (from left to right): doublet:* $H_{L\text{-tyrosine met est HCl}}$, *doublet:* $H_{L\text{-tyrosine met est HCl}}$, *singlet: HOD, triplet:* $H_{L\text{-tyrosine met est HCl}}$, *singlet:* $H_{L\text{-tyrosine met est HCl}}$, *triplet:* H_a *(tetraethylene glycol), singlet:* $H_{interior}$ *(tetraethylene glycol), triplet:* H_b *(tetraethylene glycol), multiplet:* $H_{L\text{-tyrosine met est HCl}}$*] LabArchives: Experimental Notebook/L-tyrosine methyl ester HCl Titrations Raw Data*

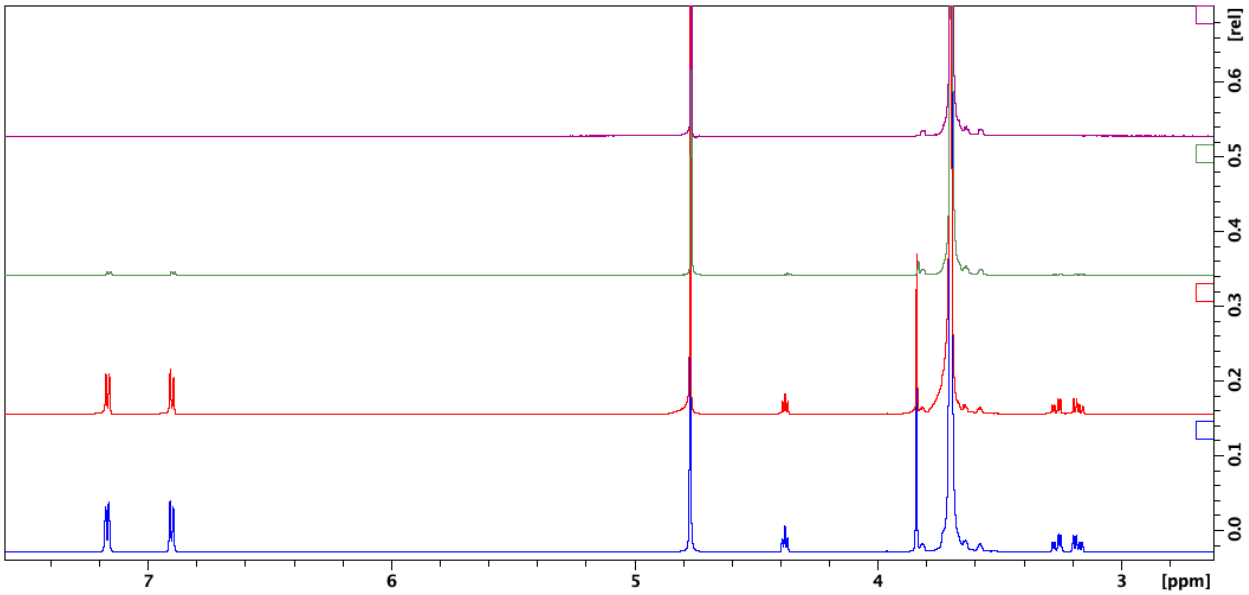

Appendix 5c: ^{1}H NMR spectra of PEG 8000 (**5**) at increasing concentrations of L-tyrosine methyl ester hydrochloride (**12**). From top to bottom: (a) 4 mM PEG 8000, 20 uM DSS, in D_2O; (b) 4 mM PEG 8000, 4 mM L-tyrosine methyl ester HCl, 20 uM DSS, in D_2O; (c) 4 mM PEG 8000, 40 mM L-tyrosine methyl ester HCl, 20 uM DSS, in D_2O; (d) 4 mM PEG 8000, 80 mM

L-tyrosine methyl ester HCl, 20 uM DSS, in D_2O. [*Peak assignments (from left to right): doublet: $H_{L\text{-tyrosine met est HCl}}$, doublet: $H_{L\text{-tyrosine met est HCl}}$, singlet: HOD, triplet: $H_{L\text{-tyrosine met est HCl}}$, singlet: $H_{L\text{-tyrosine met est HCl}}$, singlet: $H_{interior}$ (PEG 8000), multiplet: $H_{L\text{-tyrosine met est HCl}}$] LabArchives: Experimental Notebook/L-tyrosine methyl ester HCl Titrations Raw Data*

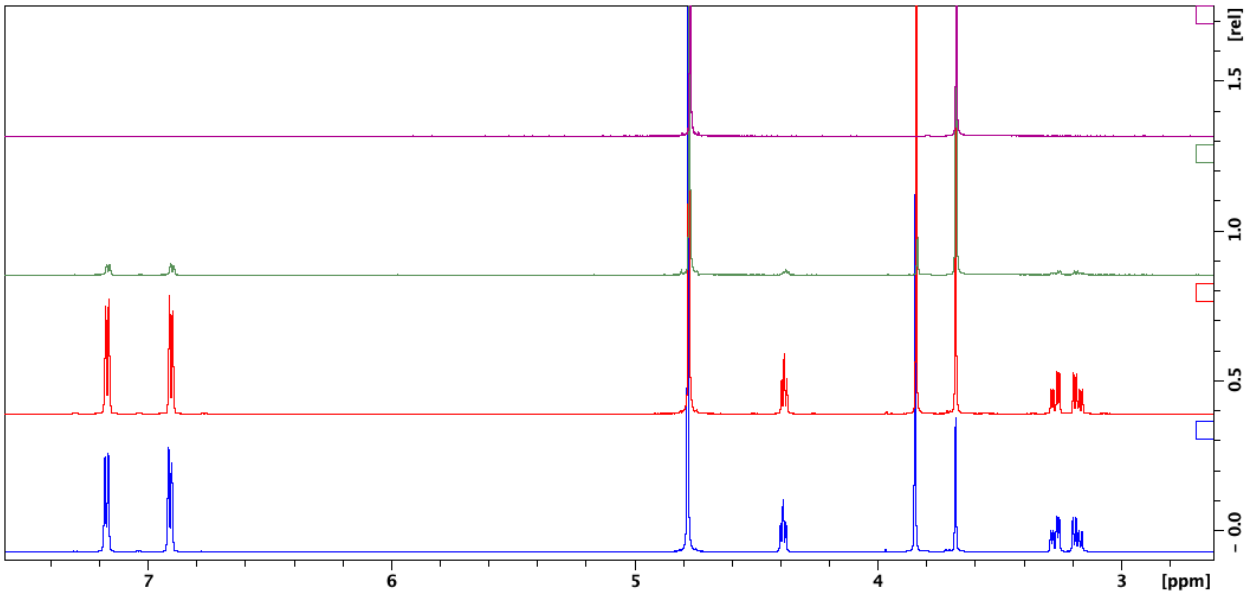

Appendix 5d: ^{1}H NMR spectra of 18-crown-6 (**7**) at increasing concentrations of L-tyrosine methyl ester hydrochloride (**12**). From top to bottom: (a) 4 mM 18-crown-6, 20 uM DSS, in D_2O; (b) 4 mM 18-crown-6, 4 mM L-tyrosine methyl ester HCl, 20 uM DSS, in D_2O; (c) 4 mM 18-crown-6, 40 mM L-tyrosine methyl ester HCl, 20 uM DSS, in D_2O; (d) 4 mM 18-crown-6, 80 mM L-tyrosine methyl ester HCl, 20 uM DSS, in D_2O. [*Peak assignments (from left to right): doublet: $H_{L\text{-tyrosine met est HCl}}$, doublet: $H_{L\text{-tyrosine met est HCl}}$, singlet: HOD, triplet: $H_{L\text{-tyrosine met est HCl}}$, singlet: $H_{L\text{-tyrosine met est HCl}}$, singlet: H_a (18-crown-6), multiplet: $H_{L\text{-tyrosine met est HCl}}$] LabArchives: Experimental Notebook/L-tryptophan methyl ester HCl Titrations Raw Data*

Appendix 6a-d: ^{1}H NMR spectra of 4-nitrophenol with various PEG-related compounds.

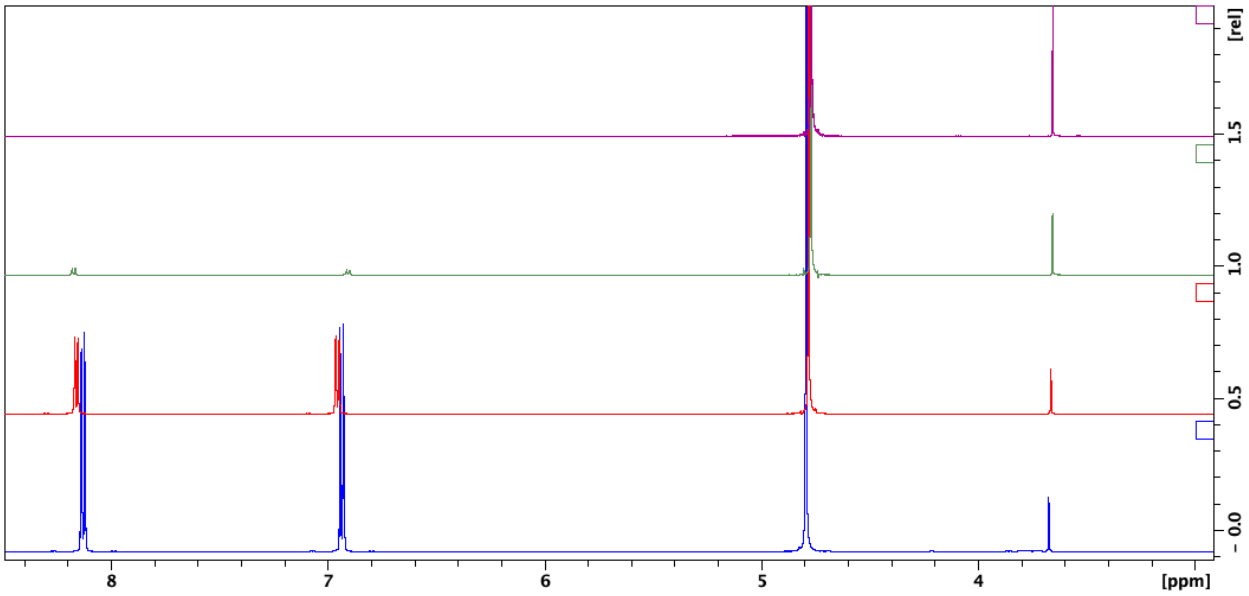

Appendix 6a: ^{1}H NMR spectra of ethylene glycol (**1**) at increasing concentrations of 4-nitrophenol (**14**). From top to bottom: (a) 4 mM ethylene glycol, 20 uM DSS, in D_2O; (b) 4 mM ethylene glycol, 4 mM 4-nitrophenol, 20 uM DSS, in D_2O; (c) 4 mM ethylene glycol, 40 mM 4-nitrophenol, 20 uM DSS, in D_2O; (d) 4 mM ethylene glycol, 80 mM 4-nitrophenol, 20 uM DSS, in D_2O. [*Peak assignments (from left to right): doublet: $H_{4\text{-nitrophenol}}$, doublet: $H_{4\text{-nitrophenol}}$, singlet: HOD, singlet: H_a (ethylene glycol)] LabArchives: Experimental Notebook/4-nitrophenol Titrations Raw Data*

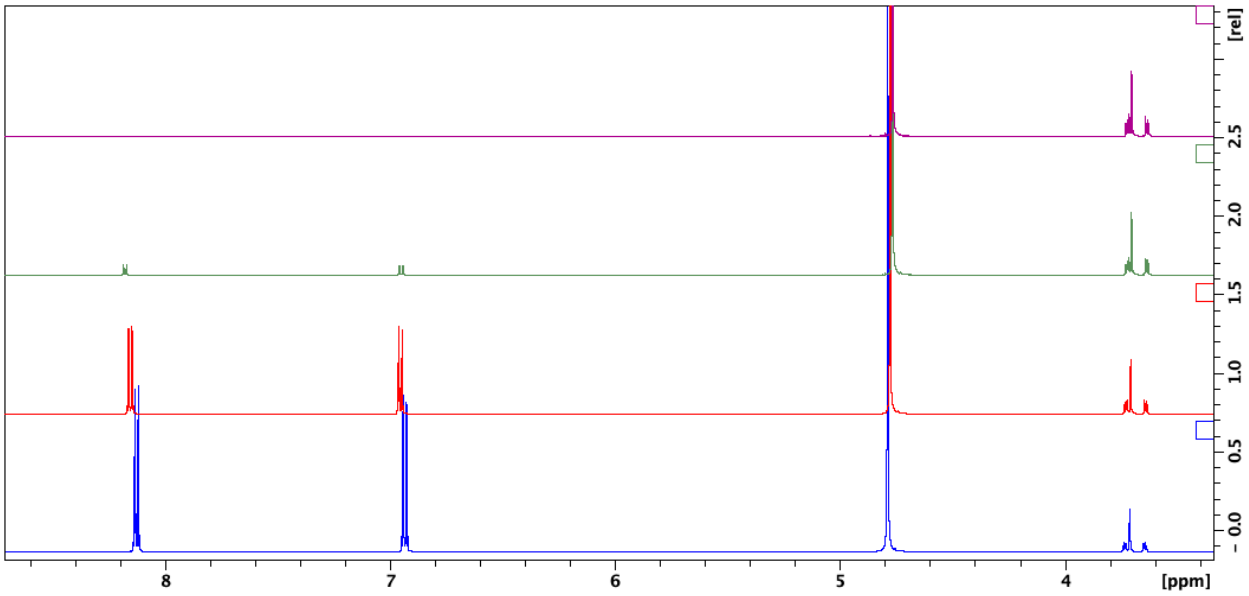

Appendix 6b: ^{1}H NMR spectra of tetraethylene glycol (**4**) at increasing concentrations of 4-nitrophenol (**14**). From top to bottom: (a) 4 mM tetraethylene glycol, 20 uM DSS, in D_2O; (b) 4 mM tetraethylene glycol, 4 mM 4-nitrophenol, 20 uM DSS, in D_2O; (c) 4 mM tetraethylene glycol, 40 mM 4-nitrophenol, 20 uM DSS, in D_2O; (d) 4 mM tetraethylene glycol, 80 mM

4-nitrophenol, 20 uM DSS, in D_2O. [*Peak assignments (from left to right): doublet: $H_{4\text{-nitrophenol}}$, doublet: $H_{4\text{-nitrophenol}}$, singlet: HOD, triplet: H_a (tetraethylene glycol), singlet: $H_{interior}$ (tetraethylene glycol), triplet: H_b (tetraethylene glycol)] LabArchives: Experimental Notebook/4-nitrophenol Titrations Raw Data*

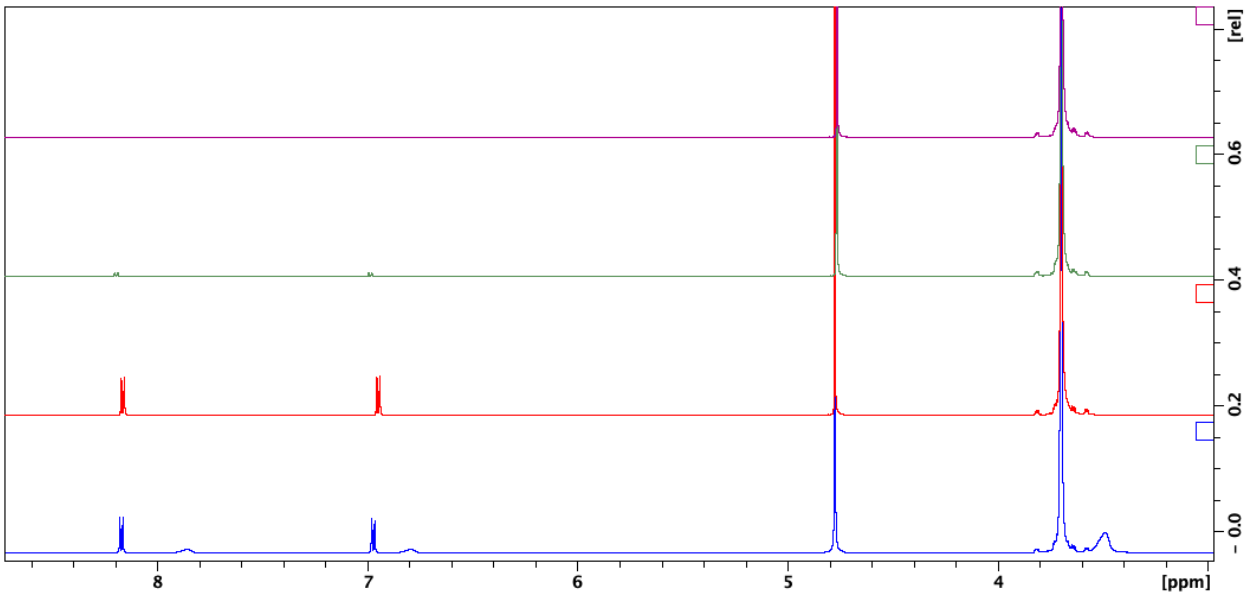

Appendix 6c: ^1H NMR spectra of PEG 8000 (**5**) at increasing concentrations of 4-nitrophenol (**14**). From top to bottom: (a) 4 mM PEG 8000, 20 uM DSS, in D_2O; (b) 4 mM PEG 8000, 4 mM 4-nitrophenol, 20 uM DSS, in D_2O; (c) 4 mM PEG 8000, 40 mM 4-nitrophenol, 20 uM DSS, in D_2O; (d) 4 mM PEG 8000, 80 mM 4-nitrophenol, 20 uM DSS, in D_2O. [*Peak assignments (from left to right): doublet: $H_{4\text{-nitrophenol}}$, doublet: $H_{4\text{-nitrophenol}}$, singlet: HOD, singlet: $H_{interior}$ (PEG 8000)] LabArchives: Experimental Notebook/4-nitrophenol Titrations Raw Data*

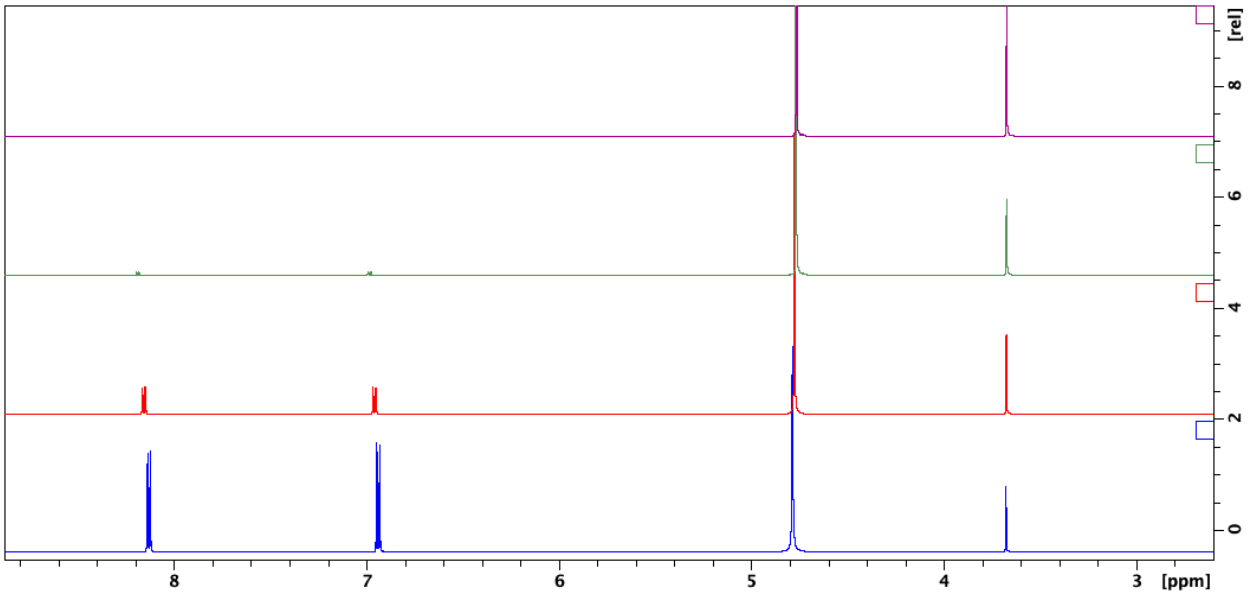

Appendix 6d: ^1H NMR spectra of 18-crown-6 (**7**) at increasing concentrations of 4-nitrophenol (**14**). From top to bottom: (a) 4 mM 18-crown-6, 20 uM DSS, in D_2O; (b) 4 mM 18-crown-6, 4

mM 4-nitrophenol, 20 uM DSS, in D_2O; (c) 4 mM 18-crown-6, 40 mM 4-nitrophenol, 20 uM DSS, in D_2O; (d) 4 mM 18-crown-6, 80 mM 4-nitrophenol, 20 uM DSS, in D_2O. [*Peak assignments (from left to right): doublet: $H_{4\text{-nitrophenol}}$, doublet: $H_{4\text{-nitrophenol}}$, singlet: HOD, singlet: H_a (18-crown-6)] LabArchives: Experimental Notebook/4-nitrophenol Titrations Raw Data*

Appendix 7a-d: ^{1}H NMR spectra of 3-cyanophenol with various PEG-related compounds.

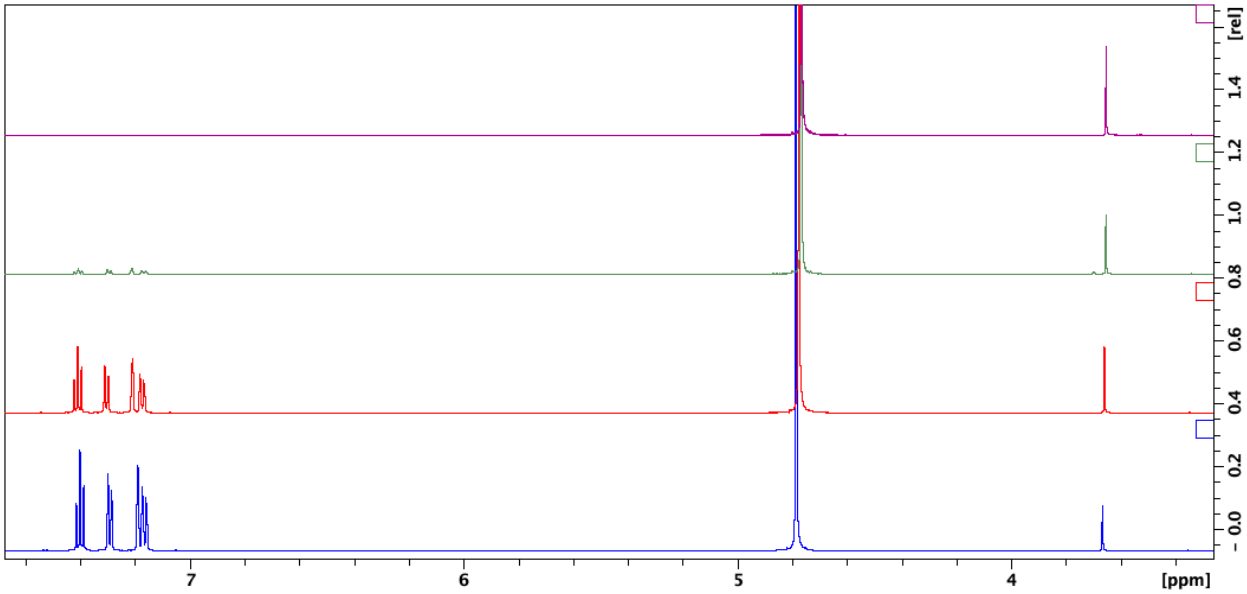

Appendix 7a: ^{1}H NMR spectra of ethylene glycol (**1**) at increasing concentrations of 3-cyanophenol (**15**). From top to bottom: (a) 4 mM ethylene glycol, 20 uM DSS, in D_2O; (b) 4 mM ethylene glycol, 4 mM 3-cyanophenol, 20 uM DSS, in D_2O; (c) 4 mM ethylene glycol, 40 mM 3-cyanophenol, 20 uM DSS, in D_2O; (d) 4 mM ethylene glycol, 80 mM 3-cyanophenol, 20 uM DSS, in D_2O. [*Peak assignments (from left to right): triplet: $H_{3\text{-cyanophenol}}$, doublet: $H_{3\text{-cyanophenol}}$, singlet: $H_{3\text{-cyanophenol}}$, doublet: $H_{3\text{-cyanophenol}}$, singlet: HOD, singlet: H_a (ethylene glycol)] LabArchives: Experimental Notebook/4-nitrophenol Titrations Raw Data*

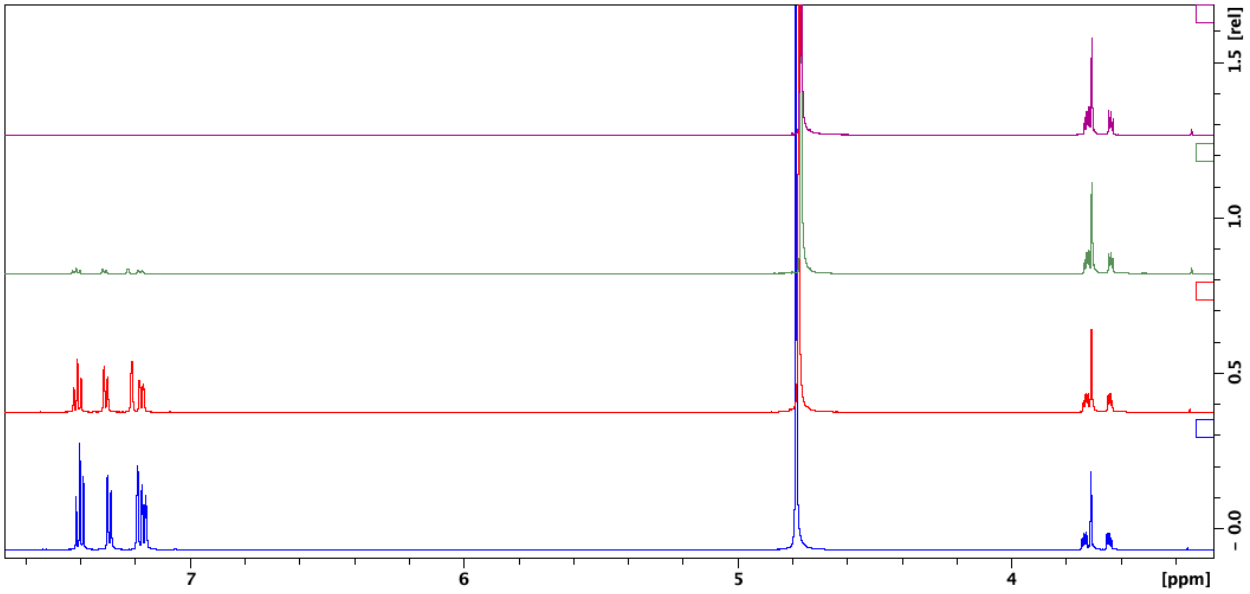

Appendix 7b: ^{1}H NMR spectra of tetraethylene glycol (**4**) at increasing concentrations of 3-cyanophenol (**15**). From top to bottom: (a) 4 mM tetraethylene glycol, 20 uM DSS, in D_2O; (b) 4 mM tetraethylene glycol, 4 mM 3-cyanophenol, 20 uM DSS, in D_2O; (c) 4 mM tetraethylene glycol, 40 mM 3-cyanophenol, 20 uM DSS, in D_2O; (d) 4 mM tetraethylene glycol, 80 mM 3-cyanophenol, 20 uM DSS, in D_2O. [*Peak assignments (from left to right): triplet: $H_{3\text{-cyanophenol}}$, doublet: $H_{3\text{-cyanophenol}}$, singlet: $H_{3\text{-cyanophenol}}$, doublet: $H_{3\text{-cyanophenol}}$, singlet: HOD, triplet: H_a (tetraethylene glycol), singlet: $H_{interior}$ (tetraethylene glycol), triplet: H_b (tetraethylene glycol)] LabArchives: Experimental Notebook/4-nitrophenol Titrations Raw Data*

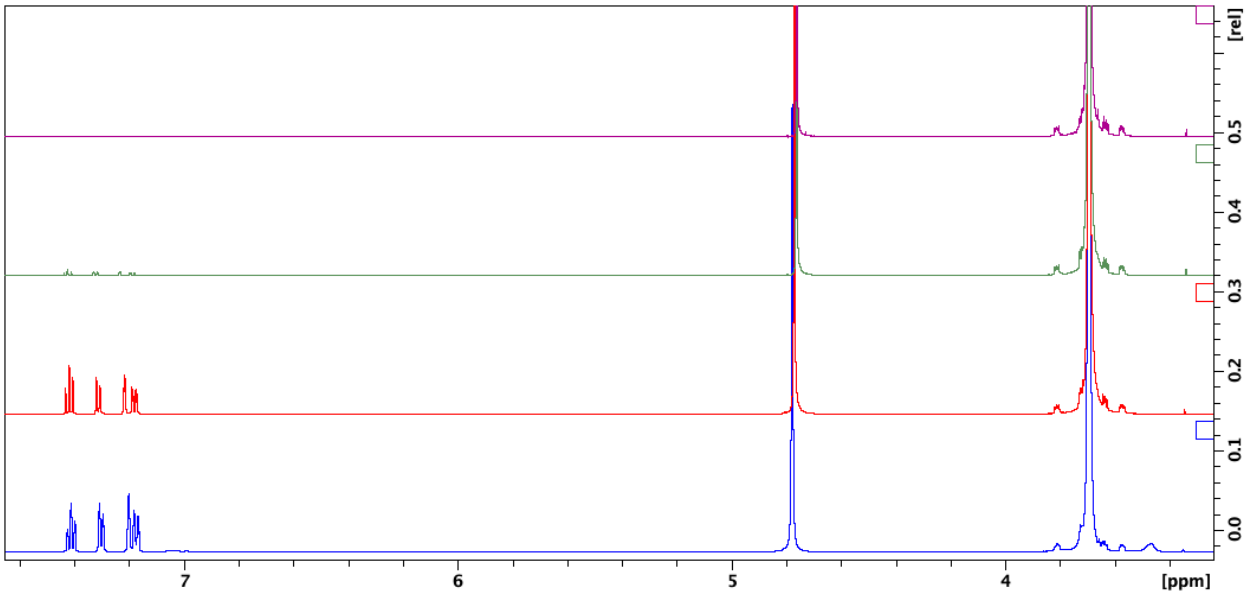

Appendix 7c: ^{1}H NMR spectra of PEG 8000 (**5**) at increasing concentrations of 3-cyanophenol (**15**). From top to bottom: (a) 4 mM PEG 8000, 20 uM DSS, in D_2O; (b) 4 mM PEG 8000, 4 mM 3-cyanophenol, 20 uM DSS, in D_2O; (c) 4 mM PEG 8000, 40 mM 3-cyanophenol, 20 uM DSS, in D_2O; (d) 4 mM PEG 8000, 80 mM 3-cyanophenol, 20 uM DSS, in D_2O. [*Peak assignments*

(from left to right): triplet: $H_{3\text{-cyanophenol}}$, doublet: $H_{3\text{-cyanophenol}}$, singlet: $H_{3\text{-cyanophenol}}$, doublet: $H_{3\text{-cyanophenol}}$, singlet: HOD, singlet: $H_{interior}$ (PEG 8000)] LabArchives: Experimental Notebook/4-nitrophenol Titrations Raw Data

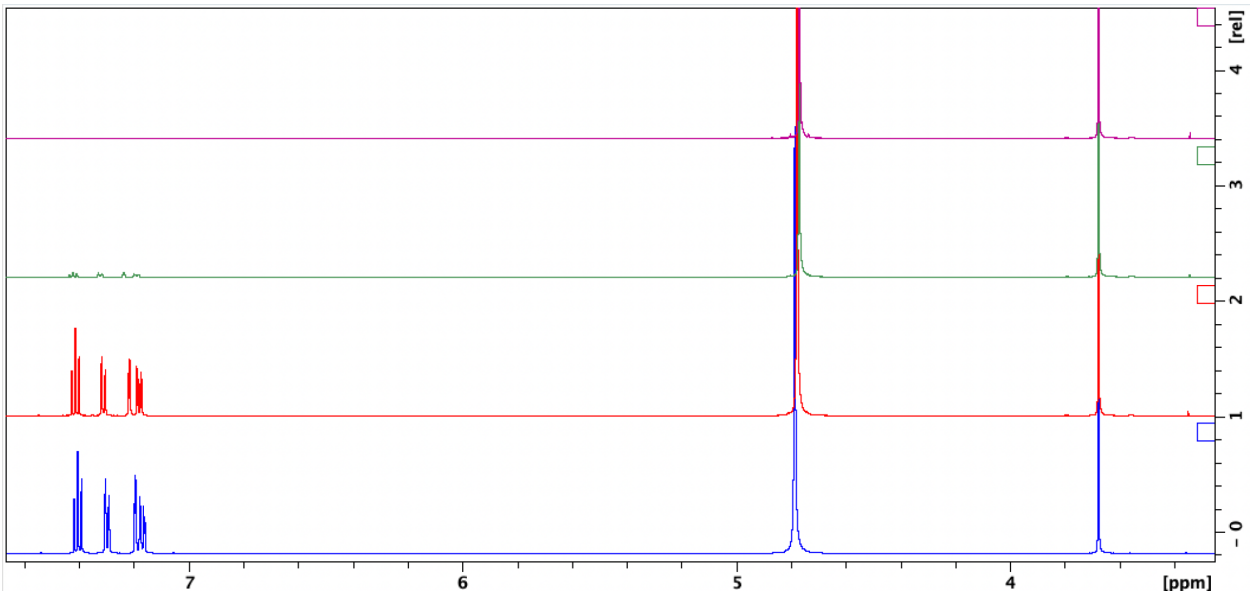

Appendix 7d: ^{1}H NMR spectra of 18-crown-6 (**7**) at increasing concentrations of 3-cyanophenol (**15**). From top to bottom: (a) 4 mM 18-crown-6, 20 uM DSS, in D_2O; (b) 4 mM 18-crown-6, 4 mM 3-cyanophenol, 20 uM DSS, in D_2O; (c) 4 mM 18-crown-6, 40 mM 3-cyanophenol, 20 uM DSS, in D_2O; (d) 4 mM 18-crown-6, 80 mM 3-cyanophenol, 20 uM DSS, in D_2O. [*Peak assignments (from left to right): triplet: $H_{3\text{-cyanophenol}}$, doublet: $H_{3\text{-cyanophenol}}$, singlet: $H_{3\text{-cyanophenol}}$, doublet: $H_{3\text{-cyanophenol}}$, singlet: HOD, singlet: H_a (18-crown-6)] LabArchives: Experimental Notebook/4-nitrophenol Titrations Raw Data*

DOSY Spectra

Appendix 8-15: DOSY NMR diffusion curves for indole (4 mM) and acetone (4 mM) in D_2O, without PEG 8000. Diffusion constants for these curves are in Table 8.

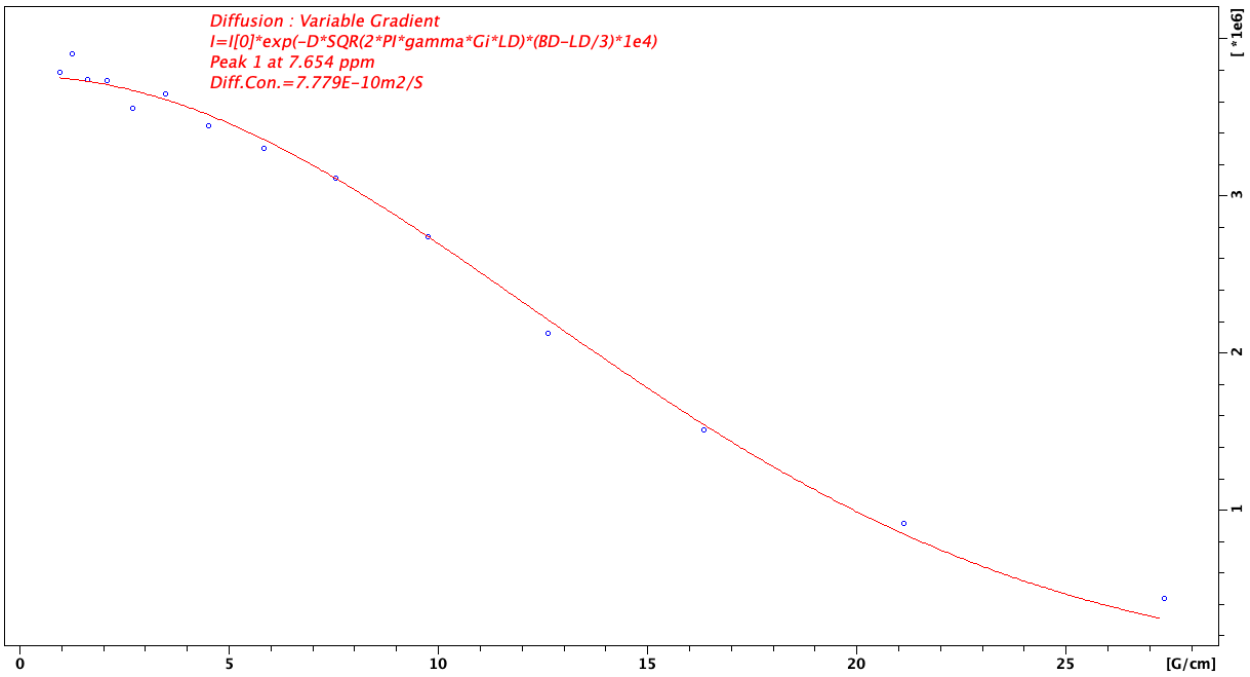

Appendix 8: H_a (indole)

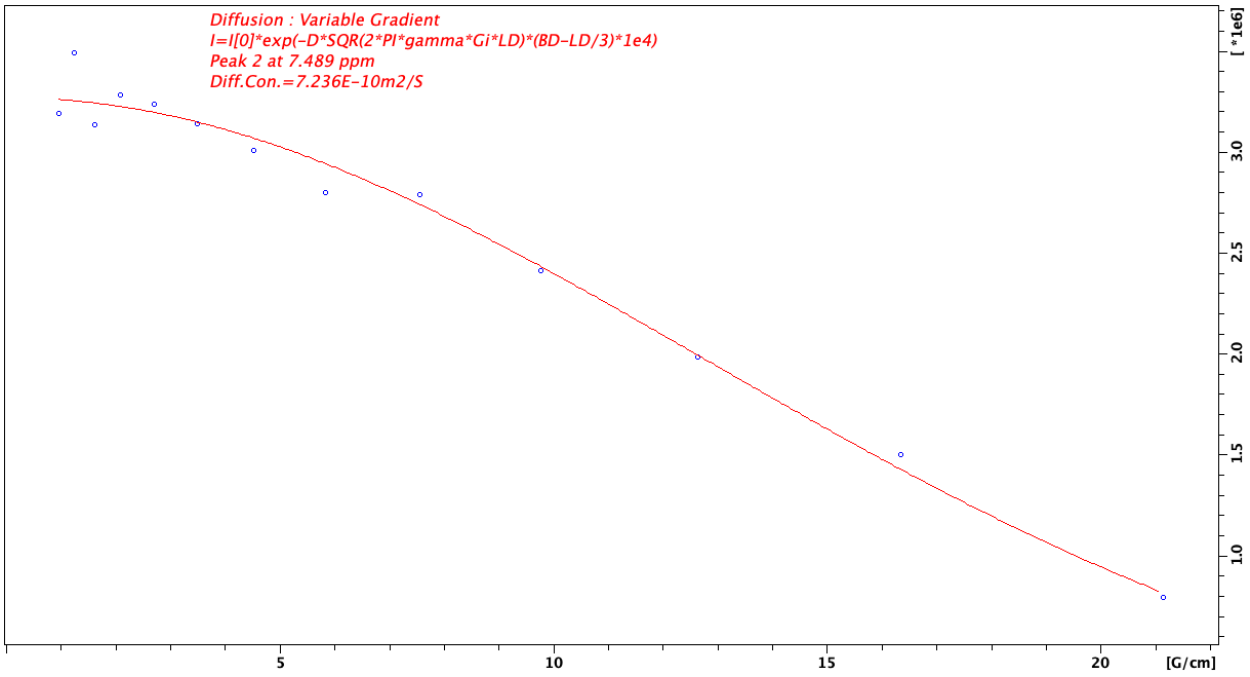

Appendix 9: H_b (indole)

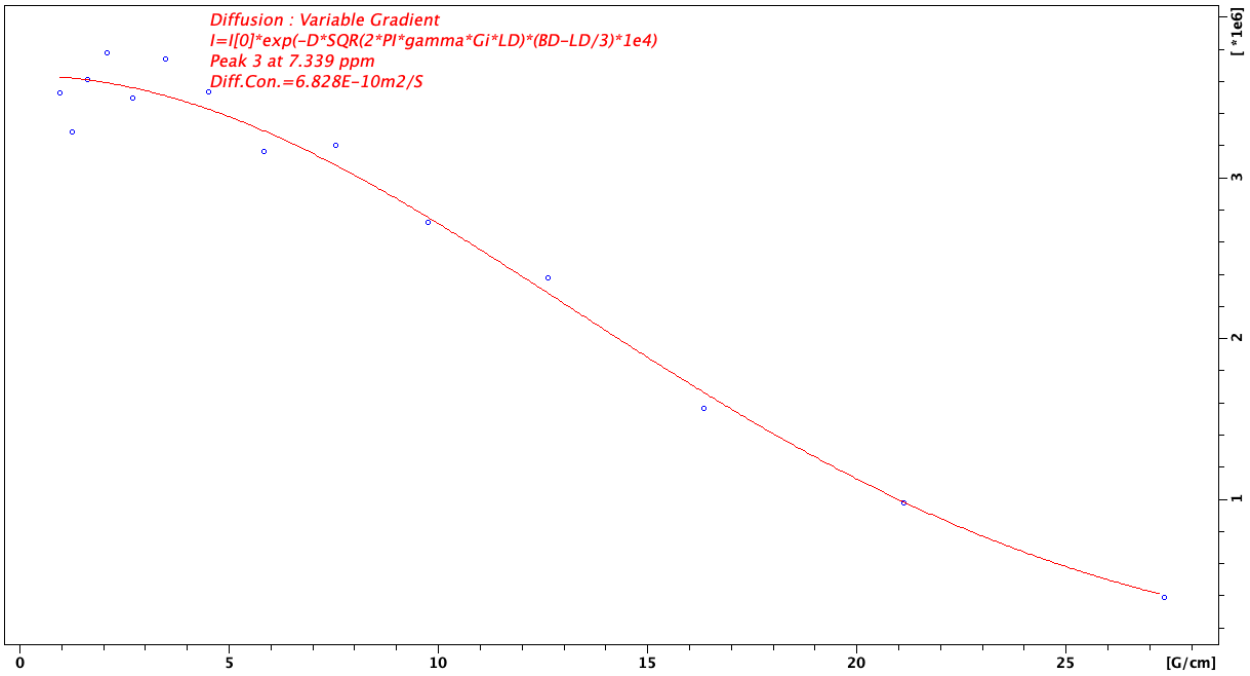

Appendix 10: H_c (indole)

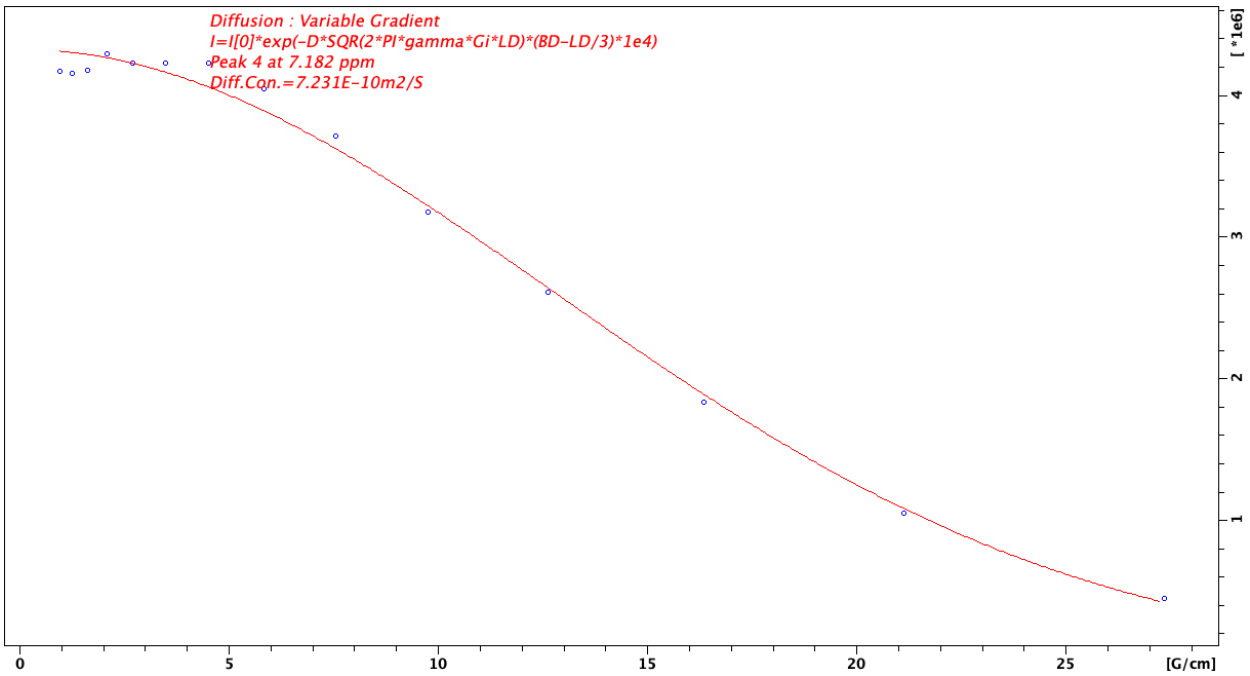

Appendix 11: H_d (indole)

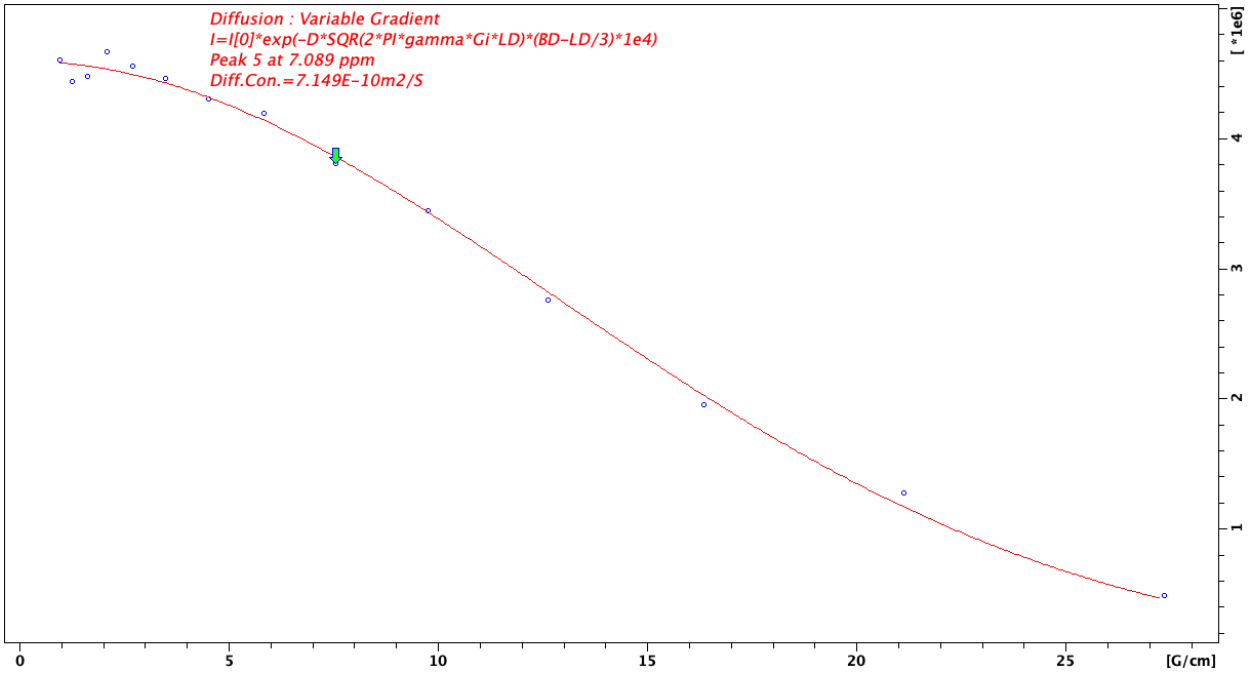

Appendix 12: H_e (indole)

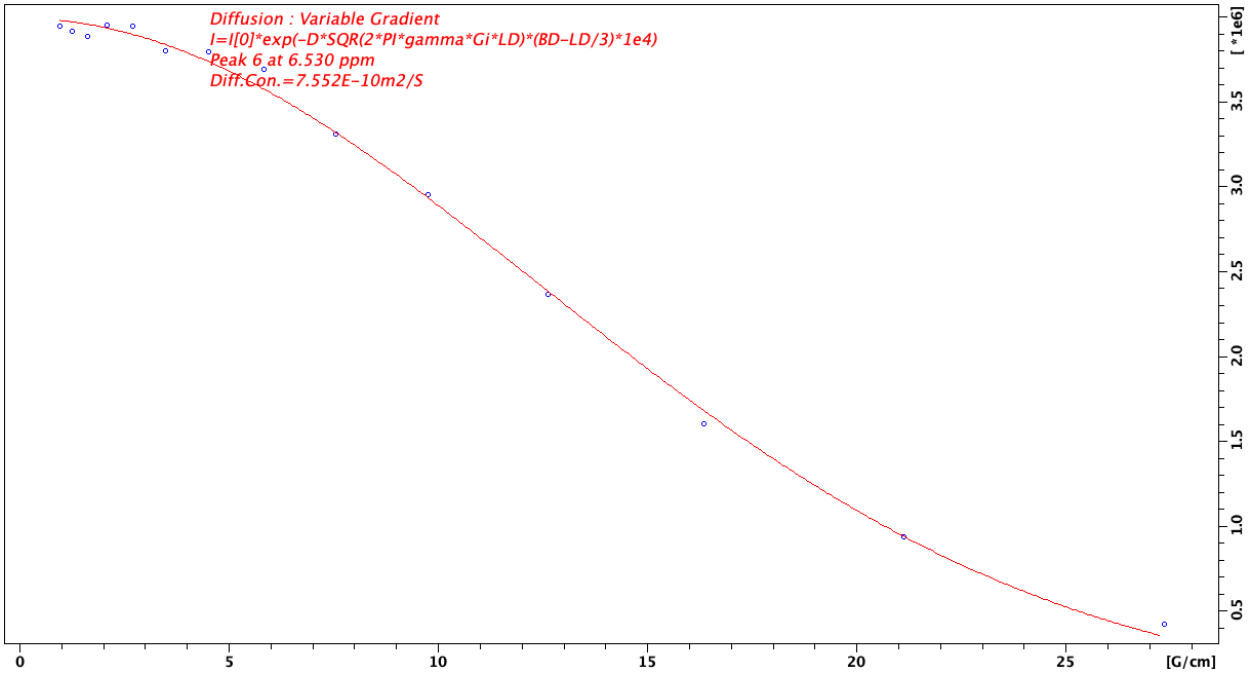

Appendix 13: H_f (indole)

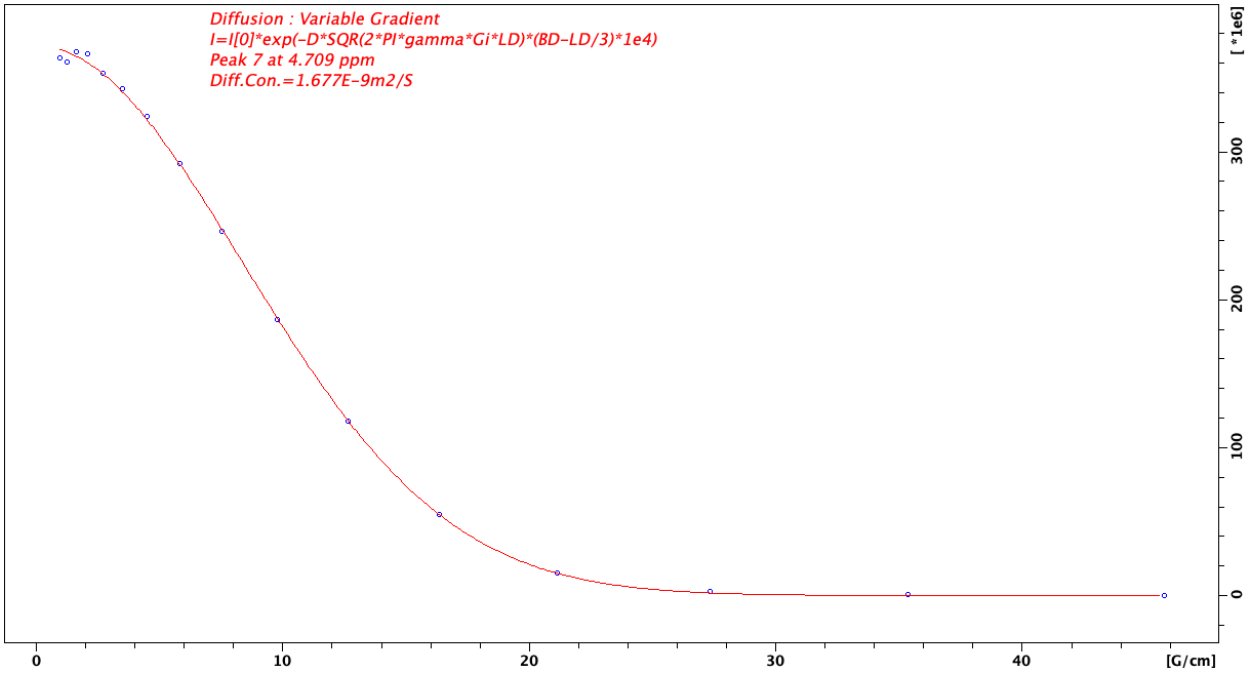

Appendix 14: HOD

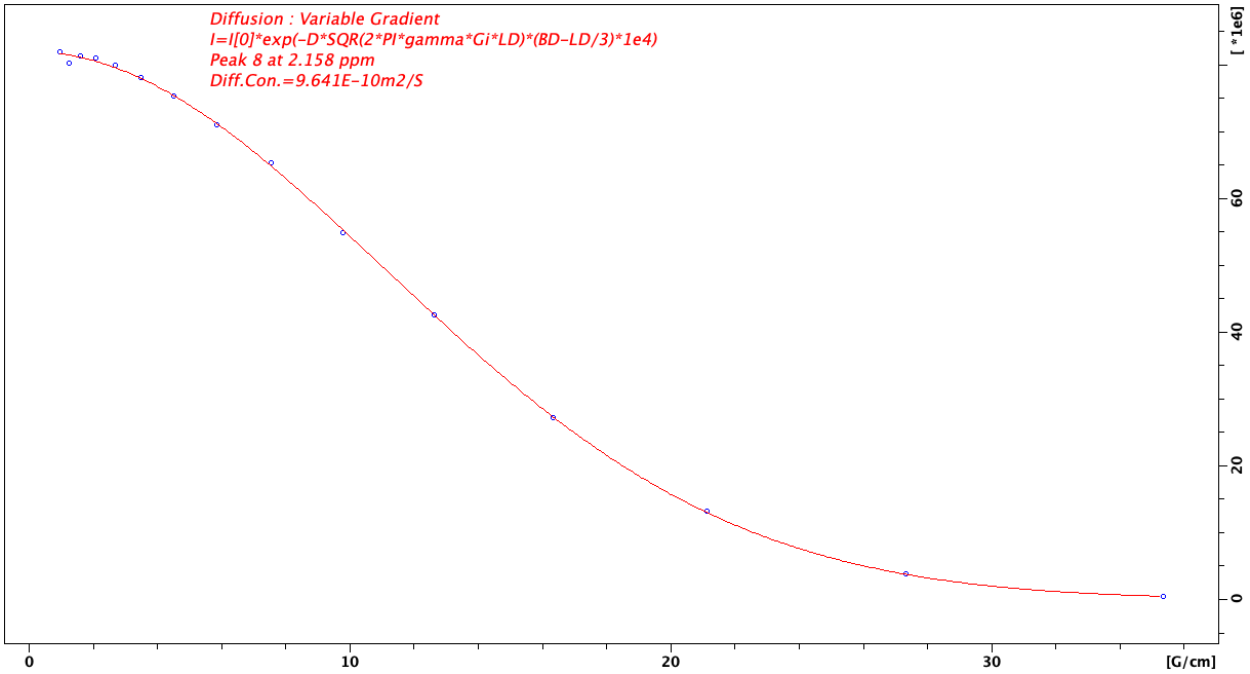

Appendix 15: H_a (acetone)

Appendix 16-24. DOSY NMR diffusion curves for indole (4 mM) and acetone (4 mM) in D_2O, with PEG 8000 (4 mM). Diffusion constants for these curves are in Table 8.

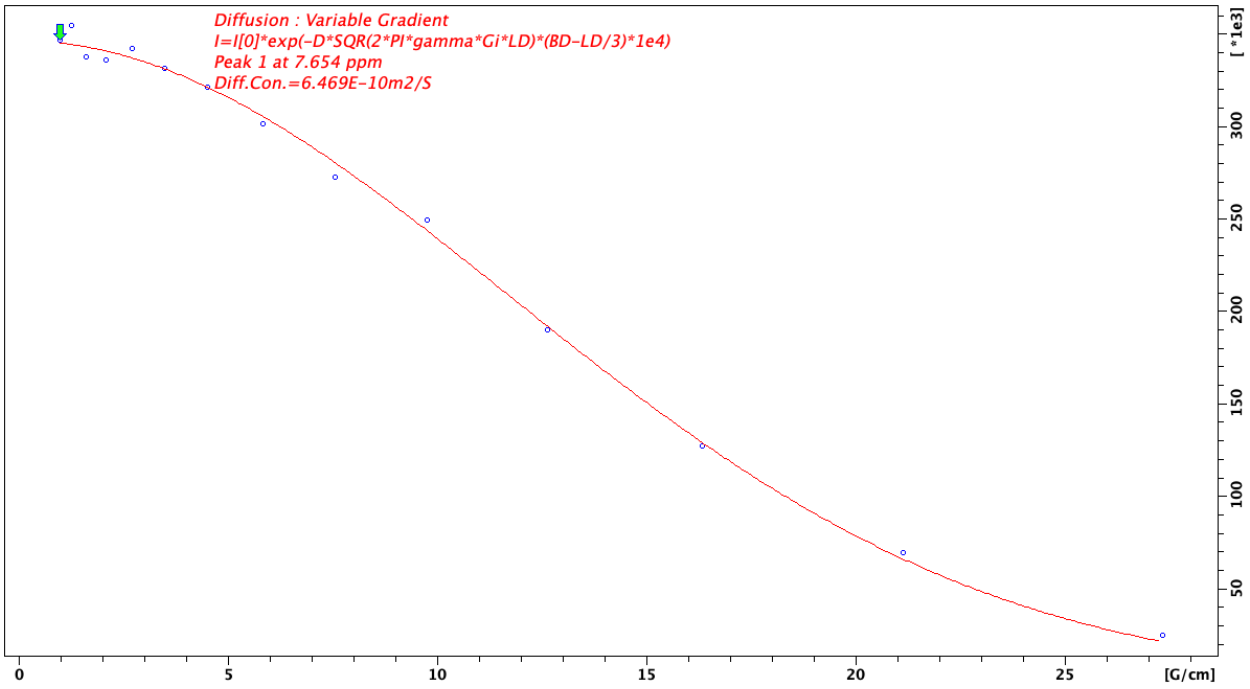

Appendix 16: H_a (indole)

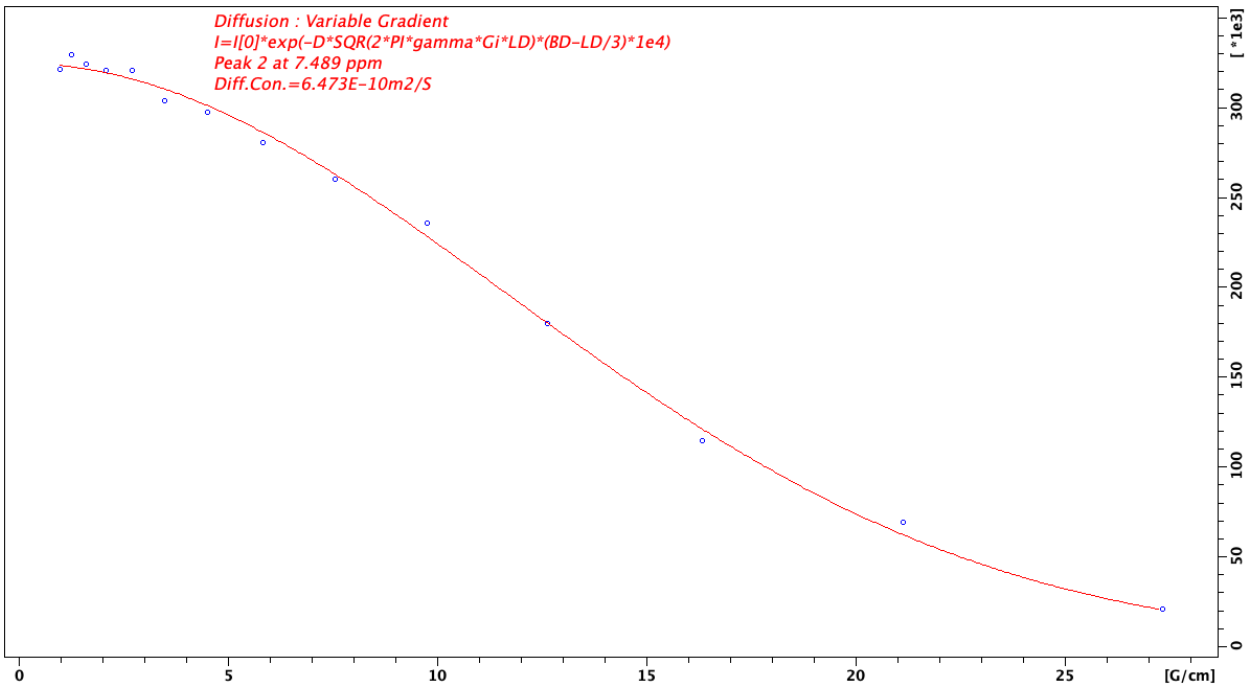

Appendix 17: H_b (indole)

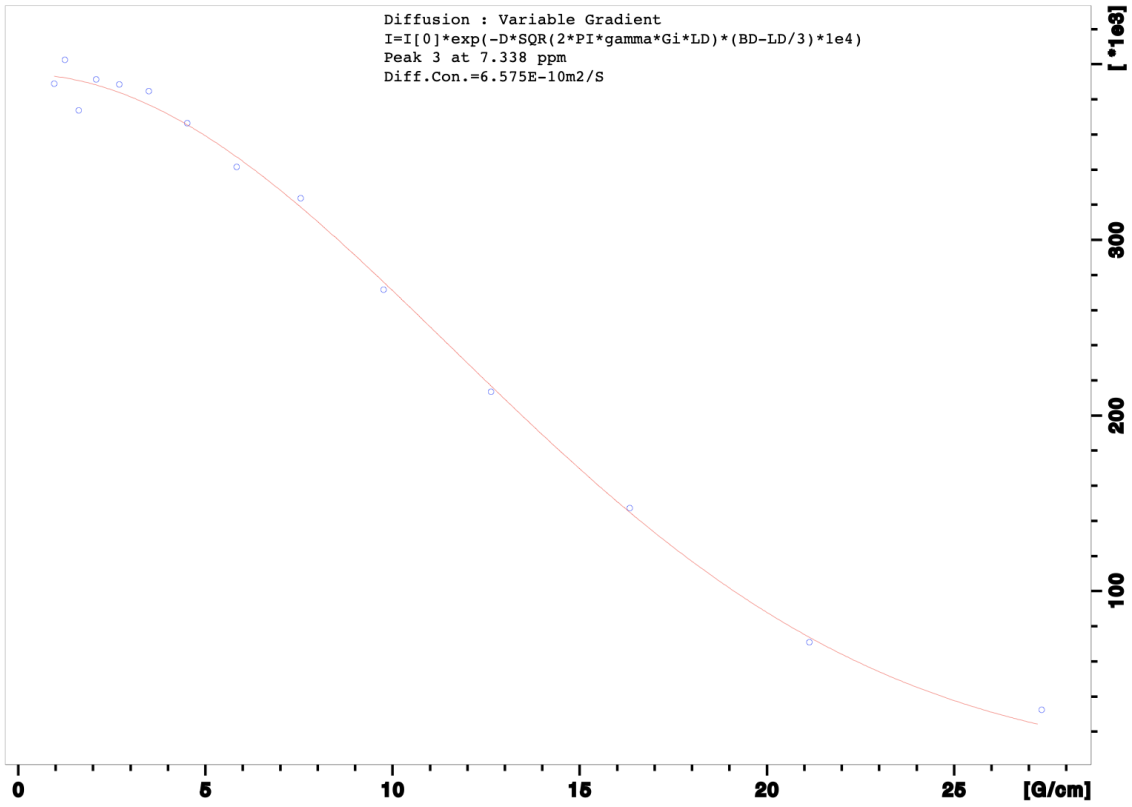

Appendix 18: H_c (indole)

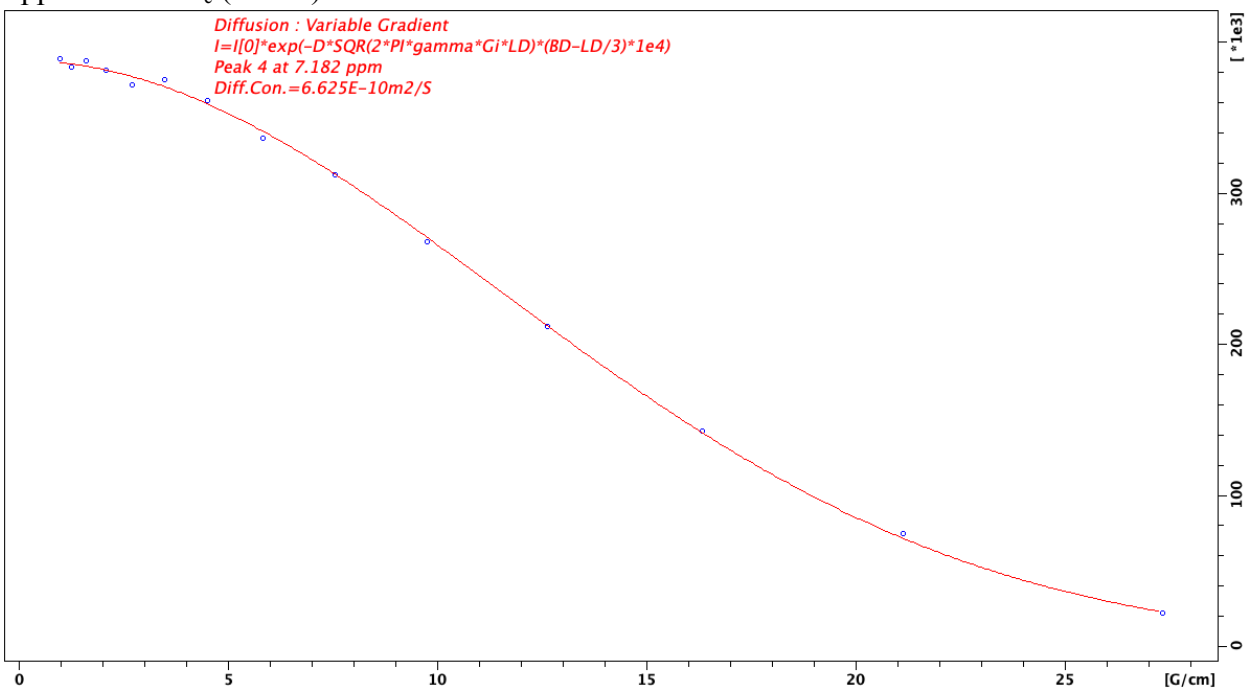

Appendix 19: H_d (indole)

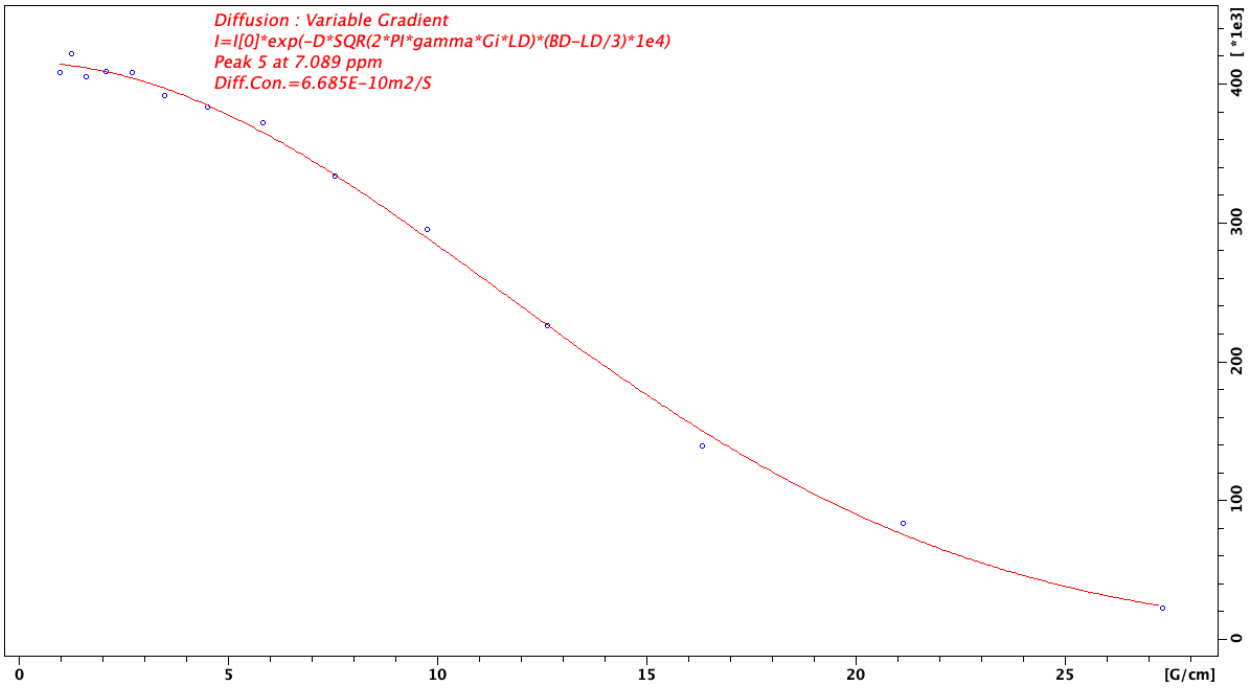

Appendix 20: H_e (indole)

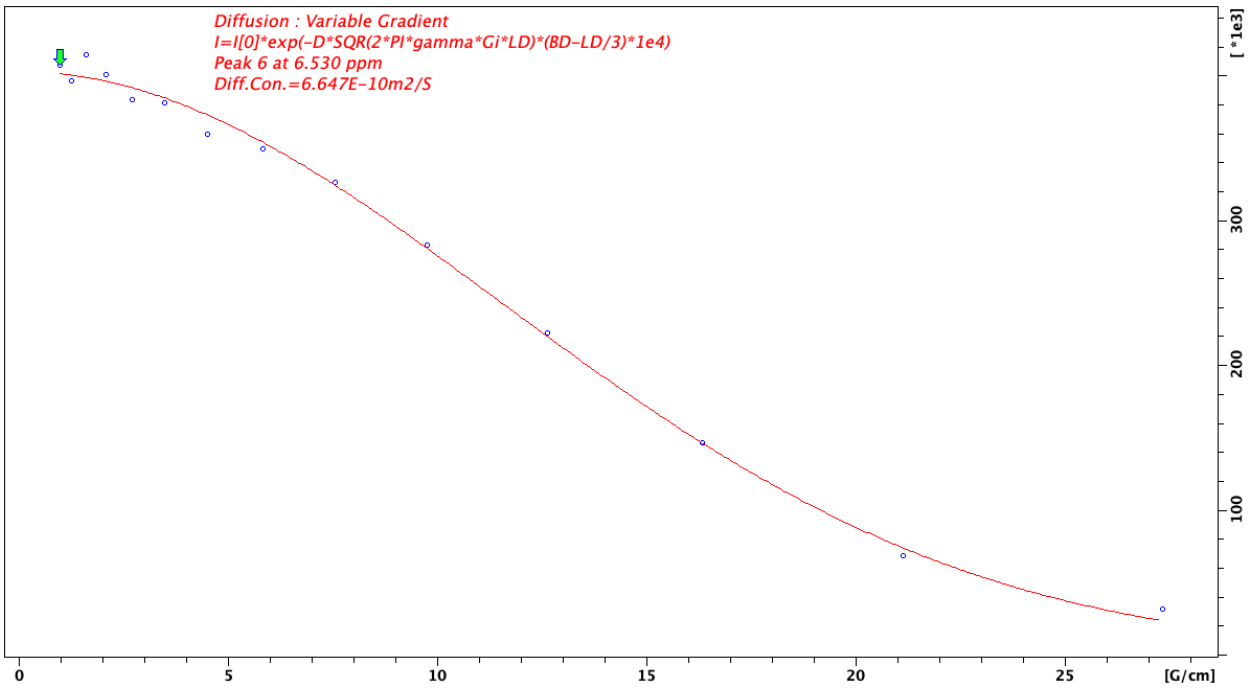

Appendix 21: H_f (indole)

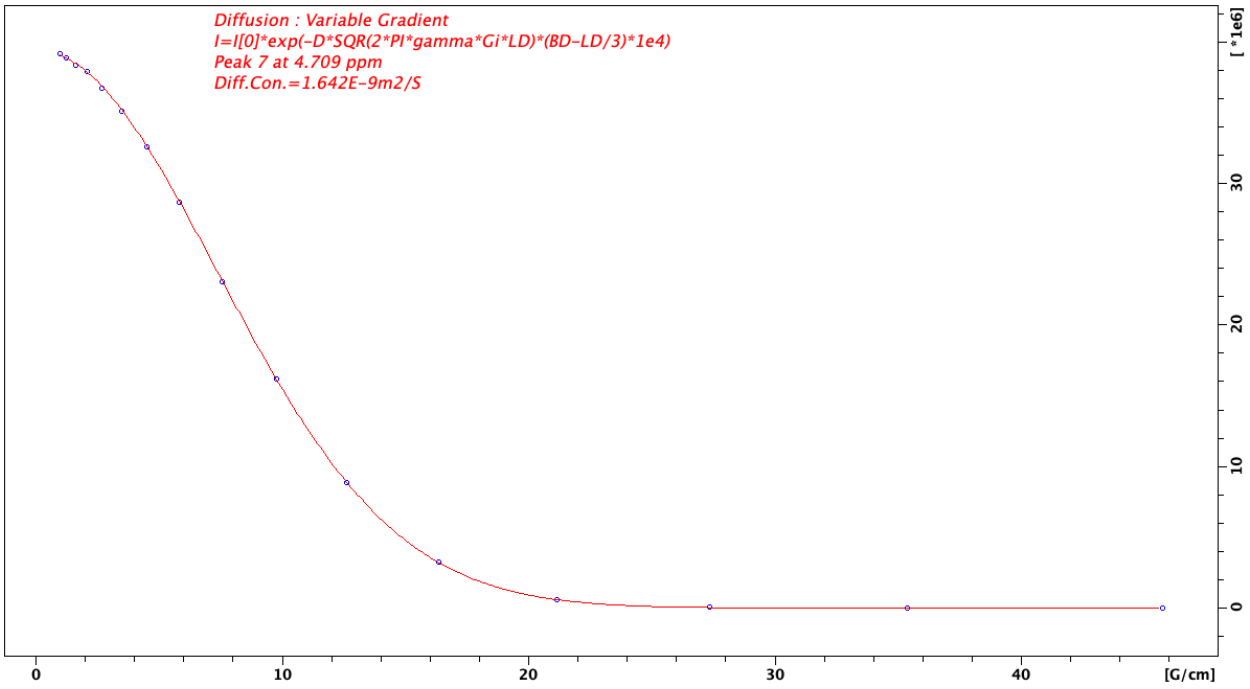

Appendix 22: HOD

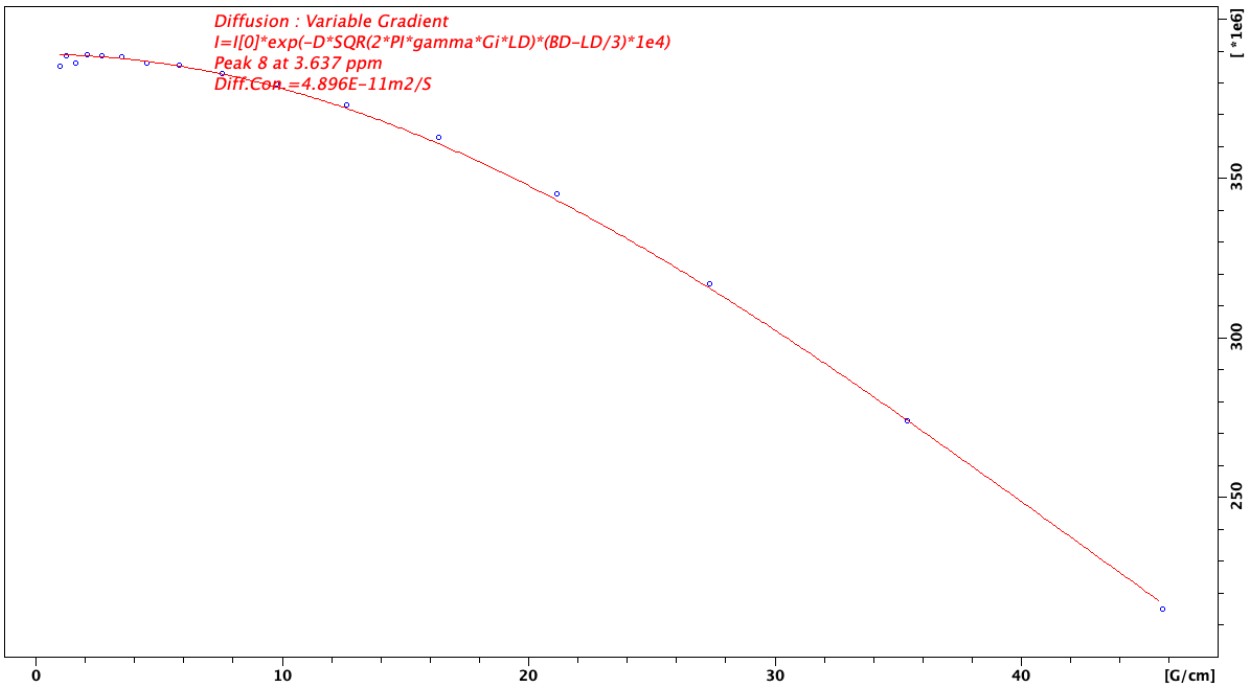

Appendix 23: $H_{interior}$ (PEG 8000)

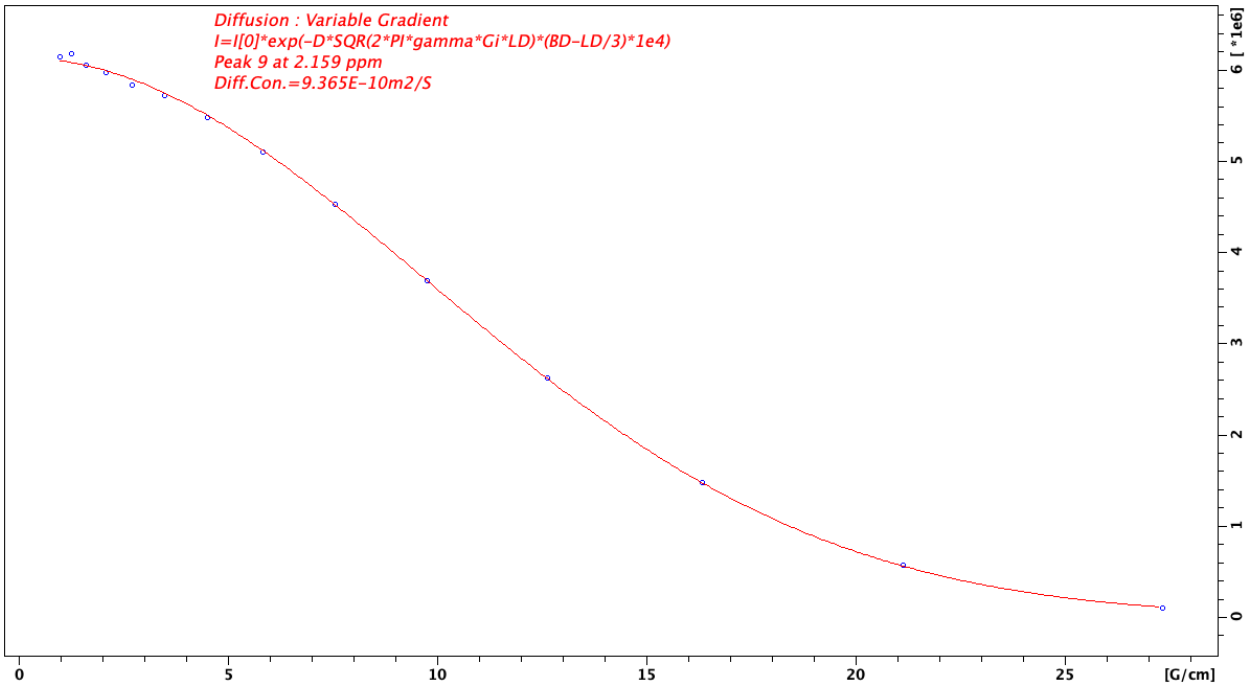

Appendix 24: H_a (acetone)

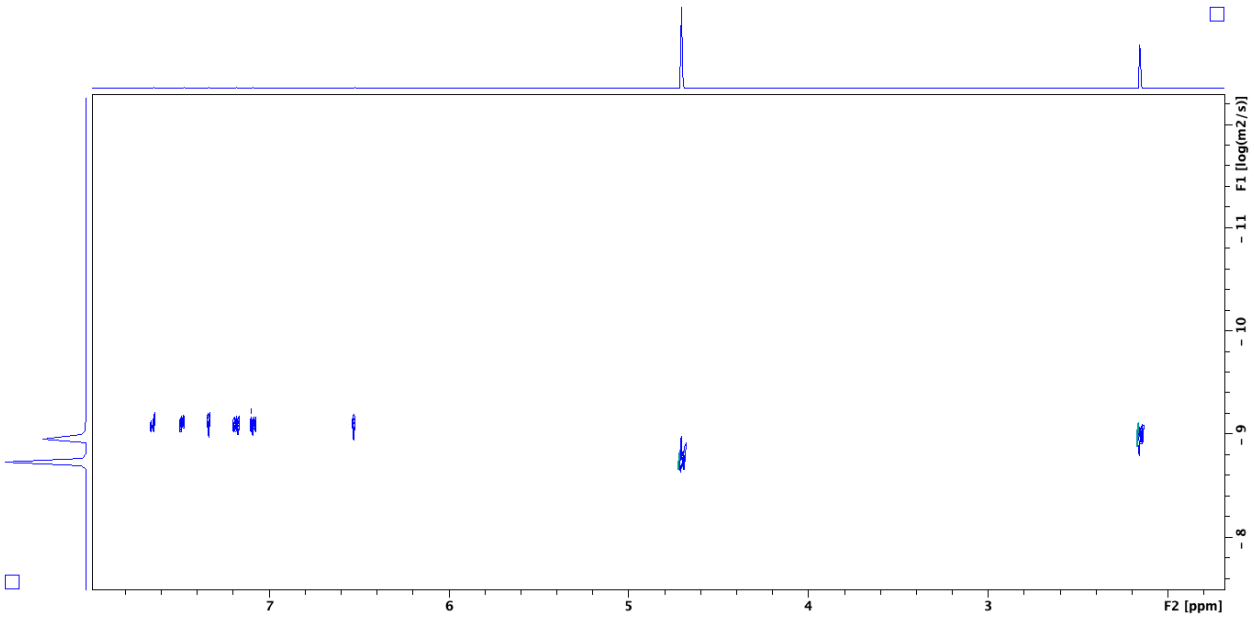

Appendix 25: DOSY NMR spectrum of 4 mM indole (**9**) and 4 mM acetone (**16**) in D_2O. (DOSY parameters: NS = 16; DS = 8; SW = 6.5495 ppm; O1P = 4.961 ppm; D20 = 0.150 s; P30 = 1.000 ms) *LabArchives: Experimental Notebook/Indole PEG 8000 Ac DOSY Raw Data*

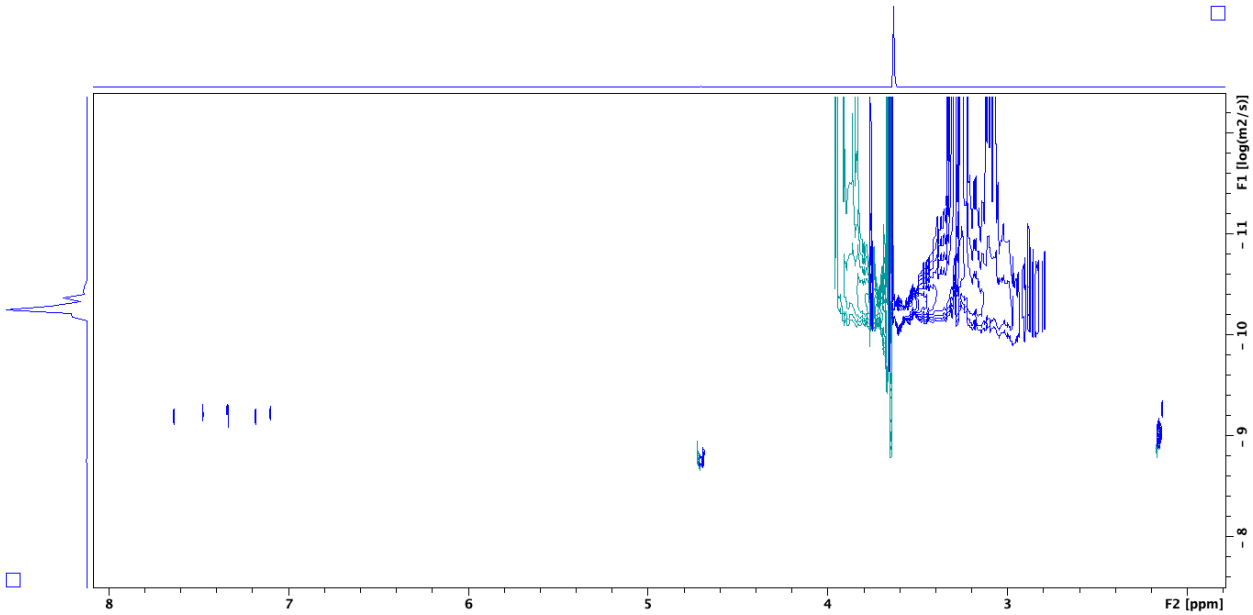

Appendix 26: DOSY NMR spectrum of 4 mM indole (**9**), 4 mM PEG 8000 (**5**) and 4 mM acetone (**16**) in D_2O. (DOSY parameters: NS = 16; DS = 8; SW = 6.2986 ppm; O1P = 4.938 ppm; D20 = 0.200 s; P30 = 1.000 ms) *Experimental Notebook/Indole PEG 8000 Ac DOSY Raw Data*